

**Signaling Mechanisms of Polyspermy Blocks**

by

**Rachel E. Bainbridge**

Bachelor of Science, West Virginia University, 2017

Bachelor of Arts, West Virginia University, 2017

Submitted to the Graduate Faculty of the  
Dietrich School of Arts and Sciences in partial fulfillment  
of the requirements for the degree of  
Doctor of Philosophy

University of Pittsburgh

2022

UNIVERSITY OF PITTSBURGH

DIETRICH SCHOOL OF ARTS AND SCIENCES

This dissertation was presented

by

**Rachel E. Bainbridge**

It was defended on

December 1, 2022

and approved by

Elias Aizenman, Professor, Neurobiology

Jeffrey Hildebrand, Associate Professor, Biological Sciences

Miler Lee, Assistant Professor, Biological Sciences

Allyson O'Donnell, Assistant Professor, Biological Sciences

Dissertation Director: Anne Carlson, Associate Professor, Biological Sciences

Copyright © by Rachel E. Bainbridge

2022

## Polyspermy Blocking Mechanisms in Sperm and Egg

Rachel E. Bainbridge, PhD

University of Pittsburgh, 2022

Fertilization is a tightly regulated process requiring numerous signaling processes. My dissertation research focused on two: PLC activation in the egg following fertilization, and zinc effects on gamete fertility.

Fertilization initiates polyspermy blocks that stop fertilization by multiple sperm. Eggs from most animals use the slow block to polyspermy, which occurs minutes after fertilization and involves the release of cortical granules to create a barrier that surrounds the nascent zygote. In external fertilizers, eggs also use the fast block, which occurs seconds after fertilization, and involves an electrical depolarization of the egg plasma membrane. In eggs of the African clawed frog, *Xenopus laevis*, the fast block depolarization is mediated by the calcium-activated chloride channel TMEM16A following a phospholipase C (PLC)- dependent calcium increase. PLC- $\gamma$ 1 is the most abundant PLC isozyme in the egg, typically activated by phosphorylation of a conserved tyrosine at the enzyme's active site. I used tyrosine kinase inhibitors during whole cell recording to observe the fast block during *X. laevis* fertilization. I found that blocking tyrosine phosphorylation did not affect the fast block depolarization, suggesting that another pathway activates the fast block to polyspermy in *X. laevis* eggs.

In contrast to the fast block, the slow block is used by eggs from most sexually reproducing animals. During the slow block, mammalian eggs have been shown to release zinc into the extracellular milieu. Here we demonstrated that *X. laevis* eggs also release zinc post-fertilization, and that at physiologic concentrations, extracellular zinc stopped fertilization in diverse external

fertilizers. By independently treating *X. laevis* sperm or eggs with zinc prior to fertilization, we demonstrated that the zinc targets both gametes to stop fertilization.

In addition to high extracellular zinc surrounding already fertilized eggs, mammalian sperm encounter high zinc concentrations as they are mixed with the seminal fluid at mating. I established a fluorometry assay using the zinc indicator FluoZin-3 to monitor cytoplasmic zinc in mammalian sperm. Because mammalian sperm both encounter varying concentrations of extracellular zinc and must undergo changes post-mating to gain the ability to fertilize an egg, we believe that zinc may alter sperm physiology.

## Table of Contents

List of Abbreviations .....	xv
Preface.....	xvi
1.0 Introduction.....	1
1.1 Physiology of fertilization .....	1
1.1.1 Post-mating preparation of sperm to fertilize .....	1
1.1.1.1 Sperm activation .....	2
1.1.1.1.1 Mammalian sperm capacitation .....	2
1.1.1.1.2 Frog sperm activation.....	5
1.1.2 Egg activation .....	5
1.1.2.1 Polyspermy block.....	8
1.1.2.2 Slow block to polyspermy .....	8
1.1.2.3 Fast block to polyspermy .....	11
1.2 Zinc plays a commanding role in the regulation of fertilization .....	15
1.2.1 Mammalian sperm encounter elevated extracellular zinc at multiple points between mating and fertilization .....	15
1.2.2 Zinc release at activation .....	16
1.3 Model organisms.....	17
1.3.1 Egg and oocyte models.....	17
1.3.1.1 The African clawed frog <i>Xenopus laevis</i> .....	17
1.3.1.2 The purple sea urchin <i>Strongylocentrotus purpuratus</i> .....	18
1.3.1.3 The cnidarian <i>Hydractinia symbiolongicarpus</i> .....	18

1.3.2 Sperm models .....	19
1.3.2.1 The house mouse <i>Mus musculus</i> .....	19
1.3.2.2 Human surplus sperm samples.....	19
1.4 Clinical importance and significance .....	20
1.4.1 Infertility worldwide .....	20
1.4.1.1 Artificial reproductive technologies .....	20
1.4.2 Significance of understanding egg signaling.....	21
1.4.3 Environmental concerns due to zinc pollution .....	21
<b>2.0 Tyrosine phosphorylation of PLC-<math>\gamma</math> is not necessary for activation of the fast block</b>	
<b>to polyspermy .....</b>	<b>22</b>
<b>2.1 Introduction .....</b>	<b>22</b>
<b>2.2 Materials and methods.....</b>	<b>25</b>
2.2.1 Reagents .....	25
2.2.2 Solutions.....	25
2.2.3 Animals .....	26
2.2.4 Collection of gametes .....	26
2.2.5 Sperm preparation and <i>in vitro</i> fertilization.....	27
2.2.6 Electrophysiology .....	27
2.2.7 Exogenous protein expression in <i>X. laevis</i> oocytes .....	28
2.2.8 Removal of egg jelly .....	28
2.2.9 Protein sample preparation and western blot .....	29
2.2.10 Quantification and statistical analyses .....	30
<b>2.3 Results.....</b>	<b>30</b>

2.3.1 Inhibition of PLC- $\gamma$ by tyrosine kinase inhibitors did not alter the fast block .....	30
2.3.2 Inhibition of PLC- $\gamma$ by tyrosine kinase inhibitors did not affect embryonic development .....	40
2.3.3 Assessment of possible sperm PLC- $\zeta$ in <i>X. laevis</i> testis .....	40
2.4 Discussion .....	45
<b>3.0 Zinc inhibition of gamete fertility is an ancient feature of sexual reproduction in animals .....</b>	<b>47</b>
3.1 Introduction .....	47
3.2 Materials and methods.....	48
3.2.1 Ethics .....	48
3.2.2 Animals .....	48
3.2.3 Reagents .....	48
3.2.4 Solutions.....	49
3.2.5 Collection of gametes .....	50
3.2.5.1 <i>X. laevis</i> oocytes .....	50
3.2.5.2 <i>X. laevis</i> sperm and eggs .....	50
3.2.5.3 <i>S. purpuratus</i> sperm and eggs .....	51
3.2.5.4 <i>H. symbiolongicarpus</i> sperm and eggs.....	51
3.2.6 Confocal microscopy of extracellular zinc during fertilization or activation .....	52
3.2.6.1 <i>X. laevis</i> egg imaging.....	52
3.2.7 Bright-field microscopy .....	52

3.2.7.1 <i>X. laevis</i> egg and embryo imaging .....	52
3.2.7.2 <i>S. purpuratus</i> egg and embryo imaging.....	53
3.2.7.3 <i>H. symbiolongicarpus</i> egg and embryo imaging .....	53
3.2.8 Fertilization and embryonic development assays.....	53
3.2.8.1 Assessment of <i>X. laevis</i> embryonic development .....	53
3.2.8.2 Assessment of <i>S. purpuratus</i> embryonic development.....	54
3.2.8.3 Assessment of <i>H. symbiolongicarpus</i> embryonic development .....	54
3.2.9 Parthenogenic egg activation .....	54
3.2.9.1 Sperm-free activation of <i>X. laevis</i> eggs.....	54
3.2.10 FluoZin-3 fluorometry .....	55
3.2.10.1 Quantification of zinc release from <i>X. laevis</i> eggs.....	55
3.2.10.2 Quantification of zinc content of egg exudate with spectofluorometry .....	55
3.2.11 Quantification of zinc content of egg exudate with ICP-MS.....	56
3.2.12 Electrophysiology .....	57
3.2.13 Proteomic and RNA-sequencing (RNA-seq) analysis .....	58
3.3 Results.....	58
3.3.1 Zinc is released from <i>Xenopus laevis</i> eggs at activation .....	58
3.3.2 Quantification of zinc release from <i>X. laevis</i> .....	62
3.3.3 Zinc inhibition of fertilization is concentration dependent.....	62
3.3.3.1 Zinc stopped <i>X. laevis</i> fertilization .....	67
3.3.3.2 Insemination in zinc inhibited embryonic development sea urchin and a cnidarian .....	67

3.3.4 Zinc inhibition of fertilization is reversible .....	70
3.3.4.1 Inhibition of embryonic development in <i>X. laevis</i> eggs was reversible with zinc chelators .....	70
3.3.5 Zinc inhibits fertilization, not development or activation .....	73
3.3.5.1 Fast block depolarizations are not present in eggs fertilized in extracellular zinc.....	73
3.3.5.2 Delayed chelator-dependent rescue of fertility demonstrates a zinc interruption of fertilization.....	76
3.3.5.3 Eggs can still be activated chemically in the presence of zinc .....	77
3.3.6 Zinc targets both sperm and egg to stop fertilization .....	79
3.3.6.1 Zinc inhibition of eggs is concentration dependent .....	79
3.3.6.2 Zinc inhibition of sperm is concentration dependent.....	81
3.3.7 Zinc fertilization of <i>X. laevis</i> sperm was reversible with zinc chelators.....	81
3.3.8 Zinc's identity as a divalent transition metal is key for its ability to block fertilization.....	82
3.3.9 Copper targets both gametes to stop fertilization .....	83
3.3.9.1 Copper block of eggs is concentration dependent.....	85
3.3.9.2 Copper block of sperm is concentration dependent .....	85
3.4 Discussion .....	85
4.0 Mammalian sperm import extracellular zinc.....	89
4.1 Introduction .....	89
4.2 Materials and methods.....	91
4.2.1 Sperm and seminal fluid sources .....	91

4.2.2	Quantification of labile zinc in seminal fluid .....	91
4.2.3	Quantification of sperm cytoplasmic zinc .....	92
4.3	Results.....	93
4.3.1	Quantification of labile zinc in semen .....	93
4.3.2	Mammalian sperm readily take up zinc .....	93
4.3.3	Cytoplasmic zinc decreases in the presence of zinc chelators and capacitating signals .....	96
4.3.4	Transcripts for zinc transporters are expressed in the developing sperm ...	99
4.4	Discussion .....	102
5.0	Discussion.....	104
5.1	Summary .....	104
5.2	Future directions .....	104
5.2.1	Further experiments .....	105
5.2.1.1	Zinc protection of fertilized eggs .....	105
5.2.1.2	Mammalian sperm uptake of extracellular zinc .....	105
5.2.2	Wider impacts .....	106
5.2.2.1	Contraceptives.....	106
5.2.2.2	Environmental concerns due to zinc and copper pollution .....	108
Appendix A	Additional Tables .....	111
Bibliography	.....	118

## List of Tables

<b>Table 1 PLC transcripts present in RNAseq of <i>X. laevis</i> testis .....</b>	<b>44</b>
<b>Table 2 Average zinc ions released from <i>X. laevis</i> eggs .....</b>	<b>63</b>
<b>Table 3 Average IC<sub>50</sub>s of transition metals on proportion of development.....</b>	<b>65</b>
<b>Appendix Table 1 Representative species used for PLC alignment.....</b>	<b>111</b>

## List of Figures

<b>Figure 1 Capacitation of mammalian sperm.....</b>	<b>4</b>
<b>Figure 2 Different Ca<sup>2+</sup> events in the activation of diverse eggs.....</b>	<b>7</b>
<b>Figure 3 The slow block to polyspermy is conserved in sexually reproducing organisms... 10</b>	<b>10</b>
<b>Figure 4 The fast block to polyspermy in frogs.....</b>	<b>14</b>
<b>Figure 5 PLC isozymes are differentiated by their activation, tied to their structure .....</b>	<b>24</b>
<b>Figure 6 Genistein does not alter the kinetics of the fast block depolarization or the development rate of embryos.....</b>	<b>35</b>
<b>Figure 7 Lavendustin A did not alter the kinetics of the fast block depolarization or the development rate of embryos.....</b>	<b>37</b>
<b>Figure 8 Genistein and Lavendustin B inhibit phosphorylation of PLC-<math>\gamma</math>.....</b>	<b>39</b>
<b>Figure 9 Radial and linear phylogenetic trees of PLC isoforms from selected representative species.....</b>	<b>43</b>
<b>Figure 10 <i>X. laevis</i> eggs release zinc at fertilization.....</b>	<b>60</b>
<b>Figure 11 Extracellular zinc protects eggs from fertilization .....</b>	<b>64</b>
<b>Figure 12 Zinc protection of eggs is conserved in invertebrate external fertilizers.....</b>	<b>69</b>
<b>Figure 13 Zinc inhibits embryonic development by binding to proteins sunrrounding the egg .....</b>	<b>72</b>
<b>Figure 14 Eggs inseminated in extracellular zinc do no not display fertilization evoked depolarizations .....</b>	<b>74</b>
<b>Figure 15 Extracellular zinc inhibits fertilization, not just development.....</b>	<b>78</b>
<b>Figure 16 Zinc inhibits fertilization by interferring with both eggs and sperm. ....</b>	<b>80</b>

**Figure 17 Divalent transition metals such as copper also interfere with fertilization, effecting eggs and sperm ..... 84**

**Figure 18 Zinc protection of eggs is an ancient phenomenon ..... 88**

**Figure 19 Mammalian sperm encounter changing conditions throughout fertilization ..... 90**

**Figure 20 Mammalian sperm import extracellular zinc ..... 95**

**Figure 21 Chelation and capacitation lead to cytoplasmic zinc loss ..... 97**

**Figure 22 BSA, but not bicarbonate leads to cytoplasmic zinc depletion ..... 98**

**Figure 23 Transcripts of known or suspected zinc importers in mammalian developing sperm ..... 100**

**Figure 24 Known cellular localization of zinc transporters in mammalian sperm ..... 101**

## List of Abbreviations

Abbreviations used (alphabetical)

ART (Artificial reproductive technology)

BSA (bovine serum albumin)

ER (endoplasmic reticulum)

hCG (human chorionic gonadotropin)

IP<sub>3</sub> (inositol trisphosphate)

IP<sub>3</sub>R (inositol trisphosphate receptor)

ICP-MS (inductively coupled plasma mass spectrometry)

IUD (intrauterine device)

IVF (*in vitro* fertilization)

MR (Modified Ringers solution)

PLC (Phospholipase C)

PDGF-R (platelet derived growth factor receptor)

opto-M1R (rhodopsin-muscarinic receptor type 1 chimera)

oocyte homogenization buffer (OHB)

SH2 (Src-homology 2)

TPEN (N,N,N',N'-tetrakis(2-pyridinylmethyl)-1,2-ethanediamine)

ZnT (zinc transporter encoded by the SLC30 gene family)

ZIP (zinc transporter encoded by the SLC39 gene family)

## Preface

I would like to thank and acknowledge my dissertation committee for advice and support throughout my years of study. My work has been supported through the T32 Training Program: Reproductive Development from Gonads to Fetuses, as well as the Andrew W. Mellon Predoctoral Fellowship.

I want to thank my parents for the incredibly important role they played in seeing a wildly pedantic little girl through to what you see here today. I am so grateful that when faced with a child who had a constant need to correct every human being she came across, instead of stifling that behavior, you saw it for what it really was, an incredible awe at the breadth of knowledge available to us, and a desperate need to share that knowledge at every opportunity. So now instead of having to listen to constant facts about mummies, you get zinc. I don't know if it got better.

I had no idea I wanted to study reproduction or be an electrophysiologist. All I knew when I started in Anne's lab was that I wanted to follow in the footsteps of incredible scientists. Anne, you have led with incredible strength and grace, and teach us to embrace our entire identity as women in science. Joel, you have been a constant vault of information and have helped shape my work in the time you've been in the lab. I also learned so much from Katie and Wase. They are fiercely independent and brilliant, and showed me who I wanted to be when I grew up. My lab mates now, Crystal and Kayla are my ride or dies. I am so thankful for the friendship we've built, and the support you've given me. I wouldn't have stayed sane this past year without you both. Bea, I'm so happy that you're starting your graduate journey. I can't think of anyone better suited to shape the world. The people I've met in this lab make me want to stay in academia. We are the future I hope for and the people I want to succeed in it.

I have made such incredible friends through this journey, especially Jon and Sarah. They are the smartest, weirdest people I've ever met, and I love them as family. I never thought I'd find people who really get me, but I have, and I am so happy we are going to spend the rest of our lives sharing our accomplishments and stupid adventures.

I spent 6 weeks this summer at a summer course in Woods Hole. There, I learned more than I ever thought possible and met 20 of my favorite people. I am so grateful for the experience, which has already shaped my future, and even more I am thankful for the FIR family I found.

Last, I want to thank my partner of 9 years, Alan, for sticking with me through all the stress and the deadlines. You are my favorite person, and I'm so happy that you've been with me through this last stage of my life, as I've grown more into the person I wanted to be, and that you'll be with me in the next stage, for whatever comes next.

*"Your work will outlive you, but those you love may not."*

## **1.0 Introduction**

Most animals are the product of successful fertilization. Yet, the success of fertilization does not occur by chance. Fertilization of an egg by multiple sperm, a condition known as polyspermy, is one of the most prevalent barriers to successful fertilization. To prevent entry of more than one sperm, eggs can employ processes that protect the nascent zygotes. Despite the importance of the process of fertilization, there are many aspects we do not yet understand. Exploring the complex signaling events of fertilization will not only lay the conceptual foundation for understanding the earliest moments of new life, but also can reveal novel contraceptive targets and areas for improvement in artificial reproductive technologies.

### **1.1 Physiology of fertilization**

#### **1.1.1 Post-mating preparation of sperm to fertilize**

Between the adult male and the site of fertilization, sperm must travel a long distance and through the harsh conditions of the external environment or the female reproductive tract to encounter an egg. Once at the site of fertilization, within the female reproductive tract of internal fertilizers or within the external environment for external fertilizers, sperm must find, penetrate, and activate the egg, in order to contribute its genetic material to the zygote.

### **1.1.1.1 Sperm activation**

#### **1.1.1.1.1 Mammalian sperm capacitation**

Mammalian sperm are distinguished from those of other animals in that they are unprepared to fertilize at mating, even if placed directly next to an egg (R Yanagimachi, 1988). As they spend time in the female reproductive tract, or are treated with incubations that simulate it, mammalian sperm gain the capacity to fertilize by undergoing processes collectively referred to as capacitation (Visconti et al., 1998). Capacitation comprises several discrete stages during which sperm change the way they swim, increase their intracellular pH, and release their acrosomal enzymes (Visconti et al., 1998). In the lab or clinic, sperm can be artificially capacitated using media that approximates signals from the female reproductive tract before *in vitro* fertilization (IVF) for artificial reproductive technologies (ART) or for fertilization research, (Visconti et al., 1998).

The first event of capacitation is called activation. Occurring at mating, this is when mammalian sperm start to vigorously beat their tail as they begin their marathon swim to meet the egg (R Yanagimachi, 1988). Activated sperm swim with a relatively straight path, enabling them to quickly traverse a long distance (Figure 1). After spending time in the female reproductive tract, however, sperm slow their swimming stroke and begin to beat their flagellum in a whip-like, asymmetric manner (R. Yanagimachi, 1970). This latter swimming pattern is called hyperactivation (Susan S. Suarez, 2008). Hyperactivation is necessary for mammalian fertilization with its purported role being to help sperm ratchet through the zona pellucida, a tough protective structure that surrounds the egg (Kay & Robertson, 1998; Stauss, Votta, & Suarez, 1995; Susan S. Suarez, 2008). Both a  $\text{Ca}^{2+}$ -permeable channel and high intracellular pH have central roles in

signaling hyperactivation (Babcock, Rufo, & Lardy, 1983; Ho, Granish, & Suarez, 2002; Lindemann & Goltz, 1988; Polina V. Lishko et al., 2012; S. S. Suarez, Vincenti, & Ceglia, 1987).

The voltage-gated,  $\text{Ca}^{2+}$ -conducting channel essential for hyperactivation is called Cation Channel of Sperm (CatSper) (Anne E. Carlson et al., 2003; P. V. Lishko et al., 2012; Qi et al., 2007). CatSper is activated during capacitation, allowing  $\text{Ca}^{2+}$  to enter the sperm, which then controls the way the tail beats (Anne E. Carlson et al., 2003).  $\text{Ca}^{2+}$  regulation of flagellar waveform was first demonstrated by experiments wherein detergent was applied to permeabilize the sperm membrane (Lindemann & Goltz, 1988). This condition equilibrates the intracellular and extracellular ion concentrations, allowing experimenters control of the  $\text{Ca}^{2+}$  concentration in the sperm flagellum. At low intracellular  $\text{Ca}^{2+}$ , symmetrical flagellar beats are observed, whereas at a high intracellular  $\text{Ca}^{2+}$ , the waveform becomes asymmetrical and approaches a whiplash-like form (Lindemann & Goltz, 1988). For mammalian sperm, an asymmetrical flagellar waveform is a defining feature of hyperactivation, and the  $\text{Ca}^{2+}$  that changes beat symmetry is conducted by the sperm specific CatSper channel (Anne E. Carlson et al., 2003).

Another important factor for sperm function is their intracellular pH. In the male, mature sperm maintain an acidic intracellular pH (N. L. Cross & Razy-Faulkner, 1997; Santi et al., 2013; Zeng, Oberdorf, & Florman, 1996). However, in the female reproductive tract, the sperm cytosolic pH becomes more basic, and this is thought to potentiate CatSper channels, and therefore alter their flagellar waveform as they progress through the reproductive tract, as well as to undergo the acrosome reaction (Polina V. Lishko et al., 2012).

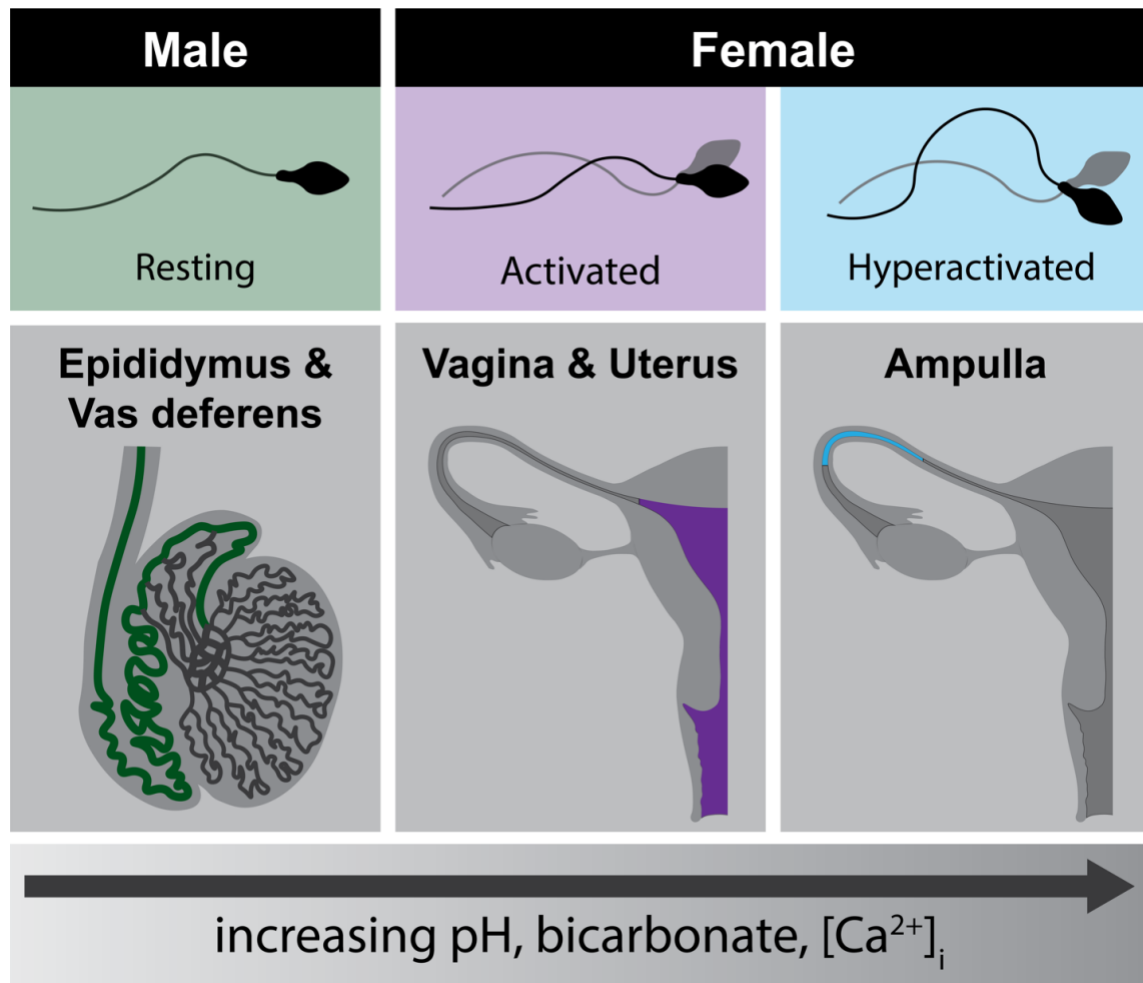


**Figure 1 Capacitation of mammalian sperm**

Following deposition in the female reproductive tract, sperm become activated and demonstrate forward motility. With increasing pH, bicarbonate, and intracellular calcium, the sperm continue to change their swimming behavior. As they pass through to the oviduct, they hyperactivate within the ampulla as they approach the egg. Hyperactivated sperm have a whiplash-like motility, which is theorized to help the sperm penetrate the egg.

#### **1.1.1.1.2 Frog sperm activation**

Sperm from external fertilizers do not spend time in the female reproductive tract. Instead, sperm from vertebrate animals that mate in aquatic environments are activated as they enter the dilute aqueous environment (Reinhart, Ridgway, & Chandler, 1998; Tholl et al., 2011). For example, in *Xenopus laevis*, osmotic shock activates sperm, which sperm experience when they are released into pond water with a lower salt content compared to osmolarities within the male or to that of standard laboratory media (Inoda & Morisawa, 1987; Reinhart et al., 1998). Once *X. laevis* sperm reach the egg, the acrosome reaction is activated by a substance derived from the female oviductal pars recta which accumulates in the jelly as the eggs pass through the oviduct during ovulation (Ueda, Yoshizaki, & Iwao, 2002).

#### **1.1.2 Egg activation**

The transition from a fertilization-competent egg into a developing embryo requires a series of highly conserved events, collectively known as egg activation. Newly fertilized eggs from animals and some plants (Denninger et al., 2014; K. Swann & Lai, 2016), display a large elevation of intracellular  $\text{Ca}^{2+}$  which activates embryonic development. This elevation can be a singular wave, or multiple oscillations (Figure 2). The channels and signaling events that give rise to these  $\text{Ca}^{2+}$  elevations vary between animals (Figure 2), and these differences are likely influenced by the varying environments for embryonic development, within the female reproductive tract or aquatic environments.

Increased intracellular  $\text{Ca}^{2+}$  activates embryonic development in the externally fertilizing frog *X. laevis*. In contrast to the oscillations in mammalian eggs, eggs from *X. laevis* have a single, prolonged elevation of intracellular  $\text{Ca}^{2+}$ . Notably, eggs from *X. laevis* are exceptionally large,

with diameters of 1.4  $\mu\text{m}$  (K. L. Wozniak et al., 2017). Thus, a wave of elevated intracellular  $\text{Ca}^{2+}$  must travel a substantial distance. For *X. laevis* eggs, intracellular  $\text{Ca}^{2+}$  remains low until fertilization, when a PLC and  $\text{IP}_3$  mediated signaling pathway activates  $\text{Ca}^{2+}$  release from the ER (Busa, Ferguson, Joseph, Williamson, & Nuccitelli, 1985; Busa & Nuccitelli, 1985). A single  $\text{Ca}^{2+}$  wave then propagates from the sperm entry site across the entire egg, persisting for several minutes (Busa & Nuccitelli, 1985; Sato, Tokmakov, Iwasaki, & Fukami, 2000). It is not yet understood how PLC is activated at fertilization. Uncovering how fertilization activates PLC in *X. laevis* eggs will reveal important insights into the first moments which lead to new life.

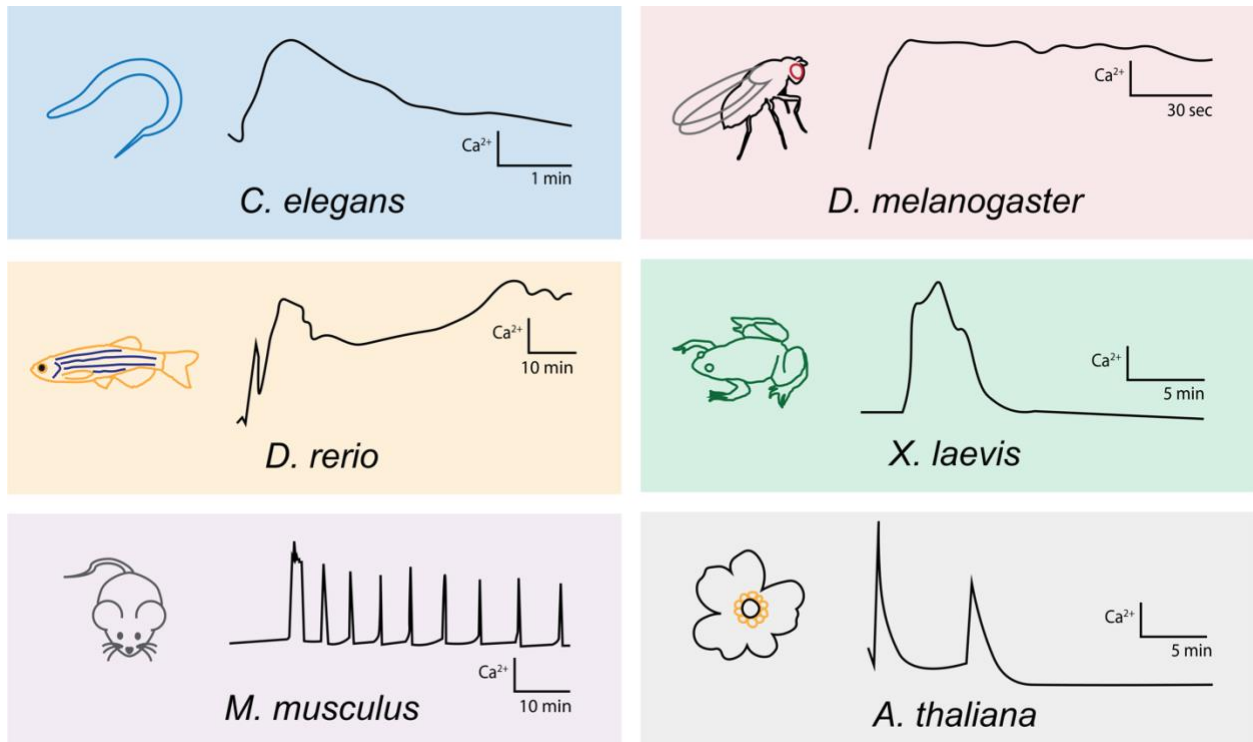


**Figure 2 Different  $\text{Ca}^{2+}$  events in the activation of diverse eggs**

Example intracellular  $\text{Ca}^{2+}$  events in eggs from various animals (Stein, Savy, Williams, & Williams, 2020) and a plant (Denninger et al., 2014), observed over time by changes in fluorescence of  $\text{Ca}^{2+}$  indicators. Relative changes of intracellular  $\text{Ca}^{2+}$  is represented on the y-axis, and time on the x-axis.

### **1.1.2.1 Polyspermy block**

In most sexually reproducing animals, only eggs fertilized by one sperm can successfully initiate embryonic development (Evans, 2020; S. Mizushima & Sasanami, 2017; Wilson, 1925). Should this golden ratio of one egg fertilized by one sperm be violated, each fertilizing sperm would bring its own chromosomes, leading to polysomy, excess centrioles, and result in asymmetric cleavages during embryonic development (Hinkley Jr & Wright, 1986; S. Mizushima & Sasanami, 2017). Eggs have evolved methods to protect themselves from multiple fertilizations, termed polyspermy blocks (S. Mizushima & Sasanami, 2017; Runft, Jaffe, & Mehlmann, 2002).

One hundred years ago, Ernest Just reported his observations of polyspermy blocking mechanisms (Just, 1919). Observing fertilization in starfish using light microscopy, Just observed the creation of the physical barrier surrounding the egg after fertilization. He deduced, however, that this physical barrier likely developed too slowly to prevent the entrance of multiple sperm in this external fertilizing animal. He predicted that a faster block must occur, and in a remarkably accurate abstraction from his observations, suggested that a “wave of negativity” overtook the starfish egg following fertilization (although directionally wrong, he correctly predicted that the fast block was electrochemical in nature) (Just, 1919).

### **1.1.2.2 Slow block to polyspermy**

Nearly all sexually reproducing animals use the slow block to polyspermy, which occurs minutes after fertilization and involves the exocytosis of cortical granules from the egg and establishment of a physical barrier around the nascent zygote (Figure 3) (Metz, 2012; J. L. Wong & Wessel, 2006). These Golgi-derived cortical granules are docked at the plasma membrane (Austin, 1956; Gulyas, 1980). Following increased cytoplasmic  $\text{Ca}^{2+}$ , the cortical granules release their contents (McPherson, McPherson, Mathews, Campbell, & Longo, 1992). Although we have

known about the slow block for more than 100 years, the molecular mechanisms that enable the contents of the cortical granules to stop sperm entry in the fertilized egg is still debated.

Most eggs are surrounded by a glycoprotein matrix, conserved in structure amongst diverse animals (Swanson & Vacquier, 2002). This extracellular matrix is referred to by various names such as the vitelline envelope in frogs, chorion in fish, and the zona pellucida in mammals. The contents of the cortical granules harden this glycoprotein matrix to make it less penetrable to sperm following fertilization (Bleil & Wassarman, 1980; Wolf, Nishihara, West, Wyrick, & Hedrick, 1976; Yurewicz, Oliphant, & Hedrick, 1975). These contents include several metalloproteases (Bleil, Beall, & Wassarman, 1981; Burkart, Xiong, Baibakov, Jiménez-Movilla, & Dean, 2012; Tian, Gong, & Lennarz, 1999) and lectins (Chamow & Hedrick, 1986; Dong, Yang, Yang, Zhang, & Gui, 2004) which contribute to the hardening of envelope proteins.

Recently it was observed that zinc is released during exocytosis of cortical granules from the eggs of several mammals (Duncan et al., 2016; Kim et al., 2011; Emily L. Que et al., 2018). We have now demonstrated that eggs from non-mammalian vertebrates including frogs, salamanders, and fish also release zinc at fertilization (Katherine L. Wozniak et al., 2020). Eggs from invertebrates such as the fruit fly *Drosophila* (Hu et al., 2020), or the round worm *Caenorhabditis elegans* (Mendoza et al., 2022) also release zinc during activation. Because zinc is released during the slow block to polyspermy, I asked whether this extracellular zinc may stop sperm from entering fertilized eggs.

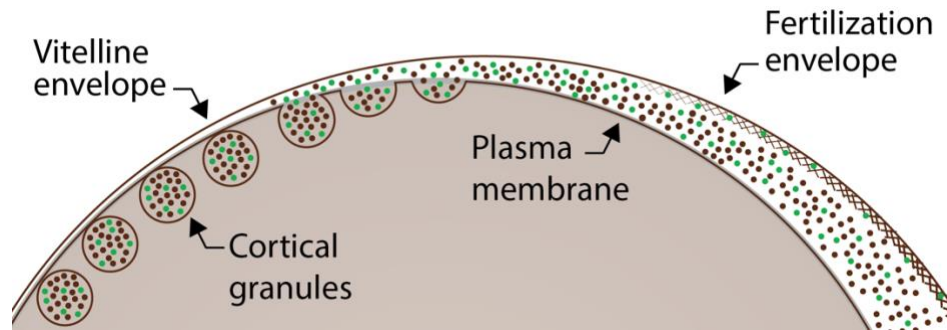


**Figure 3 The slow block to polyspermy is conserved in sexually reproducing organisms**

Depiction of the slow block to polyspermy in a *Xenopus laevis* egg. Cortical granules docked at the plasma membrane release their contents at fertilization, leading to the lifting and hardening of the vitelline envelope (termed the zona pellucida in mammals). This process and the envelope, an extracellular glycoprotein matrix, is highly conserved. Sperm cannot penetrate this hardened fertilization envelope.

### 1.1.2.3 Fast block to polyspermy

The fast block is an electrical block observed only in eggs from external fertilizers, possibly because the higher sperm to egg ratio at the site of fertilization necessitates a more immediate protection from polyspermic fertilization. Immediately following fertilization, the egg plasma membrane is depolarized (Figure 4). This membrane potential change allows sperm to bind to, but not penetrate the egg (L. A. Jaffe, 1976).

In the 1950s and earlier, several research groups working independently observed fertilization-signaled depolarizations in eggs from diverse external fertilizers, including frogs and sea urchins (Hiramoto, 1959; Hori, 1958; Maeno, Morita, & Kuwabara, 1956; Peterfi & Rothschild, 1935; Scheer, Monroy, Santangelo, & Riccobono, 1954; Tyler, Monroy, Kao, & Grundfest, 1956). Following development of the voltage clamp, scientists demonstrated that this fertilization signaled depolarization was a polyspermy block (L. A. Jaffe, 1976). Specifically, it was observed that clamping sea urchin eggs at positive potentials typically reached at fertilization stopped sperm entry until the clamp was released and the membrane repolarized to the resting potential. Once the membrane potential returned to rest, these eggs were immediately fertilized, and the membrane potential quickly depolarized. In contrast, eggs clamped at the resting potential were fertilized by multiple sperm, while unclamped eggs fertilized at the same time were monospermic. These data demonstrate that the membrane depolarization that occurs at fertilization serves as a fast block to polyspermy.

Since its original discovery, the fast block has been observed in eggs from diverse externally fertilizing animals such as starfish (Miyazaki & Hirai, 1979), sea urchin (Whitaker & Steinhardt, 1983), frogs (Charbonneau, Moreau, Picheral, Vilain, & Guerrier, 1983; Nicholas L. Cross & Elinson, 1980), including *Xenopus laevis* (Iwao, 1985), sea squirt (Goudeau, Depresle,

Rosa, & Goudeau, 1994), ribbon worm (Kline, Jaffe, & Tucker, 1985) and algae (Brawley, 1991). Notably, mammalian eggs do not depolarize upon fertilization and clamping these eggs at depolarized potentials does not prevent sperm entry (Katherine L. Wozniak & Carlson, 2020).

The fast block has been studied in several species of frogs including the American toad *Bufo americanus*, the northern leopard frog *Rana pipiens* (Nicholas L. Cross & Elinson, 1980), and the African clawed frog *Xenopus laevis* (Iwao, 1985). These were chosen for their relative abundance of gametes and amenability of these gametes to electrophysiology recordings. Indeed, most frog eggs use the fast block, and their fertilizations are monospermic. Here we will focus on the fast block in *X. laevis*, the species for which most complete signaling pathway has been established.

The fast block to polyspermy in *X. laevis* can be described in three phases (Figure 4A). First a brief step current is recorded, followed by a steep shift in membrane potential from approximately -20 mV to +5 mV. Finally, the membrane potential slowly repolarizes (Katherine L. Wozniak & Carlson, 2020).

The step current observed in the initial phase of the fast block is hypothesized to occur at the early moments of sperm-egg binding and is observed as a small current. This current could reflect a change in membrane capacitance resulting from sperm-egg fusion.

The second stage of the fast block involves the fertilization-activated depolarization, which is caused by an efflux of  $\text{Cl}^-$  from the egg. Because frogs fertilize in pond water, which is more dilute than the intracellular milieu, opening  $\text{Cl}^-$  channels allows the anion to leave the egg and collapse the membrane potential. Insemination of *X. laevis* eggs in the presence of varying concentrations of external  $\text{Cl}^-$  gave rise to differing kinetics and direction of membrane potential changes. Sufficiently high levels of extracellular  $\text{Cl}^-$  abrogates the fast block, establishing that a

Cl<sup>-</sup> efflux mediates the fast block in frog eggs (Grey, Bastiani, Webb, & Schertel, 1982; Webb & Nuccitelli, 1985).

In addition to a Cl<sup>-</sup> current, an increase of intracellular Ca<sup>2+</sup> is also needed for the fast block. The role for Ca<sup>2+</sup> in the fast block was supported by the observations that *X. laevis* eggs injected with the Ca<sup>2+</sup> chelator BAPTA did not depolarize upon fertilization. Considered alongside the fertilization-evoked efflux of Cl<sup>-</sup>, these observations gave rise to the hypothesis that a Ca<sup>2+</sup>-activated Cl<sup>-</sup> channel mediates the depolarization in *X. laevis* eggs.

Recently, the depolarizing channel has been identified as TMEM16A (or anoctamin-1, encoded by the ANO1 gene). TMEM16A is a Ca<sup>2+</sup> activated Cl<sup>-</sup> channel abundantly expressed in *X. laevis* eggs (Katherine L. Wozniak, Wesley A. Phelps, Maiwase Tembo, Miler T. Lee, & Anne E. Carlson, 2018). Fertilization activates this channel by inducing the release of Ca<sup>2+</sup> from the endoplasmic reticulum (ER) (Figure 4B). Fertilization no longer depolarized *X. laevis* eggs treated with inhibitors of the enzyme phospholipase C (PLC) or the inositol triphosphate receptor (IP<sub>3</sub>R), revealing that fertilization signals the fast block in a pathway that requires PLC and an IP<sub>3</sub>-evoked Ca<sup>2+</sup> release from the ER (Katherine L. Wozniak, Maiwase Tembo, Wesley A. Phelps, Miler T. Lee, & Anne E. Carlson, 2018). At the time of this writing, the identity of the responsible PLC, and how it is activated by fertilization is unknown.

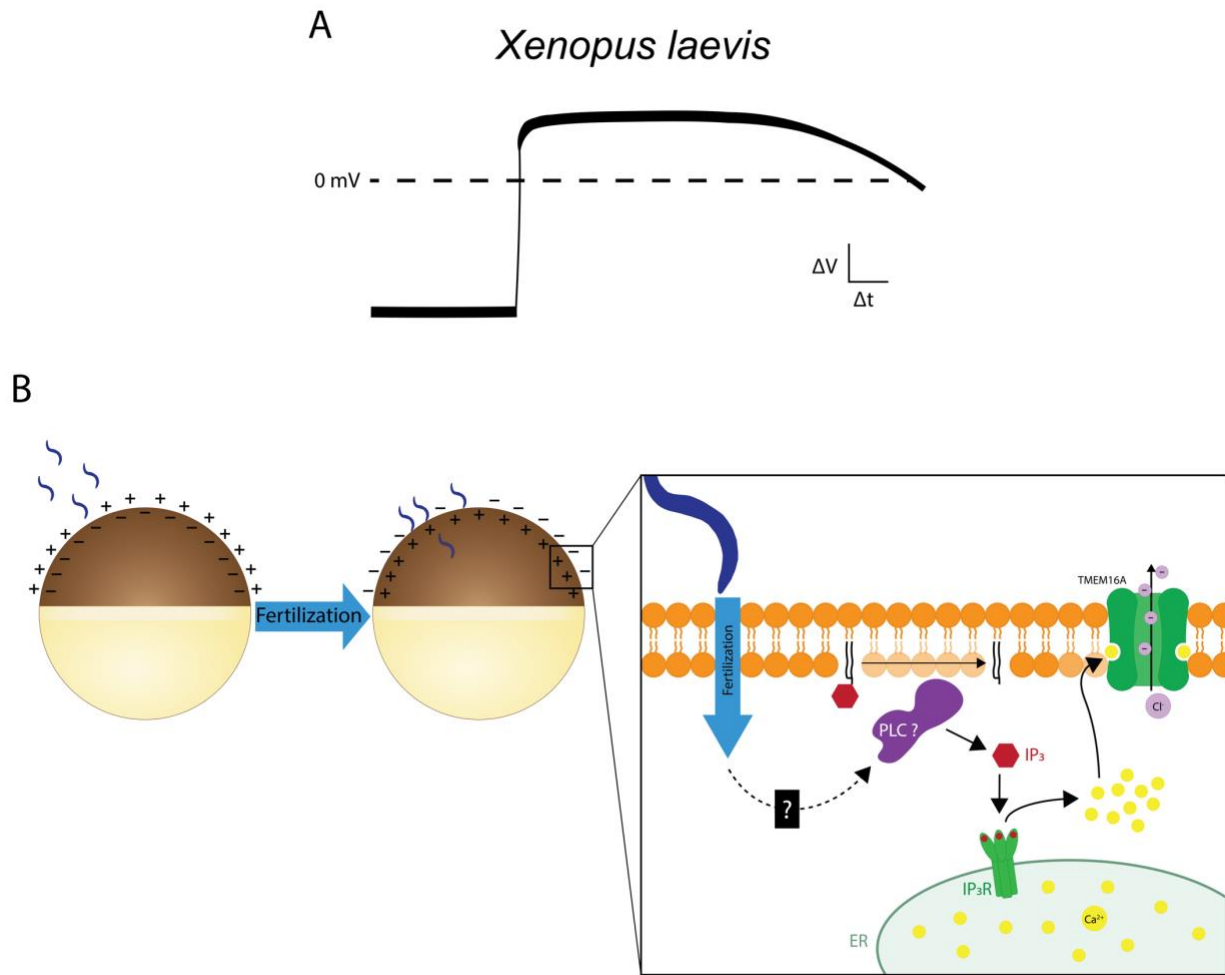


**Figure 4 The fast block to polyspermy in frogs**

Schematics of typical electrophysiology recordings made from *Xenopus laevis* during fertilization. In the *Xenopus laevis* egg (B), sperm can bind to, but not enter an egg which has depolarized. Within the egg (inset schematic), fertilization activates a PLC, freeing  $IP_3$  from the plasma membrane. This  $IP_3$  then binds its cognate receptor ( $IP_3R$ ) on the ER to increasing intracellular  $Ca^{2+}$  which activates TMEM16A channels. The efflux of  $Cl^-$  depolarizes the egg.

## **1.2 Zinc plays a commanding role in the regulation of fertilization**

Zinc is an essential mineral. Several conserved processes important for gametogenesis, egg activation, and embryonic development such as cell cycle regulation, and RNA and protein synthesis depend on proper regulation of zinc availability ("Zinc Fact Sheet," 2022). The average total zinc in the human circulatory system is 12-14  $\mu\text{M}$  (Hennigar, Lieberman, Fulgoni, & McClung, 2018; Saaranen, Suistomaa, Kantola, Saarikoski, & Vanha-Perttula, 1987). Dysregulation or deficiency leads to a number of health problems, including male and female infertility.

### **1.2.1 Mammalian sperm encounter elevated extracellular zinc at multiple points between mating and fertilization**

Between mating and fertilization, mammalian sperm encounter high concentrations of zinc at two discrete stages: when mixed with the seminal fluids at mating (Milostić-Srb et al., 2020; Riffo, Leiva, & Astudillo, 1992; Sørensen et al., 1999; Stanković & Mikac-Dević, 1976), and when encountering an already fertilized egg (Duncan et al., 2016; Kim et al., 2011; Emily L. Que et al., 2018). Seminal fluid has the highest relative zinc content in the body, with measurement of total zinc in human semen ranging from 1-3 mM (Milostić-Srb et al., 2020; Riffo et al., 1992; Sørensen et al., 1999; Stanković & Mikac-Dević, 1976). By contrast, the average concentration of total zinc in the human circulatory system is 12-14  $\mu\text{M}$  (Hennigar et al., 2018; Saaranen et al., 1987). Though much of the zinc in seminal fluid is likely bound, sperm still likely come in to contact with a significant level of labile zinc. Understanding the interaction of zinc and sperm may resolve the generally conflicting reports of the effects of zinc level on male fertility. It is also worth noting

that serum or plasma zinc levels used clinically to assess overall zinc levels can vary greatly by collection method, time, and health and lifestyle factors such as hormone level and muscle catabolism ("Zinc Fact Sheet," 2022) and may contribute to the difficulty correlating zinc status and sperm health. Direct manipulation in the lab will therefore provide a more controlled picture of the interaction between free zinc and sperm function.

### **1.2.2 Zinc release at activation**

Recently, zinc release has been observed from mammalian eggs during cortical granule exocytosis in mouse (Kim et al., 2011), cow (Suzuki, Ju, & Yang, 2000), and human (Duncan et al., 2016) eggs. It has been hypothesized that this metal may contribute to the mechanisms by which the slow polyspermy block stops additional sperm from entering already fertilized eggs (E. L. Que, Duncan, Bayer, Philips, & Roth, 2017). For example, data suggest that zinc contributes to hardening of the zona pellucida, the highly conserved extracellular glycoprotein matrix that surrounds egg cells, leading to the hypothesis that this modification is sufficient to block sperm binding to the egg (E. L. Que et al., 2017). However, previous studies have not yet directly tested whether the zinc released at fertilization can prevent sperm entry into the egg, a feature required of a true polyspermy blocking mechanism.

## 1.3 Model organisms

During my dissertation research, I leveraged the strengths of diverse animals to characterize the polyspermy blocks that ensure successful monospermic fertilizations in species millions of years diverged from one another.

### 1.3.1 Egg and oocyte models

Most research on the role of zinc released by eggs following fertilization has focused on mammalian eggs. However, similarities between mammalian and non-mammalian gametes may suggest conserved mechanisms of zinc action, while differences may give hints to specialized mechanisms. Further, eggs and oocytes from external fertilizers such as frogs and sea urchins are readily accessible, substantially larger than their mammalian counterparts, and can be easily used in the lab to perform *in vitro* fertilization under biologically relevant conditions (Lee-Liu, Méndez-Olivos, Muñoz, & Larraín, 2017; McClay, 2011). Finally, eggs from external fertilizers utilize the fast block to polyspermy, which is observed within seconds of fertilization. This provides a fantastic model for studying early moments of fertilization and embryonic development.

#### 1.3.1.1 The African clawed frog *Xenopus laevis*

The African clawed frog *Xenopus laevis* is one of the most well-established models for the study of fertilization and utilizes both the fast and slow blocks to polyspermy (J. L. Wong & Wessel, 2006). Established protocols, a deep foundation of existing knowledge, and easy access to gametes are several of the advantages of this system (S. L. Green, 2009). Induction of ovulation is so reliable in this species that they were used as a method to detect human chorionic

gonadotropin (hCG) in pregnant people prior to popularity of the at-home pregnancy test (S. L. Green, 2009). External fertilization of *X. laevis* eggs make them ideal for *in vitro* fertilization experiments. Despite being tetraploid, *X. laevis* has a fully sequenced genome (Benson et al., 2017; Session et al., 2016).

#### **1.3.1.2 The purple sea urchin *Strongylocentrotus purpuratus***

The purple sea urchin, *Strongylocentrotus purpuratus* is an echinoderm native to the west coast of the US (McClay, 2011). Sea urchins are a traditional model organism in developmental biology, and utilize both the fast and slow blocks to polyspermy (Santella, Vasilev, & Chun, 2012). During the gravid season (mid November – March for *S. purpuratus*), large amounts of gametes can be obtained with shaking or injection of KCl, with individuals spawning its entire store of gametes (Foltz, Adams, & Runft, 2004). This provides thousands of gametes for use in *in vitro* fertilization experiments. Techniques for *in vitro* fertilization are so well established and technically straightforward that they are often used in teaching settings in developmental biology labs.

#### **1.3.1.3 The cnidarian *Hydractinia symbiolongicarpus***

The clonal cnidarian *Hydractinia symbiolongicarpus* grows on the shells of hermit crabs in the wild, and on glass slides in the lab (Frank, Nicotra, & Schnitzler, 2020). The polyps of the colony spawn in response to light cues, which allows for experimenter control (Frank et al., 2020). The gametes are mixed in a petri dish for *in vitro* fertilization, and have become a popular tool for studying embryonic development, allrecognition (Karadge, Gosto, & Nicotra, 2015), and regeneration (Frank et al., 2020). This provides a useful system to study fertilization in an ancient species.

### **1.3.2 Sperm models**

I used both mouse, *Mus musculus*, and human sperm samples to start characterizing how zinc targets mammalian sperm. Mammalian sperm undergo dramatic changes in preparation to fertilize the egg (R Yanagimachi, 1988) (Figure 1). They are a useful model to understand how zinc can interfere with capacity to fertilize.

#### **1.3.2.1 The house mouse *Mus musculus***

*M. musculus* is a classic system for developmental biology, due to their small size, ability to be genetically modified, and fast generation time. We utilize commercially available Swiss Webster retired breeders as males who have proven fertility. These provide easily obtained samples from a homogenous population. Mature sperm are obtained from the epididymis of mice, and never encounter seminal fluid. This may present both strengths and weaknesses as a model for fertilizing sperm.

#### **1.3.2.2 Human surplus sperm samples**

I used human semen for various studies. These samples were surplus from fertility testing by consenting donors. These samples would have otherwise been discarded. No patient information is provided to us including all information protected under the HIPAA. Therefore, we had no information regarding patient fertility, health status, age, or other factors which can impact sperm quality. However, these samples provide powerful models for understanding how human sperm may be affected by extracellular zinc.

## **1.4 Clinical importance and significance**

### **1.4.1 Infertility worldwide**

With more than 48.5 million couples struggling with infertility worldwide (CDC), it is important to continue to develop assisted reproductive technologies (ARTs) such as *in vitro* fertilization (IVF). Better understanding of the role of zinc in fertilization has already improved fertility treatments. For example, the amount of zinc released during IVF can predict embryo quality before implantation (Duncan et al., 2016; Kong et al., 2015).

#### **1.4.1.1 Artificial reproductive technologies**

The average current success rate of IVF is less than 35% (CDC). Major improvements in ART are likely hampered due to a lack of understanding of early development (Combelles & Racowsky, 2005), such as the factors important for proper protection from polyspermy. It was estimated that 7% of embryos fertilized in IVF would become polyspermic (Feng & Gordon, 1996). Extrapolating from the 284,385 ART cycles performed in 2016 (CDC), then nearly 20,000 embryos would become polyspermic. This is based on the major underestimation that only one egg is fertilized in each cycle. When multiple sperm fertilize an egg, these embryos are not viable and therefore are not transferred into the uterus following IVF (Hummel & Kettel, 1997). With a more complete understanding of the slow polyspermy block, we can optimize the conditions and procedures used for IVF to decrease the incidence of polyspermy, and thereby reduce the number of eggs wasted. Zinc has been proposed as a supplement for IVF conditions to prevent DNA damage in frozen sperm samples (Kotdawala & Kumar, 2012) and to predict egg quality (Duncan

et al., 2016). However, I propose that we must first seek to understand the effects of zinc at the first moments of fertilization in order to design the most effective protocols for IVF.

#### **1.4.2 Significance of understanding egg signaling**

Phospholipase C (PLC) isozymes vital for signaling the fertilization evoked depolarization in *X. laevis* are highly conserved. Data in this dissertation will demonstrate that PLCs in the *X. laevis* egg do not activate during fertilization via a canonical activation pathway. This allows us an opportunity to study noncanonical activation of PLC in a fully endogenous system.

#### **1.4.3 Environmental concerns due to zinc pollution**

Zinc pollution provides little risk for human health (Bodar, Pronk, & Sijm, 2005). In fact, there are a number of uses for zinc in controlling and maintaining healthy aquatic environments which would result in an increase in environmental zinc levels. Zinc has been proposed as an algacide (P. T. S. Wong & Chau, 1990), as well as a supplement to improve the fertility of endangered fish species (Kazemi, Sourinejad, Ghaedi, Johari, & Ghasemi, 2020) (Kocabaş & Kutluyer, 2017). However, with these contradictory uses, we must understand how zinc affects gametes and early embryos, so that we can carefully plan to protect the entire ecosystem we'd be affecting.

## **2.0 Tyrosine phosphorylation of PLC- $\gamma$ is not necessary for activation of the fast block to polyspermy**

### **2.1 Introduction**

The ratio of one sperm to one egg is important for maintaining proper ploidy and for successful initiation of the delicate cascade of developmental processes that will take the nascent zygote to a new life. The egg is largely responsible for maintaining this ratio, using processes known as polyspermy blocks to prevent subsequent fertilization by multiple sperm. The slow block to polyspermy is ubiquitous in animals (discussed in Chapter 3). In external fertilizers, there is an additional polyspermy block, the fast block which activates within seconds following fertilization. The fast block is an electrical depolarization at the egg plasma membrane, which allows sperm to bind to, but not penetrate the egg (L. A. Jaffe, 1976). It is not yet understood how the fast block is initiated in any species, nor has the signaling pathway been completely mapped in any species.

We best understand the molecular mechanisms of the fast block in the African clawed frog, *Xenopus laevis* (Figure 4B). In all frogs, a  $\text{Ca}^{2+}$ -activated  $\text{Cl}^-$  current depolarizes the egg shortly after fertilization (Nicholas L. Cross & Elinson, 1980; David Glahn & Nuccitelli, 2003; Grey et al., 1982; Kline, 1988; Runft et al., 2002; Webb & Nuccitelli, 1985). Previous work from our lab identified that the  $\text{Ca}^{2+}$ -activated  $\text{Cl}^-$  channel TMEM16A mediates this depolarization (Katherine L. Wozniak, Wesley A. Phelps, et al., 2018). The  $\text{Ca}^{2+}$  which activates TMEM16A is released via a phospholipase C (PLC)-dependent increase in  $\text{IP}_3$  (Katherine L. Wozniak, Maiwase Tembo, et al., 2018). We do not know how fertilization turns on PLC activity to signal the fast block. I sought to identify the pathway by which fertilization activates PLC. Different PLC isozymes are activated

by different signaling pathways. By querying published proteomics datasets acquired from the fertilization competent eggs, and RNA-sequencing datasets from developing oocytes and egg, we have found three PLC isozymes in *X. laevis* eggs present at different concentrations: PLC- $\gamma$ 1 (85.21 nM), PLC- $\beta$ 1 (3.91 nM), and PLC- $\beta$ 3 (4.30 nM) (Session et al., 2016; Wühr et al., 2014).

We can distinguish the activity of different PLC isozymes by targeting their specific method of activation (Figure 5). PLC- $\gamma$  is typically activated by phosphorylation of a tyrosine residue in the active site (Nishibe et al., 1990). Therefore, we can use tyrosine kinase inhibitors to stop these pathways from activating PLC- $\gamma$  and determine whether this interferes with the fast block to polyspermy. We utilized the general tyrosine kinase inhibitors genistein (Akiyama et al., 1987; Akiyama & Ogawara, 1991) and lavendustin A and B (Hsu et al., 1991; Onoda et al., 1989). These inhibitors have been used in *X. laevis* eggs to examine the role of PLC- $\gamma$  in  $\text{Ca}^{2+}$  release following egg activation. It has been observed that injection of these inhibitors into *X. laevis* eggs led to a decrease in sperm induced egg activation, assessed by cortical contraction (Sato et al., 1998). In another study, it was observed that injection of lavendustin A into *X. laevis* eggs led to a decrease in the incidence of cortical contraction, fertilization envelope lifting, and  $\text{Ca}^{2+}$  wave generation, all events associated with egg activation (D. Glahn, Mark, Behr, & Nuccitelli, 1999). The authors of these two studies concluded that tyrosine phosphorylation of PLC- $\gamma$  is essential for *X. laevis* egg activation. However, this conclusion is controversial. For example, another group inhibited PLC- $\gamma$  activation via tyrosine phosphorylation by injecting Src-homology 2 (SH2) domain into the eggs, which has been shown to outcompete PLC- $\gamma$ 1 as substrate for tyrosine phosphorylation. This domain was able to outcompete the native PLC- $\gamma$  for activation via exogenously expressed receptor tyrosine kinase for the platelet derived growth factor. It was observed that the  $\text{Ca}^{2+}$  release at fertilization was not altered (Runft, Watras, & Jaffe, 1999). Our

study will examine whether tyrosine phosphorylation of PLC-  $\gamma$  is needed for the fast block to polyspermy in *X. laevis* eggs.

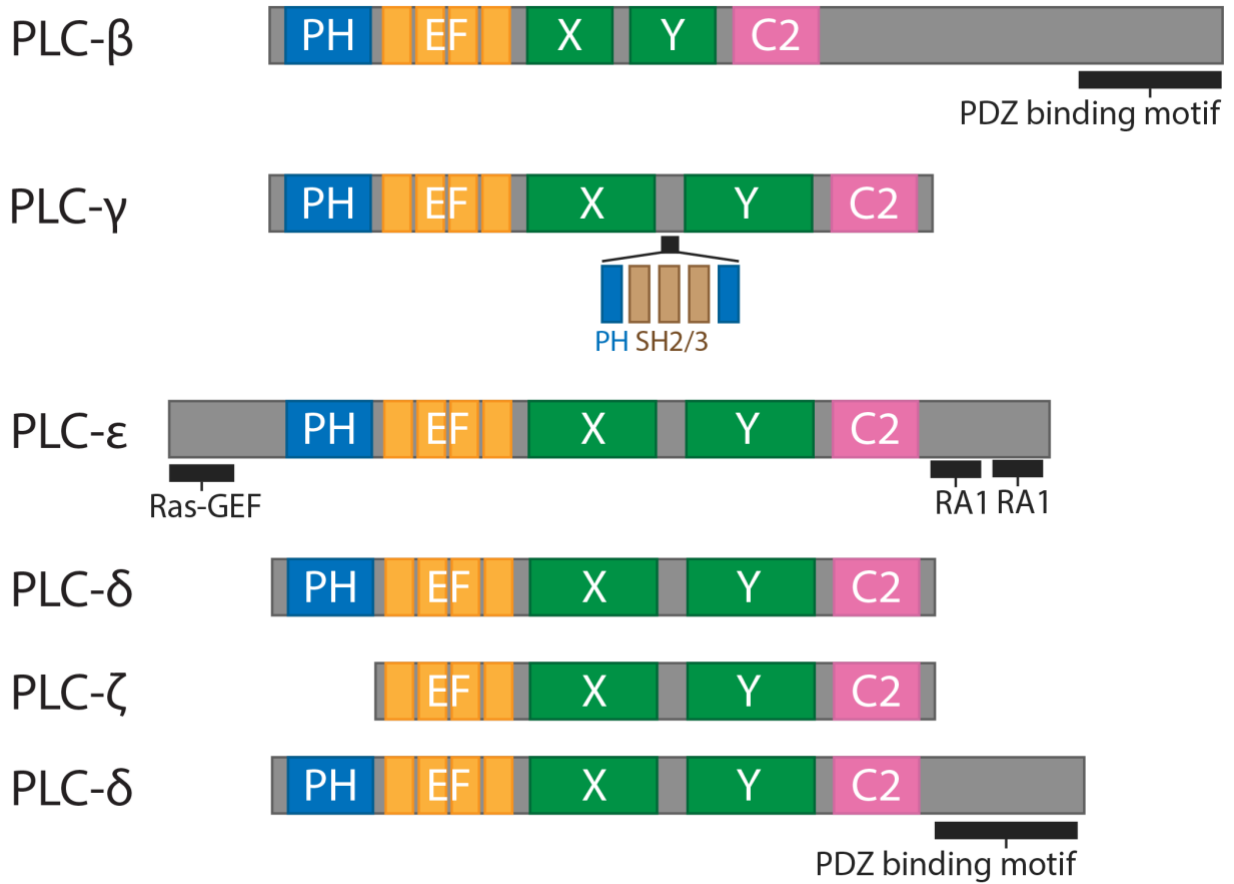


**Figure 5 PLC isozymes are differentiated by their activation, tied to their structure**

Different PLC isozymes are differentiated by their mechanism of activation. This is tied to their structure. Though many of the subunits are the same, such as the catalytic X-Y linker, the membrane-associating PH domain, and the  $\text{Ca}^{2+}$ -sensitive EF hand, others such as the SH2/3 domains of PLC- $\gamma$  are tied to their activation (Bill & Vines, 2020; Kadamur & Ross, 2013).

To do so, we made whole cell recordings of *X. laevis* eggs inseminated in the presence of these general tyrosine kinase inhibitors which suggest that tyrosine phosphorylation of PLC- $\gamma$  is not required to activate the fast block. We observed no change in kinetics of the fast block depolarization in the presence of these inhibitors, or on the incidence of polyspermy. We also did not observe any effects on the incidence of fertilization in the presence of these inhibitors. This suggests that tyrosine phosphorylation of PLC- $\gamma$ 1 is not essential for the fast block or for egg activation. It is possible that the pathways shown to be necessary for egg activation and those necessary for initiation of the fast block have novel features.

## **2.2 Materials and methods**

### **2.2.1 Reagents**

Genistein was obtained from Alfa Aesar (Thermo Fisher Scientific; Tewksbury, MA) and Lavendustin A/B obtained from Santa Cruz Biotechnology (Dallas, TX). Leibovitz's-15 (L-15) medium (without L-glutamine) was purchased from Sigma-Aldrich. All other materials, unless noted, were purchased from Thermo Fisher Scientific.

### **2.2.2 Solutions**

Modified Ringer's (MR) solution was used as the base for all fertilization and recording assays in this study (100 mM NaCl, 1.8 mM KCl, 2.0 mM CaCl<sub>2</sub>, 1.0 mM MgCl<sub>2</sub>, 5.0 mM HEPES, pH 7.8). The MR solution was filtered using a sterile, 0.2- $\mu$ m polystyrene filter (Heasman et al.,

1991). Development assays were performed in 33% MR solution (MR/3) with or without inhibitors. Fertilization recordings were performed in 20% MR (MR/5) with or without inhibitors. Following fertilization recordings, eggs were incubated in MR/3 without inhibitors for 2 hours.

MR solutions containing inhibitors were prepared from concentrated stock solutions, kept in DMSO. Final DMSO content was maintained below 2% of total volume of solution.

### **2.2.3 Animals**

All animal procedures were conducted using acceptable standards of human animal care and approved by the Animal Care and Use Committee at the University of Pittsburgh. *X. laevis* adults were obtained commercially (Research Resource Identifier NXR\_0.0031; NASCO) and housed at 20°C with a 12-h/12-h light/dark cycle.

### **2.2.4 Collection of gametes**

To obtain mature, fertilization-competent eggs, sexually mature *X. laevis* females were induced to ovulate via injection of 1,000 IU human chorionic gonadotropin into the dorsal lymph sac and overnight incubation at 14-16°C for 12-16 hours (K. L. Wozniak et al., 2017). Females typically began to lay eggs within 2 hours after being moved to room temperature. Eggs were collected on dry Petri dishes and used within 10 minutes of laying.

To obtain sperm, testes were harvested from sexually mature *X. laevis* males (K. L. Wozniak et al., 2017). Males were first euthanized by a 30-minute immersion in 3.6 g/L tricaine-S, pH 7.4, testes were then harvested and cleaned. Testes were then stored at 4°C in MR for use on the day of the dissection, or in L-15 medium for use up to 1 week later.

### **2.2.5 Sperm preparation and *in vitro* fertilization**

For *in vitro* fertilizations during whole cell recordings, sperm suspensions were made by macerating 1/10 of the *X. laevis* testis in MR/5. This solution was kept at 4°C for up to 1 hour for use. Up to three sperm additions were added to each egg during whole cell recording, with 10 minutes between additions. To monitor for embryonic development after recording, inseminated eggs were transferred to MR/3 and incubated at room temperature for 2 hours. Development was assessed based on the appearance of cleavage furrows (K. L. Wozniak et al., 2017).

To assess the incidence of polyspermy with or without inhibitors, cleavage furrows were observed 90-120 minutes following sperm addition (Grey et al., 1982). Approximately 11-70 eggs were inseminated in MR/3 with or without inhibitors and incubated for 10 minutes at room temperature. To inseminate, sperm suspension was added to eggs in each experimental condition, pipetting the suspension directly on top of the eggs. Symmetrical cleavage furrows were scored as successful monospermic fertilization, while polyspermic fertilization was defined by asymmetric patterns of cleavage furrows (Elinson, 1975; Grey et al., 1982).

### **2.2.6 Electrophysiology**

Electrophysiological recordings were made using TEV-200A voltage clamps (Dagan Co.) and digitized by Axon Digidata 1550A (Molecular Devices). Data were acquired with pClamp Software (Molecular Devices) at a rate of 5kHz.

Pipettes used to impale the *X. laevis* eggs for recordings were pulled from borosilicate glass for a resistance of 5-15 M $\Omega$  and filled with 1 M KCl. Resting and fertilization potentials were quantified ~10s before and after the depolarization, respectively. Depolarization rates of each

recording were quantified by determining the maximum velocity of the quickest 1-mV shift in the membrane potential.

### **2.2.7 Exogenous protein expression in *X. laevis* oocytes**

The cDNAs encoding the platelet derived growth factor receptor (PDGF-R) (Gagoski et al., 2016) were purchased from Addgene (plasmid 67130) and were engineered into the GEMHE vector using overlapping extension PCR. The sequences for all constructs were verified by automated sequencing (Gene Wiz or Plasmidsaurus). The cRNAs were transcribed using the T7 mMessage mMachine (Ambion). Defolliculated oocytes were injected with cRNA and used 3 days following injection.

### **2.2.8 Removal of egg jelly**

For procedures requiring the removal of jelly, eggs were incubated at room temperature for 5 minutes before insemination with sperm suspension prepared as described previously (Katherine L. Wozniak & Carlson, 2020). Activated eggs, identified by their tendency to roll so the animal pole faced up and displaying a contracted animal pole, were used for western blot preparations. To remove the jelly, eggs were placed on agar in a 35 mm petri dish, in MR/3 with 45 mM  $\beta$ -mercaptoethanol (BME), pH 8.5. During the BME incubation, eggs were gently agitated for 1-2 minutes, until their external jelly visibly dissolved, as indicated by close nestling of the eggs and loss of visible jelly. To remove the BME solution, de-jellied eggs were then moved with a plastic transfer pipette to a petri dish coated with 1% agar in MR/3 pH 6.5 and agitated for an additional

minute. Eggs were then transferred three times to additional agar coated dishes with MR/3 pH 7.8, swirling gently and briefly in each.

### **2.2.9 Protein sample preparation and western blot**

Fertilization incompetent, developmentally immature oocytes, and mature eggs were lysed using a Dounce homogenizer and ice-cold oocyte homogenization buffer (OHB) (10 mM HEPES, 250 mM sucrose, 5 mM MgCl<sub>2</sub>, 5% glycerol supplemented with protease and phosphatase inhibitors in a 1:100 dilution) (Hill et al., 2005). 100 µL of OHB was used per 10 eggs or oocytes. Cellular debris was removed by centrifugation at 500 RCF for 5 mins at 4 °C and the resulting pellet was then resuspended in 100 µL OHB. The sample was again sedimented and the supernatant from both the successive sedimentations was pooled and again centrifuged at 18,213 RCF for 15 mins at 4 °C. The supernatant was then sedimented at 18,213 RCF for 15 mins at 4 °C. 30 µL of this supernatant was combined with 10 µL sample buffer (50 mM Tris pH 6.8, 2% SDS, 10% glycerol, 1% β-mercaptoethanol, 12.5 mM EDTA, 0.02% bromophenol blue) before incubating at 95 °C for 1 min.

Samples were resolved by electrophoresis on precast 4-12% BIS-TRIS PAGE gels (Invitrogen) run in TRIS-MOPS (50 mM MOPS, 50 mM Tris, 1 mM EDTA, 0.1% SDS) running buffer, followed by wet transfer to a nitrocellulose membrane at 10 V for 1 hour in Bolt (Invitrogen) transfer buffer. Loading was evaluated by Ponceau S. Blocking was performed for 1 hour at room temperature using Superblock (Thermo) buffer. Primary antibody incubation was performed overnight at 4 °C with anti-PLCγ [pY783] (Abcam) (1:1000) and secondary antibody was performed for 1 hour at room temperature using goat anti-rabbit HRP (Invitrogen) (1:10000).

All washes were performed using TBST (20 mM Tris, 150 mM NaCl, 0.1% Tween-20, pH 8). Blots were resolved using Supersignal Pico (Pierce) on a GE/Amersham 600RGB imager using chemiluminescence settings. Gel was stained with SYPRO Ruby Protein Gel Stain (Lonza) to demonstrate equal protein loading.

### **2.2.10 Quantification and statistical analyses**

All electrophysiology recordings were analyzed with Igor (Wave-Metrics), Excel (Microsoft), and Prism9 (GraphPad, Dotmatics). Data for each experimental condition are displayed in Tukey box plot distributions, where the box contains the data between 25% and 75% and the whiskers span 10-90%. All conditions contain trials conducted on multiple days with gametes from multiple females. Unpaired *T* tests were used to determine differences between inhibitor treatments. Depolarization rates were  $\log_{10}$  transformed before statistical analyses.

## **2.3 Results**

### **2.3.1 Inhibition of PLC- $\gamma$ by tyrosine kinase inhibitors did not alter the fast block**

*X. laevis* eggs inseminated during whole cell recording depolarize several minutes after sperm addition (Figure 6A, 13 eggs). Before the depolarization, the eggs exhibited a stable resting potential with an average of -13.8 mV ( $\pm$  0.9; Figure 6C). Following insemination in control conditions, the plasma membrane reached an average potential of 12.67 mV ( $\pm$  0.87; Figure 6D) at 3.78 minutes following insemination on average ( $\pm$  3.00). We quantified the rate of the

depolarization by calculating the rate of the fastest 1 mV increment during depolarization (Katherine L. Wozniak, Wesley A. Phelps, et al., 2018; Katherine L. Wozniak, Maiwase Tembo, et al., 2018). Eggs inseminated in control conditions had an average depolarization rate of 2.45 mV/s ( $\pm 0.87$ ; Figure 6E, 7E). Importantly, these average potentials and depolarization rate agree with data published in our lab previously (Katherine L. Wozniak, Wesley A. Phelps, et al., 2018; Katherine L. Wozniak, Maiwase Tembo, et al., 2018). The depolarization rate is directly proportional to the TMEM16A channels open during the depolarization (Katherine L. Wozniak, Wesley A. Phelps, et al., 2018). Therefore, if the signaling pathway that precedes the fast block depolarization is inhibited, fewer channels will open, and the depolarization rate will be slowed. Thus, we will use depolarization rate as a readout for inhibition of the fast block signaling pathway. Following whole cell recordings, these eggs were monitored for development, and all develop the symmetric cleavage furrows that indicate monospermic fertilization. These data highlight our ability to record the depolarization that follows fertilization and establishes a standard to which our below experiments can be compared.

Due to the higher relative abundance of PLC- $\gamma$ 1, present at 80 nM, 20-fold higher than either PLC $\beta$ 1 or PLC $\beta$ 3 (Session et al., 2016; Wühr et al., 2014), we hypothesized that this isoform initiates the fast block. PLC- $\gamma$  enzymes are typically activated by tyrosine phosphorylation. Therefore, I utilized cell permeant tyrosine kinase inhibitors genistein and lavendustin A and B to prevent tyrosine phosphorylation of PLC- $\gamma$ 1 during fertilization and, determine whether this interfered with the fast block depolarization.

To establish efficacy of tyrosine kinase inhibitors in *Xenopus laevis* eggs, Kayla Komondor and Joel Rosenbaum assayed for their ability to reduce tyrosine phosphorylation. As positive control, the receptor tyrosine kinase for platelet derived growth factor (PDGF-R) was expressed

in *X. laevis* oocytes. Application of platelet derived growth factor to PDGF-R expressing oocytes increased tyrosine phosphorylation of PLC- $\gamma$ 1 on position Y776 of PLC- $\gamma$ 1 (homologous to position Y783 of mouse PLC- $\gamma$ 1) (Kadamur & Ross, 2013) as observed with Western blot (Figure 8A). Oocytes treated with 100  $\mu$ M genistein did not experience increased tyrosine phosphorylation of PLC- $\gamma$ 1 with application of PDGF (Figure 8A, Lane G). Treatment of 100 nM lavendustin B was less effective in reducing PDGF-signaled tyrosine phosphorylation (Figure 8A, Lane LB), but more effective than the analog lavendustin A (Hsu et al., 1991; Onoda et al., 1989) which had no effect (Figure 8A, Lane LA). We also determined that tyrosine phosphorylation of PLC- $\gamma$ 1 on position Y776 did not occur at fertilization in *X. laevis* eggs (Figure 8 B-C). However, with the possibility that PLC- $\gamma$ 1 tyrosine phosphorylation at fertilization is below threshold of detection in Western blot, I still interrogated the ability of tyrosine kinase inhibitors to interrupt PLC- $\gamma$ 1 signaling in the fast block depolarization.

To test the hypothesis that PLC- $\gamma$ 1 signals the fast block, I performed whole cell recordings of eggs inseminated in the presence of cell-permeant tyrosine kinase inhibitors genistein (Akiyama et al., 1987; Akiyama & Ogawara, 1991) as well as lavendustin B and analog lavendustin A (Hsu et al., 1991; Onoda et al., 1989). Because our Western blot data demonstrated that these inhibitors effectively stopped PDGF-signaled tyrosine phosphorylation of PLC- $\gamma$ 1 (Figure 8A). I was confident that application of these inhibitors in the bath solution, without injection into the eggs, would be sufficient to stop any fertilization activated tyrosine phosphorylation of Y776 of PLC- $\gamma$ 1.

Freshly laid eggs were placed in either 100  $\mu$ M genistein, 100 nM lavendustin A, or 100 nM lavendustin B for whole cell recording (Figs 6A, 7A). Eggs were incubated for 5 minutes in the solution after impalement with the electrodes to ensure steady resting potential. Sperm from *X.*

*laevis* testis minced with the same inhibitor solution, to prevent inhibitor dilution, were then added to the egg. The membrane potential of the egg before depolarization (resting potential), following fertilization evoked depolarization (fertilization potential), and rate of depolarization (fertilization rate) were all quantified from each whole cell recording (Figs 6 C-E, 7 C-H). Temperature was variable in the lab at time of experimentation, so controls were date matched to treatment. Eggs inseminated in control solution at the same time as genistein recording displayed average resting potential of  $-15.1 \pm 1.7$  mV, fertilization potential of  $3.8 \pm 2.9$  mV, and depolarization rate of  $1.0 \pm 0.46$  mV/ms. Eggs inseminated in genistein displayed average resting potential of  $-17.6 \pm 1.9$  mV, fertilization potential of  $2.4 \pm 2.6$  mV, and depolarization rate of  $8.9 \pm 3.1$  mV/ms. There was no statistical difference between any examined metric with or without genistein (resting potential  $P = 0.36$ , fertilization potential  $P = 0.76$ , log depolarization rate  $P = 0.08$ ). For eggs inseminated in control solution at the same time as lavendustin A, average resting potential was  $-10.7 \pm 3.1$  mV, fertilization potential was  $16.0 \pm 4.9$  mV, and depolarization rate was  $0.29 \pm 0.18$  mV/ms. Eggs inseminated in lavdendustin A had an average resting potential of  $-7.9 \pm 2.4$  mV, fertilization potential of  $19.7 \pm 3.9$  mV, and depolarization rate of  $0.66 \pm 0.49$  mV/ms. There was no statistical difference between any metric of recording with or without lavendustin A (resting potential  $P = 0.50$ , fertilization potential  $P = 0.58$ , log depolarization rate  $P = 0.74$ ). For eggs inseminated in control solution at the same time as lavendustin B, average resting potential was  $-7.7 \pm 2.1$  mV, fertilization potential was  $23.7 \pm 1.4$  mV, and depolarization rate of  $0.03 \pm 0.01$  mV/ms. Eggs inseminated in lavdendustin B had an average resting potential of  $-8.1 \pm 2.5$  mV, fertilization potential of  $19.8 \pm 3.8$  mV, and depolarization rate of  $0.26 \pm 0.2$  mV/ms. There was no statistical difference between any metric of recording with or without lavendustin B (resting potential  $P = 0.91$ , fertilization potential  $P = 0.27$ , log depolarization rate  $P = 0.37$ ). These data demonstrate that

stopping tyrosine phosphorylation- mediated activation of PLC- $\gamma$  did not interfere with the fast block to polyspermy in *X. laevis* eggs. This is also supported by the observation that tyrosine phosphorylation of Y776 of PLC- $\gamma$ 1 was not observed following fertilization in *X. laevis* eggs (Figure 8B).

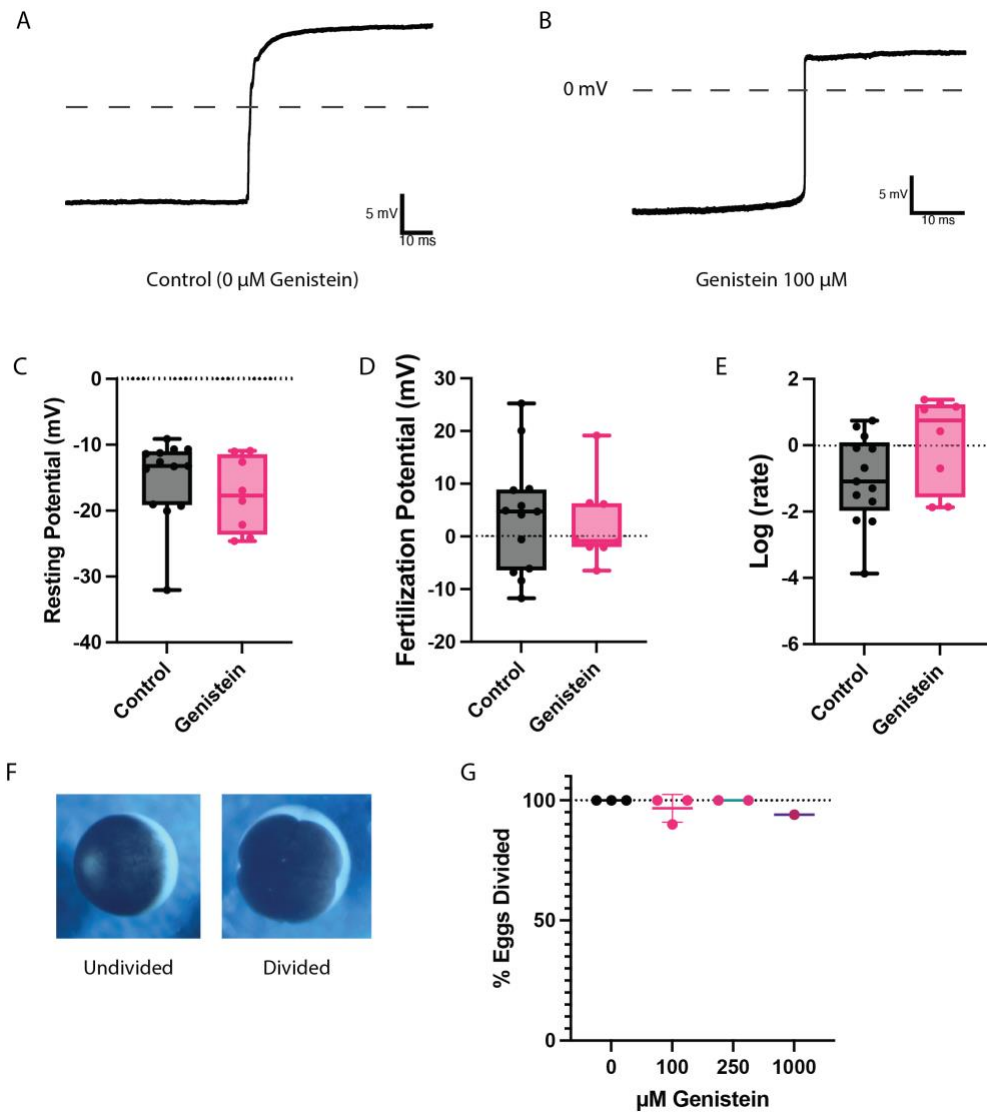


**Figure 6 Genistein does not alter the kinetics of the fast block depolarization or the development rate of embryos**

A-B) Representative whole cell electrophysiology recordings of *X. laevis* eggs made during *in vitro* fertilization. Fertilization evoked depolarizations are observed with or without genistein. C-E) Box plots showing the resting potential, the membrane potential prior to the depolarization, D) fertilization potential, the membrane potential following the depolarization, E) depolarization

rate (mV/mS) of fertilization evoked depolarization (calculated from the fastest 1 mV increment of the depolarization) in recordings made with or without genistein. F) Representative images of an undivided, unfertilized egg and a symmetrically divided fertilized egg. G) Percent of embryos that present with symmetrical cleavage furrows following *in vitro* fertilization in the presence of increasing concentrations of genistein.

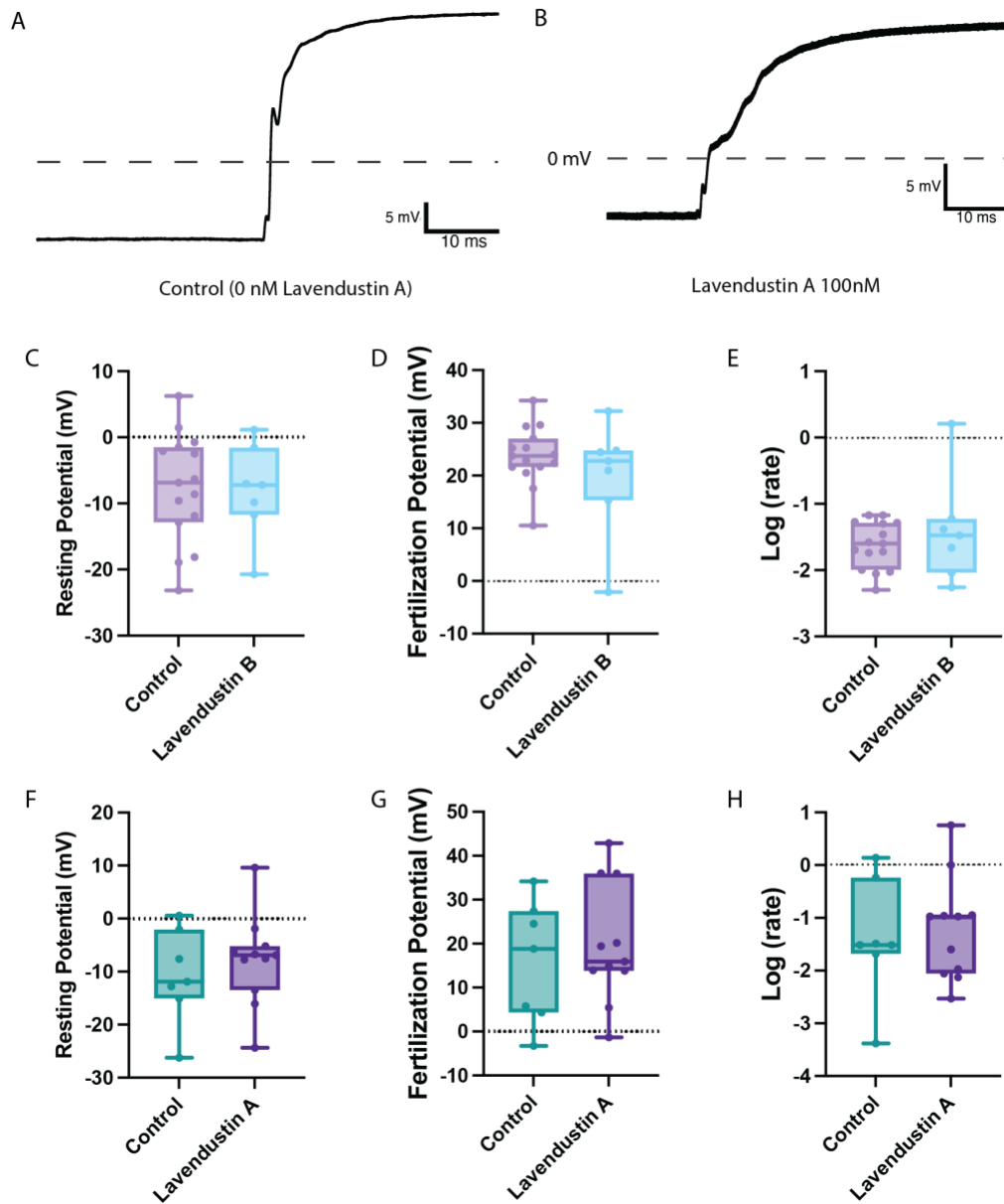


**Figure 7 Lavendustin A did not alter the kinetics of the fast block depolarization or the development rate of embryos**

A-B) Representative whole cell electrophysiology recordings of *X. laevis* eggs made during *in vitro* fertilization. Fertilization evoked depolarizations are observed with or without lavendustin A. C-E) Box plots showing (C) the resting potential, the membrane potential prior to the

depolarization, (D) fertilization potential, the membrane potential following the depolarization, and (E) depolarization rate (mV/mS) of fertilization evoked depolarization (calculated from the fastest 1 mV increment of the depolarization) in recordings made with or without lavendustin B. F-H) Box plots showing (F) the resting potential, the membrane potential prior to the depolarization, (G) fertilization potential, the membrane potential following the depolarization, and (H) depolarization rate (mV/mS) of fertilization evoked depolarization (calculated from the fastest 1 mV increment of the depolarization) in recordings made with or without the inactive analog lavendustin A.

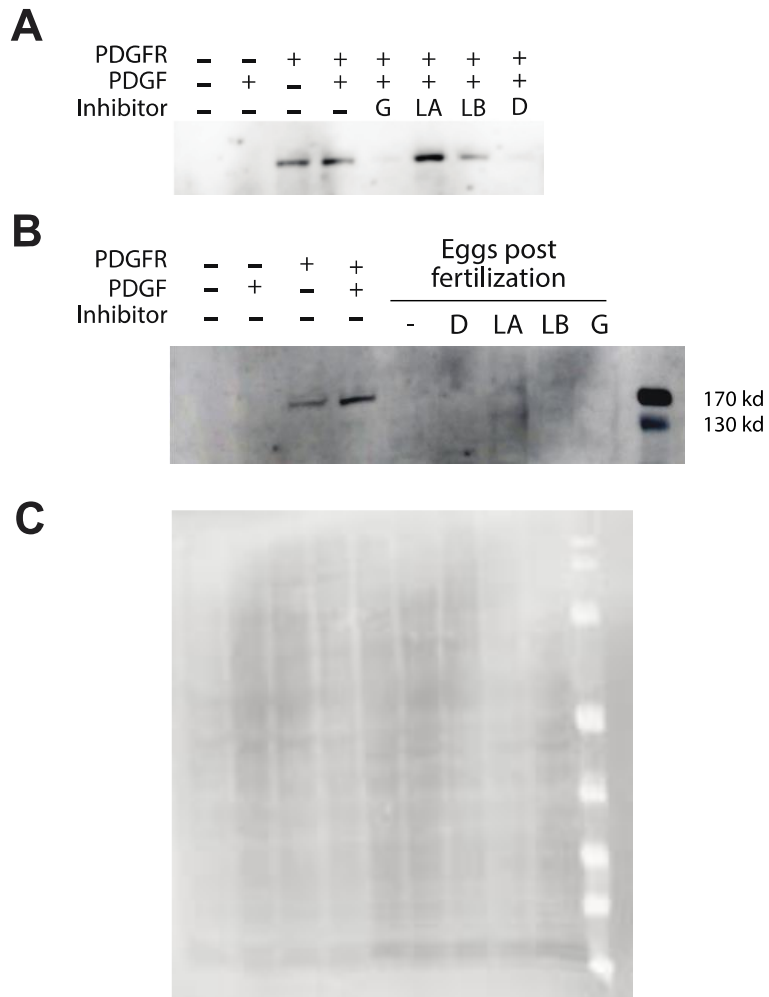


**Figure 8 Genistein and Lavendustin B inhibit phosphorylation of PLC- $\gamma$**

(A) Western blot probing for tyrosine phosphorylation of PLC $\gamma$ 1-Y776 in *X. laevis* oocytes expressing platelet-derived growth factor receptors (PDGFR). Blot probed for PLC $\gamma$ 1-Y776 phosphorylation in the presence of tyrosine kinase inhibitors (G: Genistein, LA: Lavendustin A, LB: Lavendustin B). (B) *X. laevis* eggs were fertilized and processed for western blot revealed that PLC $\gamma$ 1-Y776 was not phosphorylated following fertilization. (C) Loading control for (B).

### **2.3.2 Inhibition of PLC- $\gamma$ by tyrosine kinase inhibitors did not affect embryonic development**

It has been observed that injection of genistein inhibits egg activation (measured by cortical contraction and  $\text{Ca}^{2+}$  wave generation) which precedes embryonic development after fertilization (D. Glahn et al., 1999; Sato et al., 1998). It would also be expected that if inhibition of PLC- $\gamma$  affects the fast polyspermy block, then inhibitors should lead to an increase in the incidence of polyspermic fertilization. I performed *in vitro* fertilization to assess embryonic development in the presence of genistein. In these assays, the ratio of normal development, assessed by the appearance of symmetrical cleavage furrows is used to determine if fertilization occurred (Figure 6 F). Despite the previous findings that genistein interrupts egg activation, there was no difference in rate of normal development between eggs inseminated in concentrations up to 1 mM genistein, and control conditions (Figure 6 G). These data suggest that this inhibitor does not affect polyspermy blocking, egg activation, or embryonic development.

### **2.3.3 Assessment of possible sperm PLC- $\zeta$ in *X. laevis* testis**

Next, I considered the possibility that a sperm-derived PLC may increase intracellular  $\text{Ca}^{2+}$  in the egg. In mammals, PLC- $\zeta$  is a sperm-derived soluble enzyme that signals egg activation by increasing  $\text{IP}_3$ , and in turn, intracellular  $\text{Ca}^{2+}$  (Karl Swann, 2020). The gene encoding PLC- $\zeta$ , PLCZ1, has not been annotated in *X. laevis*, thereby suggesting that these frogs may lack PLC- $\zeta$  altogether. I considered the possibility that *X. laevis* have PLCZ1 that has not been annotated yet.

We sought to understand how PLC isozymes evolved and are related across varying classes of vertebrates. We surveyed representative species from diverse animals, including mammals,

birds, reptiles, amphibians, and used a lungfish species as our outgroup (Appendix Table 1). This spectrum covers evolutionary time between our *X. laevis* and mammals, where PLC- $\zeta$  was discovered and is best understood. It also represents several species with known PLC- $\zeta$  function (mammals and some birds) (Coward et al., 2005; Shusei Mizushima et al., 2007; Nomikos, Swann, & Lai, 2012) as well as species with annotated PLC- $\zeta$  genes with unknown function (reptiles and amphibians), and a species with no annotated PLC- $\zeta$  (lungfish). In a phylogenetic tree of all PLC isozymes from these representative species, it is observed that with one exception, each PLC isozyme groups together, regardless of species (Figure 9A). A cladogram of this same data demonstrates that within each grouping of PLC isoforms, PLCs from a species in the same class tend to group together (Figure 9B). It is from these alignments we understand how and why PLCZ1 genes in amphibians were annotated as PLC- $\zeta$ s, despite the fact that they lack functional features. It is very likely that even though they do look like PLC- $\zeta$  genes overall, they are possibly fractionated PLC genes that occur within the genome and have no known, and possibly no real, function. This may account for the fact that not all amphibians have an annotated PLC- $\zeta$  gene (*Xenopus* species vs *Bufo bufo* and *Rana temporaria*).

In order to determine whether a not-yet annotated PLC- $\zeta$  or PLC- $\zeta$ -like isozyme might be present in *X. laevis* sperm, we performed RNAseq on *X. laevis* testis. Mature sperm are transcriptionally quiescent, and we reason that any protein that would be present in the mature sperm would be present as a transcript in the testis, as the spermatids develop.

I performed RNAseq on RNA isolated from the testes of 3 individual male frogs. Overall, of 34,694 genes annotated in the *X. laevis* genome, 33,377 genes showed  $\geq 1$  transcript in at least 1 frog. Transcripts from PLC- $\beta$ , PLC- $\delta$ , and PLC- $\gamma$  isoforms were present (Table 1). The most abundant was the PLC- $\delta 4$  isoform, encoded by the gene *PLCD4*. PLC- $\delta$  most resembles PLC- $\zeta$  in

structure, and with the high abundance of *PLCD4*, it is a good candidate to act as a PLC- $\zeta$ -like isozyme.

To identify a PLC isoform with possible PLC- $\zeta$ -like activity, we identified unique PLC- $\zeta$  characteristics from the literature. Typically, PLC enzymes are comprised of a pleckstrin homology (PH) domain, four EF-hand motifs, the catalytic X&Y domains, and a single C2 domain at the C-terminus (Nomikos, Kashir, & Lai, 2017) (Figure 5). Uniquely, PLC- $\zeta$  lacks a PH domain. Typically, the PH domain of PLC anchors the enzyme at the membrane. Instead, PLC- $\zeta$  includes a longer stretch of positively charged residues between the X-Y domain relative to that in other PLC isoforms; these basic residues have been proposed to target PLC- $\zeta$  to the membrane (Nomikos et al., 2011). We reasoned that a PLC- $\zeta$ -like isozyme would have a basic stretch in the X-Y linker (Nomikos et al., 2011), no PH domain, and a highly Ca<sup>2+</sup>-sensitive EF hand (Nomikos et al., 2017). Therefore, we performed alignments of the protein sequence of all PLC isozymes present in the *X. laevis* testis with previously annotated PLCZ1 from the toad *Bufo bufo*, which is of the closest relatives to *X. laevis* with an annotated PLC- $\zeta$ , as well as PLCZ1 from the mouse *M. musculus*, as the gold standard PLC- $\zeta$ . In our alignment, we observed no basic stretch in the X-Y linker of any PLC isozyme in *X. laevis*, nor the PLCZ1 of *B. bufo*. This X-Y linker has been shown to be necessary for binding the negative charges of PIP<sub>2</sub> needed for hydrolytic activity (Nomikos et al., 2011). This suggests that no functional PLC- $\zeta$  exists in *X. laevis* and that the PLCZ1 annotated in *B. bufo* is not a functional PLC- $\zeta$ .

The search for the PLC contributing to the fast block depolarization therefore likely should remain in the egg.

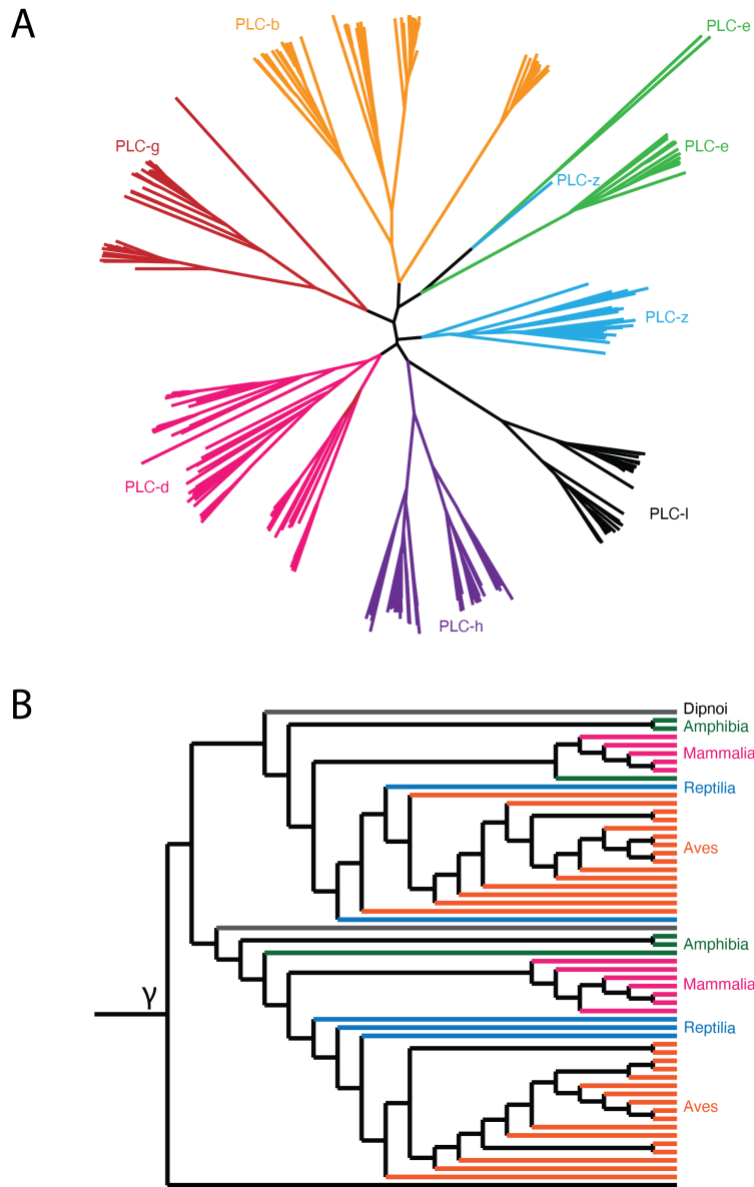


**Figure 9 Radial and linear phylogenetic trees of PLC isoforms from selected representative species**

A) Radial phylogenetic tree representing alignment of protein sequence of PLC proteins from representative mammalian, bird, reptile, amphibian, and lungfish species. PLC proteins group together primarily based on isoform. B) Section of linear cladogram made from the same alignment of PLC proteins in A, which demonstrates grouping of PLC isozyme sequences by organism class.

**Table 1 PLC transcripts present in RNAseq of *X. laevis* testis**

<b>PLC Isozyme</b>	<b>Average TPM</b>
plcd4.L	107.84
plcd1.L	8.65
plcb3.L	7.47
plcxd2.L	4.90
plcg1.S	4.80
plcd3.L	4.29
plcb1.S	3.36
plcg1.L	3.25
plcb2.L	3.20
plcg2.L	3.00
plcxd1.L	2.98
plcb4.S	1.81
plcd1.S	1.33
plcd3.S	1.25
plcb4.L	0.95
plcd4.S	0.42

## 2.4 Discussion

In the first moments following fertilization from eggs of several externally fertilizing species such as *X. laevis*, the egg undergoes a rapid depolarization. This prevents the entry of supernumerary sperm into the fertilized egg. It was previously established in the Carlson lab that in *X. laevis*, this depolarization depends on the action of Ca<sup>2+</sup>-activated Cl<sup>-</sup>-channel, TMEM16A (K. L. Wozniak, W. A. Phelps, M. Tembo, M. T. Lee, & A. E. Carlson, 2018) and that activation of this channels is a result of a PLC-dependent IP<sub>3</sub>-mediated release of Ca<sup>2+</sup> from the endoplasmic reticulum (K. L. Wozniak, M. Tembo, W. A. Phelps, M. T. Lee, & A. E. Carlson, 2018). However, which PLC isozyme was responsible for activation of this pathway was disputed (Runft et al., 1999; Sato et al., 1998). Here I showed that inhibition of the canonical activation of the most abundant PLC in the *X. laevis* egg is not sufficient to abrogate or diminish the fast block depolarization, in agreement with the work of Runft et al. This conflicts with other studies which suggest that inhibition of PLC- $\gamma$  activation was sufficient to inhibit Ca<sup>2+</sup>-driven activation of *X. laevis* eggs. However, this study introduced inhibitors via injection into the egg (Sato et al., 1998), which could result in activation via a different pathway than activation via fertilization. In fact, we never observed the tyrosine phosphorylation on residue Y776 of PLC $\gamma$ 1 after fertilization that previous studies sought to disrupt. Instead, we argue that either the activating PLC comes from another source, as occurs in mammalian species, or non-canonical activation of PLC occurs, perhaps by a bolus of calcium introduced at fertilization.

Though data suggest there is not a PLC- $\zeta$ , or PLC- $\zeta$ -like isozyme in *X. laevis* testis, there is still possibility that another sperm contributed factor could signal the fast block. Another mammalian sperm factor, PAWP (postacrosomal sheath WW domain binding protein) can also

induce egg activation when injected into mouse eggs (Aarabi et al., 2014; Aarabi, Qin, Xu, Mewburn, & Oko, 2010). Though no PLC- $\zeta$  has been observed in the sperm of nonmammalian species such as *X. laevis*, it is possible that a similar, so far unidentified, sperm factor could also trigger the fast block depolarization. It is debated whether a sperm factor could be fast enough to produce the nearly immediate response of the fertilization-evoked depolarization.

It is also possible that non-canonical activation of egg PLCs function within the fast block pathway. In other systems, elevated  $\text{Ca}^{2+}$  is sufficient to activate PLCs (Hwang, Jhon, Bae, Kim, & Rhee, 1996; Ryu, Cho, Lee, Suh, & Rhee, 1987; Wahl, Jones, Nishibe, Rhee, & Carpenter, 1992). Our own lab has demonstrated  $\text{Ca}^{2+}$ -concentration dependent activation of PLCs in excised *X. laevis* oocyte membrane patches (Tembo, Lara-Santos, Rosenbaum, & Carlson, 2022). Introduction of a bolus of cytoplasmic  $\text{Ca}^{2+}$  at fertilization may also be sufficient to activate the egg PLC and the downstream pathway that results in the fertilization-dependent depolarization, a hypothesis previously termed the “Calcium bomb” by Lionel Jaffe (L. F. Jaffe, 1983)

Though it may feel like a step back, the confirmation that tyrosine phosphorylation of PLC- $\gamma$  does not activate the fast block depolarization is an important clue to understanding the signaling processes that immediately follow fertilization. We do not understand what property of the sperm-egg interaction at fertilization leads to the signaling cascade or cascades that result in the fast block or egg activation. Now knowing that PLC- $\gamma$ 1 tyrosine phosphorylation is not necessary for the fertilization-evoked depolarization allows us to explore other candidates, namely other PLCs, possible sperm factors, or alternative activation of PLC- $\gamma$  that can, once identified, guide us through the signaling events to the exact moment where fertilization occurs.

### **3.0 Zinc inhibition of gamete fertility is an ancient feature of sexual reproduction in animals**

#### **3.1 Introduction**

Fertilization of an egg by more than one sperm, a condition known as polyspermy, is lethal for most animals. To prevent these catastrophic consequences, eggs use several strategies to shield already-fertilized eggs from penetration by additional sperm (J. L. Wong & Wessel, 2006); the two most common are referred to as the *fast* and *slow blocks to polyspermy*. Most sexual reproducers use the slow block (L. A. Jaffe & Gould, 1985; J. L. Wong & Wessel, 2006). During the slow block to polyspermy, eggs release materials that transform them into an impenetrable fortress minutes after fertilization (Bianchi, Doe, Goulding, & Wright, 2014; Burkart et al., 2012).

Recently, zinc release upon fertilization has been shown in eggs from various mammals including humans (Duncan et al., 2016), mice (Kim et al., 2011), and cows (Emily L. Que et al., 2018). This extracellular zinc has been proposed to participate in the slow block to polyspermy (E. L. Que et al., 2017; Tokuhiro & Dean, 2018). Using experimentation on fertilization and activation of eggs from five non-mammalian species, we now demonstrate that the zinc release from fertilized eggs is an ancient phenomenon and that this extracellular zinc protects fertilized eggs from polyspermy.

## 3.2 Materials and methods

### 3.2.1 Ethics

All vertebrate animal procedures were conducted using accepted standards of humane animal care and were approved by the Animal Care and Use Committee at the University of Pittsburgh.

### 3.2.2 Animals

*Xenopus laevis* (frog) adults were obtained commercially (NASCO, Fort Atkinson, WI), and housed separately at 18°C with a 12/12-hour light/dark cycle.

*Strongylocentrotus purpuratus* (purple sea urchin) gametes were obtained from commercially purchased adults (Marinus Scientific, Long Beach CA). *Hydractinia symbiolongicarpus* (cnidaria) were sexually mature, lab bred colonies (MN291-10 and MN295-8, male and female, respectively) grown on glass microscope slides and housed at 22-23°C with an 8/16-hour light/dark cycle.

### 3.2.3 Reagents

1 M MgSO<sub>4</sub> solution and 0.1 M ZnCl<sub>2</sub> stock solution in water were purchased from Sigma-Aldrich (St. Louis, MO). TPEN was purchased from Tocris (Bristol, United Kingdom) and human chorionic gonadotropin (hCG) was purchased from Covetrus (Melville, NY). Unless noted otherwise, all materials were purchased from Thermo Fisher Scientific (Waltham, MA).

### 3.2.4 Solutions

Modified Ringers (MR) solution was used for *X. laevis* fertilization experiments. MR contains (in mM): 100 NaCl, 1.8 KCl, 2.0 CaCl<sub>2</sub>, 1.0 MgCl<sub>2</sub>, and 5.0 HEPES, pH 7.8, and is filtered using a sterile, 0.2 µm polystyrene filter (Heasman, Holwill, & Wylie, 1991). Embryonic development assays were performed in 33% MR diluted in DDH<sub>2</sub>O (MR/3). Various chemicals were added to MR or MR/3, which contained final concentrations of <0.5% DMSO or ethanol.

Oocyte Ringers 2 (OR2) solution was used to rinse *X. laevis* oocytes after collagenase treatment. OR2 is comprised of (in mM): 82.5 NaCl, 2.5 KCl, 1 MgCl<sub>2</sub>, and 5 mM HEPES, pH 7.6, and is filtered using a sterile, 0.2 µm polystyrene filter (Wallace, Jared, Dumont, & Sega, 1973).

ND96 was used to store *X. laevis* oocytes. ND96 is comprised of (in mM): 96 NaCl, 2 KCl, 1 MgCl<sub>2</sub>, 10 HEPES, pyruvic acid, and 10 mg/L gentamycin at pH 7.6 and is filtered with a sterile 0.2 µm polystyrene filter (Schroeder, Cheng, Jan, & Jan, 2008).

Lab-made artificial sea water (spASW) was used for *S. purpuratus* development assays. The spASW is comprised of (in mM): 470 NaCl, 10 KCl, 11 CaCl<sub>2</sub>, 29 MgSO<sub>4</sub>, 27 MgCl<sub>2</sub>, and 2.5 NaHCO<sub>3</sub>, pH 8, and is filtered using a sterile, 0.2 µm polystyrene filter (Shen & Buck, 1993).

Commercial artificial sea water (hsASW) was used for *H. symbiolongicarpus* development assays. The hsASW is comprised of solubilized Instant Ocean Reef Crystals (Instant Ocean Spectrum Brands) at 28 parts per thousand.

### **3.2.5 Collection of gametes**

#### **3.2.5.1 *X. laevis* oocytes**

Oocytes were collected from ovarian sacs obtained from *X. laevis* females anesthetized with a 30-min immersion in 1.0 g/liter tricaine-S (MS-222), pH 7.4. Following excision, ovarian sacs were manually pulled apart, then dispersed by a 90-minute incubation in ND96 supplemented with 1 mg/ml collagenase. Collagenase was removed by repeated washes with OR2, and healthy oocytes were sorted and stored at 14°C in ND96 with sodium pyruvate and gentamycin (Tembo et al., 2022).

#### **3.2.5.2 *X. laevis* sperm and eggs**

Eggs were collected from sexually mature females. Egg laying was stimulated by injection with 1,000 IU of hCG into their dorsal lymph sac. Following injection, females were housed overnight for 12-16 hours at 14-16°C. Typically, egg-laying began within 2 hours of moving to room temperature. Eggs were collected on dry petri dishes and used within 10 minutes of being laid.

Sperm were obtained from testes harvested from sexually mature *X. laevis* males (K. L. Wozniak et al., 2017). Following euthanasia by a 30-minute immersion in 3.6 g/L tricaine-S (pH 7.4), testes were dissected and cleaned by manual removal of residual fat and vasculature. Cleaned testes were stored at 4°C in MR for use on the day of dissection or in L-15 medium for use up to one week later. Sperm were extracted by mincing 1/10 of a testis in 200-500 µL of MR and were used within 1 hour of collection (K. L. Wozniak et al., 2017).

For experiments sequentially treating eggs with different conditions, eggs were incubated in an initial experimental solution, washed three times by moving between petri dishes containing

the final treatment using a plastic transfer pipette, and then placed in the final treatment solution. Two types of these sequential treatment assays are reported here: transfer before insemination (*e.g.* Fig 10 D) and transfer after insemination (*e.g.* Fig 12 B). When transferred before fertilization, eggs were incubated in the starting solution for 15 minutes and inseminated in the transfer solution. When transferred after insemination, eggs and sperm were incubated together in the starting solution for 30 minutes, then transferred.

### **3.2.5.3 *S. purpuratus* sperm and eggs**

Gametes were collected from spawning *S. purpuratus* adults. Spawning was induced by manual agitation or injection with 100-500  $\mu$ L of 0.5 M KCl followed by agitation (Shen & Buck, 1993). Sperm were collected directly from the animal using a 10  $\mu$ L pipette and then transferred into a 1.7 mL capped tube. Eggs were collected following release into a beaker containing spASW, then filtered through a 100  $\mu$ m filter.

### **3.2.5.4 *H. symbiolongicarpus* sperm and eggs**

*H. symbiolongicarpus* gametes were collected from spawning adults. Upon the first light exposure for the day, spawning was induced following separation of male and female colonies (Sanders et al., 2018). Gametes were released within 60-90 minutes of light exposure. Eggs were collected from the water surrounding spawning females, filtered through a 20  $\mu$ m strainer, and maintained in hsASW. Sperm were collected from the water surrounding spawning males using a 1 mL pipette and maintained in hsASW.

### **3.2.6 Confocal microscopy of extracellular zinc during fertilization or activation**

Zinc release from *X. laevis* gametes was imaged using FluoZin-3 and a TCS SP5 confocal microscope (Leica Microsystems, Wetzlar, Germany) equipped with a Leica 506224 5X objective. FluoZin-3 was excited with a 488 nm visible laser, and the emission between 500-600 nm was collected. Using a galvo scanner with unidirectional (600 Hz) scanning, FluoZin-3 and bright-field images were taken every 3-5 seconds for up to 25 minutes. Images were analyzed using LAS AF (version 3.0.0 build 834) and ImageJ (Schneider, Rasband, & Eliceiri, 2012) software packages.

#### **3.2.6.1 *X. laevis* egg imaging**

To image extracellular zinc during *X. laevis* fertilization, sperm were added to dejellied eggs bathed in MR/3 with 50  $\mu$ M FluoZin-3. Sperm prepared in MR/3, was pipetted near the eggs 1 minute after image acquisition had begun. Control experiments used the same experimental design with 1.5 mM TPEN. A similar experimental design was employed to image extracellular zinc during activation where *X. laevis* eggs or oocytes were activated with 10 or 200  $\mu$ M ionomycin treatment respectively in MR/3 with no sperm addition.

### **3.2.7 Bright-field microscopy**

#### **3.2.7.1 *X. laevis* egg and embryo imaging**

A stereoscope (Leica Microsystems, Wetzlar, Germany) equipped with a Leica 10447157 1X objective and DFC310 FX camera was used to image *X. laevis* eggs and embryos. Images were analyzed using LAS (version 3.6.0 build 488) software and Photoshop (Adobe) or ImageJ (Schneider et al., 2012). For the jelly removal assay, *X. laevis* eggs were imaged using an Edmund

Optics stereomicroscope with a 10X objective, fitted with a pixiLINK digital camera and the  $\mu$ Scope Essential 64x software pixiLINK, Canada). The diameter of the egg and the surrounding jelly coat were determined in Adobe Illustrator (San Jose, CA).

### **3.2.7.2 *S. purpuratus* egg and embryo imaging**

Eggs and embryos from *S. purpuratus* were imaged on an inverted Olympus IX73 stereoscope equipped with an Olympus UPlanFL N 10X objective, Olympus TL4 light source, and Olympus U-LS30-3 camera. Images were analyzed using Photoshop (Adobe).

### **3.2.7.3 *H. symbiolongicarpus* egg and embryo imaging**

Eggs and embryos were imaged using Zeiss Discovery.V20 stereoscope equipped with a Lumenera Infinity3s camera and Zeiss KL1500 LCD light source. Images were analyzed using Photoshop (Adobe).

## **3.2.8 Fertilization and embryonic development assays**

### **3.2.8.1 Assessment of *X. laevis* embryonic development**

For each experimental trial, development of *X. laevis* embryos was assessed from approximately 20-40 eggs in each experimental condition. 20-90  $\mu$ L of the sperm suspension was used to fertilize eggs depending on the volume of the dish. Approximately 90-120 minutes after insemination, the appearance of cleavage furrows was used to assess the initiation of embryonic development (K. L. Wozniak et al., 2017). For some experiments assaying for the timing of cleavage furrow appearance, eggs were imaged every 10 minutes beginning at 60 minutes post

insemination to assess for development to the 2-cell stage. Each assay was repeated at least three times with gametes from different males and females and on different experiment days.

#### **3.2.8.2 Assessment of *S. purpuratus* embryonic development**

*S. purpuratus* sperm were activated by 5:1,000 dilution into spASW. 30  $\mu$ L of activated sperm were added to a 4 mL suspension of eggs in spASW supplemented with varying concentration of ZnSO<sub>4</sub>. Successful fertilization was visually confirmed 2 minutes after sperm addition by the raising of the fertilization envelope. Development was assayed 90-120 minutes post-fertilization based on the appearance of cleavage furrows.

#### **3.2.8.3 Assessment of *H. symbiolongicarpus* embryonic development**

For development assays, equal volumes of *H. symbiolongicarpus* sperm and egg solutions were mixed in varying concentrations of ZnSO<sub>4</sub>. Development was assayed at 60 minutes post-fertilization based on the appearance of cleavage furrows.

### **3.2.9 Parthenogenic egg activation**

#### **3.2.9.1 Sperm-free activation of *X. laevis* eggs**

To activate eggs parthenogenically, eggs were placed in 10  $\mu$ M ionomycin for 7 minutes, washed in MR/3 three times, and incubated in MR/3 for 120-150 minutes before assessment of appearance of cleavage furrows.

### 3.2.10 FluoZin-3 fluorometry

#### 3.2.10.1 Quantification of zinc release from *X. laevis* eggs

To quantify extracellular zinc released during fertilization or parthenogenic activation, jelly was removed from batches of 30-100 freshly ovulated eggs. Jelly-free eggs were then inseminated with sperm or activated with 10  $\mu$ M ionomycin. The solution (MR/3) surrounding the eggs was collected 45 minutes after sperm addition or 30 minutes after ionomycin addition. The fertilization solutions were then sedimented at 3000 rpm for 5 minutes to pellet sperm, and the supernatant was transferred to a new tube.

#### 3.2.10.2 Quantification of zinc content of egg exudate with spectofluorometry

FluoZin-3 tetrapotassium salt was dispensed from a 1 mM stock in water for a final experimental concentration of 60 nM. Fluorescence intensity measurements were recorded in a 1 mm quartz cuvette, in a Fluorolog3 spectrophotometer with FluoEssence software (both from HORIBA, Jobin Yvon). FluoZin-3 containing samples were excited with 492 nm light, and emission was recorded at 514 nm with 3 nm slit widths. The raw photometric signals were corrected for by subtracting the FluoZin-3 free background, collected prior to adding FluoZin-3 to each sample. The zinc was quantified using a standard curve (A. E. Carlson et al., 2005; K. L. Wozniak et al., 2017) calculated with the following equation:

$$[Zn^{2+}] = K^* \times \frac{R - R_{min}}{R_{max} - R}$$

where the constants  $R_{min}$  (1 nM),  $R_{max}$  (100 nM), and  $K^*$  were obtained from MR/3 supplemented with known amounts of  $ZnSO_4$  ranging from 100 pM to 1  $\mu$ M fitted to a Hill equation (A. E. Carlson et al., 2005; K. L. Wozniak et al., 2017). Although there was little variability between

experiments, standard curves were generated for each experimental trial using the exact solution used for fertilization or activation.

To determine the number of zinc ions released with fertilization or parthenogenic activation, the total zinc concentration measured by FluoZin-3 photometry was multiplied by the dilution factor for that sample and Avogadro's number and divided by the total volume of solution in which eggs were inseminated from each trial and the number of eggs per trial.

*X. laevis* eggs reportedly contain  $65.8 \pm 4$  ng/egg of zinc per egg (Nomizu, Falchuk, & Vallee, 1993). The number of zinc ions contained by each *X. laevis* egg was calculated by dividing the zinc mass by the atomic mass of zinc (65.38), then multiplying by Avogadro's number.

### **3.2.11 Quantification of zinc content of egg exudate with ICP-MS**

Eggs were dejellied and transferred to a clean 35 mm dish containing MR/3. All transfers were performed with disposable glass transfer pipettes. Eggs were activated with 100 nM to 10  $\mu$ M ionomycin (free acid) application and incubated at room temperature for 30 minutes. Solution was then transferred to 15-mL conical tubes for storage at -20°C with up to 2.5% nitric acid prior to analysis by ICP-MS. Eggs were transferred to fresh MR/3 to assess activation 60-90 minutes after ionomycin. Biological controls included eggs in MR/3 (no ionomycin), MR/3 alone, and MR/3 with 100 nM ionomycin.

Released zinc was quantified with a PerkinElmer NexION 300X ICP-MS. On each experimental day, the instrument was calibrated with a five-point calibration curve. A blank consisting of 2% sub-boil-distilled trace metal-grade nitric acid was run every 7-10 samples to rule out signal memory effects. Reported values reflect the zinc concentration from the number of

activated eggs, following subtraction of the solution background (obtained from the egg-free MR/3 with ionomycin control).

### **3.2.12 Electrophysiology**

Electrophysiological recordings were made using TEV-200A amplifiers (Dagan Co.) and digitized by Axon Digidata 1550A (Molecular Devices). Data were acquired with pClamp Software (Molecular Devices) at a rate of 5kHz.

Pipettes used to impale the *X. laevis* eggs for recordings were pulled from borosilicate glass for a resistance of 5-15 M $\Omega$  and filled with 1 M KCl.

In the case of whole cell recording, resting and fertilization potentials were quantified ~10s before and after the depolarization, respectively. Depolarization rates of each recording were quantified by determining the maximum velocity of the quickest 1-mV shift in the membrane potential.

In the case of two-electrode voltage clamp recording, eggs were clamped at -80 mV to record IP<sub>3</sub>-evoked currents. Each oocyte was injected with a 200  $\mu$ M caged IP<sub>3</sub> stock made in DDH<sub>2</sub>O to reach a final concentration of 5  $\mu$ M within the oocyte, and incubated for at least 30 minutes away from light at 18°C before recording (Schroeder et al., 2008). IP<sub>3</sub> was released from nitrophenyl cage by flash photolysis via 250 ms UV light exposure (Ultra High Power White LED Illuminator, 380–603 nm; Prizmatix). The bath solution in our recording chamber (RC-26G; Warner Instruments) was changed with the gravity-fed, pinch valve VC-8 solution changer (Warner Instruments).

### **3.2.13 Proteomic and RNA-sequencing (RNA-seq) analysis**

Zinc-transporters expressed in *X. laevis* eggs were identified by interrogating proteomic (Wühr et al., 2014) and RNA-seq (Session et al., 2016) datasets for SLC30 or SLC39 gene names.

## **3.3 Results**

### **3.3.1 Zinc is released from *Xenopus laevis* eggs at activation**

To determine whether eggs from an external fertilizer release zinc, Dr. Katherine Wozniak and I monitored extracellular zinc before and after fertilization of eggs from the African clawed frog, *Xenopus laevis*. To do so, we used confocal microscopy with the cell-impermeant, fluorescent zinc indicator FluoZin-3, before and after sperm addition. Within minutes of sperm addition, *X. laevis* eggs released zinc as a single wave that slowly wrapped around the eggs (Figure 10 A-B) (Katherine L. Wozniak et al., 2020). In mammalian eggs, zinc is released from cortical granules during the slow block to polyspermy (Kong et al., 2015; Emily L. Que et al., 2018). If zinc release also occurred during the slow block in *X. laevis* eggs, we predicted that the appearance of extracellular zinc would coincide with lifting of the envelope, a marker of the slow block. Following sperm entry, the envelope lifts from the egg as exocytosed proteases cleave contacts between this extracellular matrix and the egg's plasma membrane (Runft et al., 2002; J. L. Wong & Wessel, 2006). Appearance and localization of extracellular zinc was in sync with the lifting of the envelope (Figure 10 A red arrows). All imaged eggs underwent cortical contraction (Figure 10

C), indicating successful fertilization (Elinson, 1975). These data reveal that, as in mammals, *X. laevis* eggs release zinc upon fertilization.

We explored whether signaling the slow block without fertilization would similarly increase extracellular zinc around *X. laevis* eggs. To do so, we imaged extracellular zinc before and after application of the calcium ionophore ionomycin (Snow, Yim, Leibow, Saini, & Nuccitelli, 1996), which increases cytosolic calcium to initiate cortical granule release. In both eggs and *in vitro* matured oocytes, a zinc release quickly appeared with ionomycin application (Figure 10 D-G) and coincided with lifting of the envelope (Katherine L. Wozniak et al., 2020). Envelope lifting and cortical contraction verified successful activation (Figure 10 C).

To confirm that the change in FluoZin-3 fluorescence was due to zinc release, we fertilized *X. laevis* eggs in the zinc chelator TPEN (Arslan, Virgilio, Beltrame, Tsien, & Pozzan, 1985). Under these conditions, the fluorescence was quenched (Figure 10 H) (Katherine L. Wozniak et al., 2020). Finally, we queried proteomic (Wühr et al., 2014) and RNA-sequencing (Session et al., 2016) datasets to verify that *X. laevis* eggs express zinc transporters needed to acquire and regulate the metal (Figure 10 I). Indeed, both ZnTs and ZIPs are present in *X. laevis* eggs. All together, these results reveal that *X. laevis* eggs release zinc at fertilization during the slow polyspermy block.

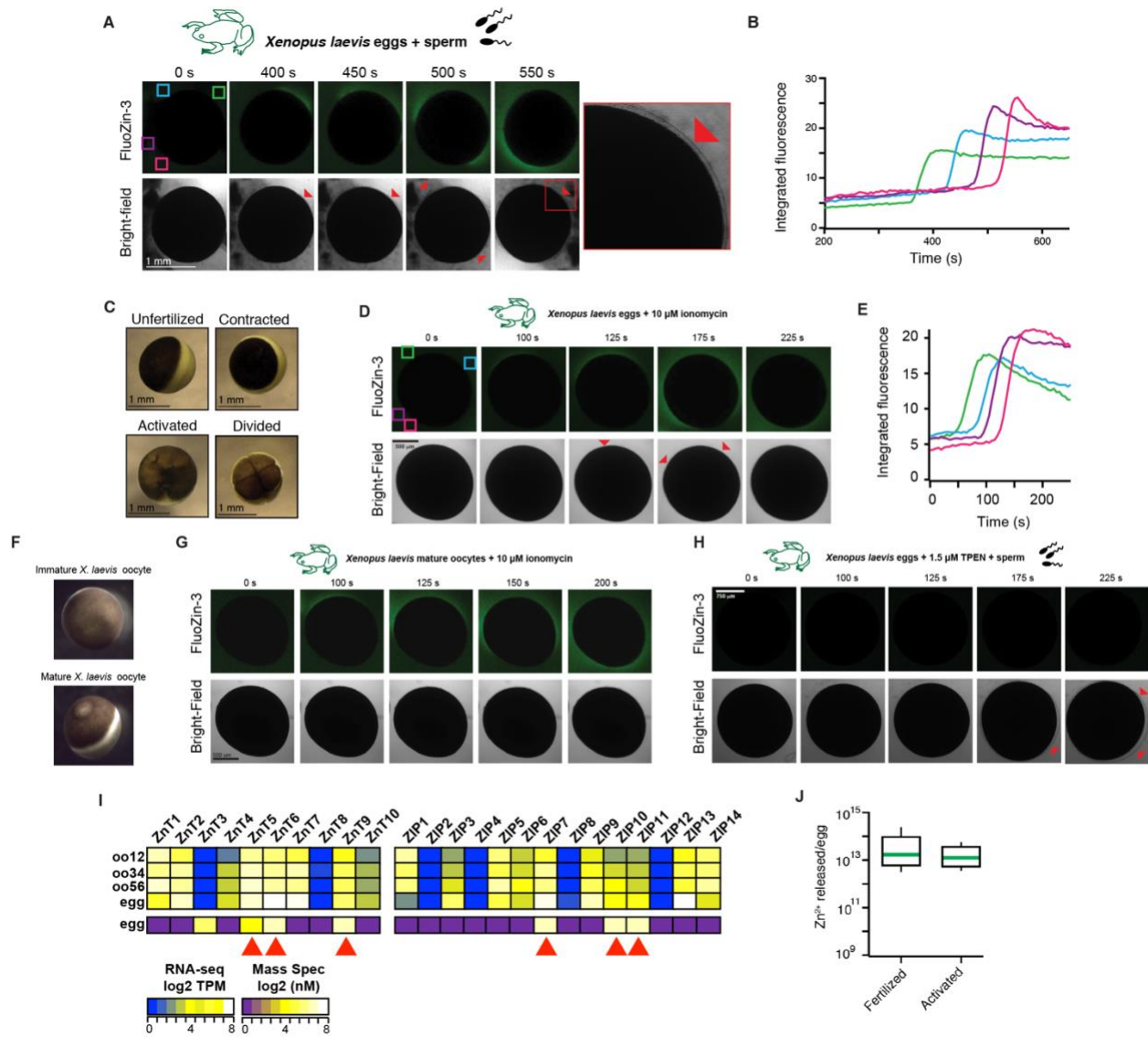


**Figure 10** *X. laevis* eggs release zinc at fertilization

(A) Representative fluorescence and bright-field images of *X. laevis* eggs in FluoZin-3, before and after sperm application (0s indicating time of sperm addition). Zinc release coincided with lifting and hardening of the envelope (red arrowheads and insert). (B) Integrated fluorescence, relative to time of sperm addition, detected by region of interest analysis, indicated by colored boxes in panel A demonstrates the single wave of zinc release around the egg. (C) Representative

images of *X. laevis* eggs and embryos. An unfertilized egg is marked by an equal animal (pigmented) pole and vegetal (unpigmented) pole, while a contracted egg, an early phenotype of egg activation, presents with a shrunken animal pole, which tends to orient upward. An egg which has been parthenogenetically activated demonstrates terminal asymmetric cleavage, while a dividing embryo cleaves symmetrically. (D-F) Parthenogenetic activation in FluoZin-3 via the calcium ionophore ionomycin leads to zinc release in both the mature, fertilization competent, *Xenopus laevis* egg (D, E) as well as the immature oocyte (F, G). (H) Fertilization in the presence of FluoZin-3 and zinc chelator TPEN abolished fluorescence. (I) Heatmaps of the expression levels of the two known families of zinc transporters ZnTs (encoded by the SLC30 gene family) and ZIPs (encoded by the SLC39 gene family) at the developmental stages indicated. Transcript levels (from (Session et al., 2016)) as determined by RNA-seq-based transcriptomics study, depicted in log<sub>2</sub> transcripts per million (TPM) (upper). Protein concentrations (from (Wühr et al., 2014)) as determined by mass spectrometry-based proteomics study, depicted in log<sub>2</sub> nanomolar (lower). Arrowheads highlight the six zinc transporters with both RNA and protein present in *X. laevis* eggs: ZnT5, ZnT6, ZnT9, ZIP7, ZIP10, and ZIP11. (J) Box plot distribution of zinc ions released per *X. laevis* egg upon fertilization or activation with 10 μM ionomycin as detected by FluoZin-3 fluorometry.

### 3.3.2 Quantification of zinc release from *X. laevis*

The zinc released from *X. laevis* eggs was quantified by collecting the solution surrounding fertilized or activated eggs and subjecting it to FluoZin-3 fluorometry. Fertilization and activation with ionomycin induced an average release of  $5.5 \pm 2.7 \times 10^{13}$  and  $1.9 \pm 1.0 \times 10^{13}$  zinc ions/egg, respectively (Figure 10 J, Table 2). Using ICP-MS, eggs activated with ionomycin release an average of  $8.7 \pm 5.2 \times 10^{12}$  zinc ions/egg (Table 2) (Katherine L. Wozniak et al., 2020). This substantiates our findings with fluorometry. Based on atomic absorption microscopy, *X. laevis* eggs reportedly have an average of  $6 \times 10^{14}$  zinc ions (Nomizu et al., 1993), thereby revealing that each egg loses less than 10% of their total zinc during the slow block. Together, these results demonstrate that an abundance of zinc ions are released from *X. laevis* eggs following fertilization and artificial activation.

### 3.3.3 Zinc inhibition of fertilization is concentration dependent

We next explored whether zinc contributes to the slow polyspermy block by inseminating *X. laevis* eggs in varying concentrations of extracellular zinc and monitoring the appearance of cleavage furrows. If extracellular zinc protects eggs from sperm entry, we predicted that signs of successful fertilization and embryonic development including the appearance of cleavage furrows would only appear in eggs inseminated in minimal zinc solution.

**Table 2 Average zinc ions released from *X. laevis* eggs**

<b>Method</b>	<b>Average ions released/egg</b>	<b>SEM</b>
<b>Fertilization (fluorometry)</b>	5.5 x 10 <sup>13</sup> (21-59 eggs in 9 trials)	2.7 x 10 <sup>13</sup>
<b>Activation (fluorometry)</b>	1.9 x 10 <sup>13</sup> (21-59 eggs in 5 trials)	9.7 x 10 <sup>12</sup>
<b>Activation (ICP-MS)</b>	8.7 x 10 <sup>12</sup> (48-122 eggs in 4 trials)	5.2 x 10 <sup>12</sup>

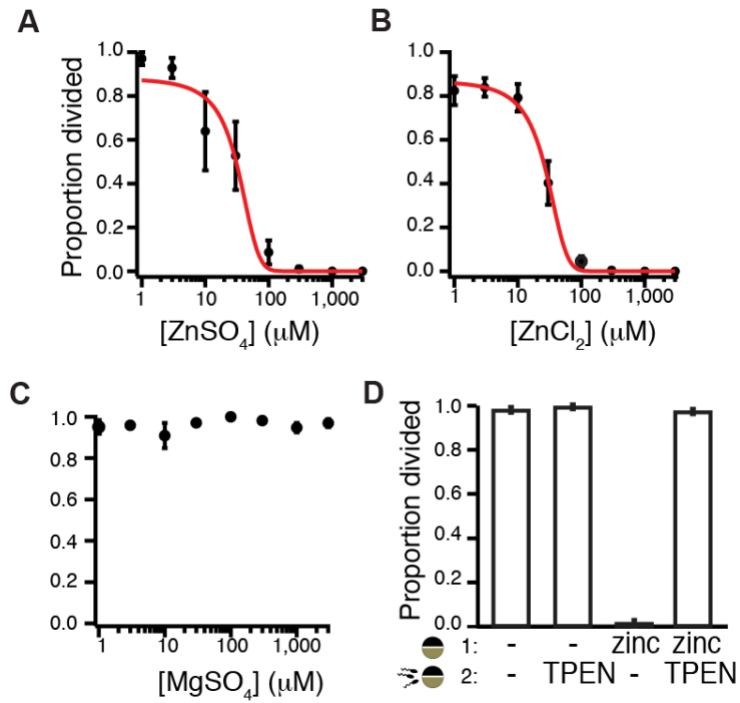


**Figure 11 Extracellular zinc protects eggs from fertilization**

(A-C) Proportion of inseminated eggs that developed cleavage furrows in indicated concentrations of ZnSO<sub>4</sub>, ZnCl<sub>2</sub>, or MgSO<sub>4</sub>. Plots in A and B were fit with sigmoidal functions. (D) Proportion of development of jelly-free eggs subjected to a 15 min pre-treatment with 0 or 300 μM ZnSO<sub>4</sub> (solution 1) then washed and moved to solution (2) with 0 or 300 μM TPEN for sperm addition (N=68 - 259 eggs, 5 trials).

**Table 3 Average IC<sub>50</sub>s of transition metals on proportion of development**

	<i>Xenopus laevis</i>	<i>X. laevis</i> (egg)	<i>X. laevis</i> (sperm)	<i>Strongylocentrotus purpuratus</i>	<i>Hydractinia symbiolongicarpus</i>
<b>ZnSO<sub>4</sub></b>	31 ± 10 μM (169 – 269 eggs in 7 trials)	73.5 ± 8.3 μM (93-255 eggs in 6 trials)	524 ± 102 μM (121-181 eggs in 5-21 trials)	9 ± 1 μM (120-684 eggs in 5 trials)	4 ± 2 μM (143 – 1,463 eggs in 5-6 trials)
<b>ZnCl<sub>2</sub></b>	30 ± 8 μM (157-326 eggs in 8 trials)				
<b>MgSO<sub>4</sub></b>	No inhibition (182 – 383 eggs in 5 trials)				
<b>CuCl<sub>2</sub></b>	9.1 ± 3.0 μM (230-321 eggs in 5 trials)				

<b>CuSO<sub>4</sub></b>		121.7 ± 23.2 μM (198-336 eggs in 5 trials)	517.9 ± 516.3 μM (121-254 eggs in 4 trials)		
<b>NiCl<sub>2</sub></b>	224 ± 23 μM  (136 – 283 eggs in 5 trials)				
<b>CoCl<sub>2</sub></b>	971 ± 92 μM  (148 – 295 eggs in 5 trials)				

### 3.3.3.1 Zinc stopped *X. laevis* fertilization

We found that ZnSO<sub>4</sub> inhibited the appearance of cleavage furrows in a concentration-dependent manner (Figure 11 A, Table 3), with no development evident from eggs inseminated in  $\geq 300 \mu\text{M}$  ZnSO<sub>4</sub>. A sigmoidal fit of the incidence of development versus ZnSO<sub>4</sub> concentration showed that half the eggs developed cleavage furrows at a zinc concentration (half-maximal inhibitory concentration, IC<sub>50</sub>) of  $31 \pm 10 \mu\text{M}$  (Figure 11 A). To confirm that zinc (Zn<sup>2+</sup>), and not sulfate (SO<sub>4</sub><sup>2-</sup>), was responsible for disrupting fertilization and embryonic development, *X. laevis* eggs were fertilized in varying concentrations of ZnCl<sub>2</sub> ( $30 \pm 8 \mu\text{M}$ ) or MgSO<sub>4</sub> (Figure 11 B-C). Whereas ZnCl<sub>2</sub> inhibited development with a nearly identical concentration response to ZnSO<sub>4</sub>, MgSO<sub>4</sub> had no effect (Table 3) (Katherine L. Wozniak et al., 2020). To further demonstrate that zinc is responsible for the inhibition of development, eggs were incubated in zinc, then transferred to and inseminated in a solution with the cell-permeant zinc chelator TPEN (Arslan et al., 1985) (N = 68 – 259 eggs, 5 trials; Figure 11 D). Nearly all eggs pretreated with zinc and subsequently inseminated in TPEN underwent cleavage, thereby revealing that extracellular zinc effects on *X. laevis* eggs are reversible (Katherine L. Wozniak et al., 2020).

### 3.3.3.2 Insemination in zinc inhibited embryonic development sea urchin and a cnidarian

Until this point, our study of zinc and fertilization had been performed on vertebrate eggs. To determine the conservation of zinc-inhibition of fertilization and early embryonic development in invertebrates, we fertilized eggs from the sea urchin *Strongylocentrotus purpuratus*, and the cnidarian *Hydractinia symbiolongicarpus*, in varying concentration of ZnSO<sub>4</sub>. For both animals, embryonic development was blocked in a concentration-dependent manner, as assessed by the appearance of cleavage furrows. ZnSO<sub>4</sub> inhibited development in *S. pupuratus* with an IC<sub>50</sub> of  $9 \pm$

1  $\mu\text{M}$  (Figure 12 A-B, Table 3). Inhibition of *H. symbiolongicarpus* gametes occurred with an  $\text{IC}_{50}$  of  $4 \pm 2 \mu\text{M}$ . (Figure 12 C-D, Table 3) (Katherine L. Wozniak et al., 2020). Together, these results reveal that zinc can inhibit fertilization and development in vertebrates and invertebrates alike. Notably, these species, though also external fertilizers, are highly diverged from *X. laevis*, and demonstrate the diversity of species where inhibition of fertilization by extracellular zinc occurs.

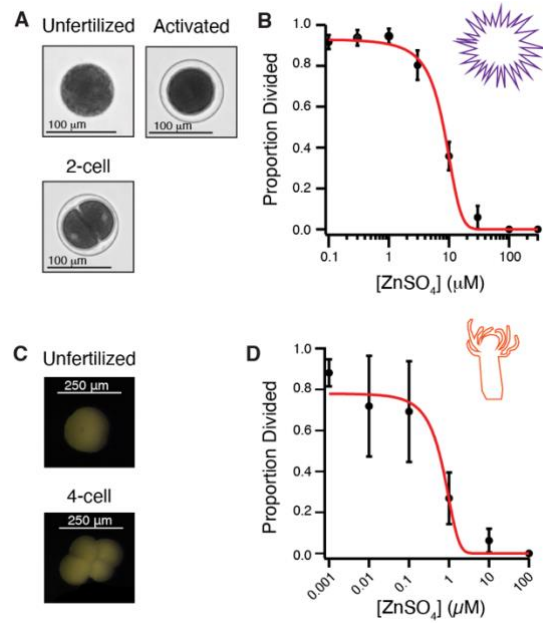


**Figure 12 Zinc protection of eggs is conserved in invertebrate external fertilizers**

A) Representative images of *S. purpuratus* eggs and embryos. B) Development was blocked in a concentration-dependent manner for *S. purpuratus* eggs in  $\text{ZnSO}_4$  (N=120-684 eggs, 5 trials). C) Representative images of *H. symbiolongicarpus* unfertilized eggs and dividing embryos. (D) Development was blocked in a concentration-dependent manner for *H. symbiolongicarpus* eggs inseminated in extracellular  $\text{ZnSO}_4$  (N=143-1463 eggs, 5-6 trials). Plots are fit with sigmoidal functions. Errors are s.e.m.

### 3.3.4 Zinc inhibition of fertilization is reversible

To understand the reversibility of the zinc effect on fertilization, I used the cell-permeant zinc chelator TPEN (Arslan et al., 1985). Determining whether TPEN reverses the zinc block of fertilization will uncover whether zinc regulates the gametes via non-covalent or covalent interactions. The cell-impermeant zinc chelator ZX1 (Pan et al., 2011) is utilized to examine the impacts of extracellular zinc on fertilization.

#### 3.3.4.1 Inhibition of embryonic development in *X. laevis* eggs was reversible with zinc chelators

To demonstrate that zinc pretreatment can inhibit fertilization, I incubated *X. laevis* eggs in solution with 300  $\mu\text{M}$   $\text{ZnSO}_4$ , before transferring to a solution without zinc for insemination. I assayed for the appearance of cleavage furrows to indicate the occurrence of fertilization. Zinc pre-treated eggs did not develop cleavage furrows ( $0 \pm 0\%$ ; Figure 13 A). As controls, eggs pretreated in zinc-free solution and inseminated without zinc developed at a high rate  $96.5 \pm 2\%$ , while eggs inseminated in the presence of zinc, regardless of pretreatment did not ( $2.5 \pm 2.5\%$  -  $2.4 \pm 2.4\%$ ) (Katherine L. Wozniak et al., 2020).

To demonstrate that dilution is not sufficient to reverse zinc inhibition of fertilization, we inseminated eggs in 1 mM  $\text{ZnSO}_4$  and then moved them to a zinc-free solution. These do not develop cleavage furrows ( $2.0 \pm 1.3\%$ ;  $N = 52 - 258$  eggs, 6 trials; Figure 13 B), unlike the controls which were inseminated in a solution with no added zinc ( $85.5 \pm 8.2\%$ ) (Katherine L. Wozniak et al., 2020).

To test the ability of a zinc chelator to reverse zinc inhibition of fertilization, I incubated eggs in 1 mM ZnSO<sub>4</sub> for 15 minutes before transfer to a solution containing 1 mM TPEN for insemination. In this condition, I observed the successful development of cleavage furrows ( $96.4 \pm 1.2\%$ , Figure 11 D). This treatment with TPEN results in a rate of development similar to those of eggs which were never in the presence of zinc ( $97.1 \pm 1.3\%$ ). This indicates that zinc modifies the egg in a non-covalent manner, reversible with a chelator. We never observed TPEN-induced activation of eggs, and insemination of eggs pre-treated in zinc-free solution before insemination in TPEN did not alter incidence of fertilization ( $98.5 \pm 1.1\%$ ) (Katherine L. Wozniak et al., 2020).

To further explore the chelator rescue of zinc inhibition of fertilization, I also utilized a cell-impermeant zinc chelator, ZX1. When zinc pre-treated eggs were inseminated in a solution containing 300  $\mu$ M ZX1, cleavage furrows developed in  $100 \pm 2\%$  of eggs, similar to those who had no contact with zinc or chelators ( $95 \pm 3\%$ ) or those which were inseminated in the presence of TPEN ( $95 \pm 5\%$ ; Figure 13 C). No effect on development was seen in eggs which had no contact with zinc but were inseminated in ZX1 ( $98 \pm 2\%$ ; Figure 13 C). The extracellular chelator ZX1 either buffered extracellular zinc important for the zinc block of fertilization or altered the zinc gradient in such a way that intracellular zinc important for the block leaves the egg.

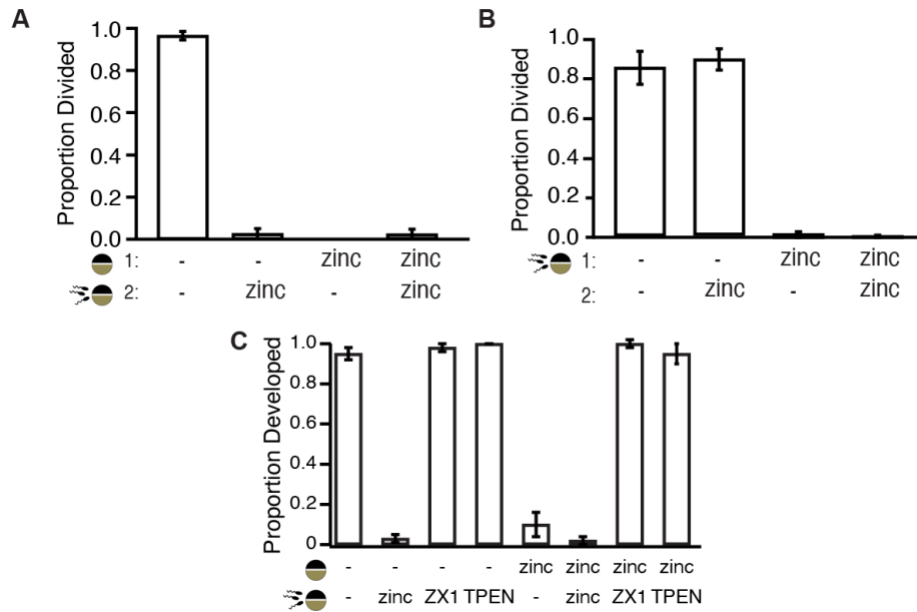


**Figure 13 Zinc inhibits embryonic development by binding to proteins surrounding the egg**

A) Incidence of development of eggs pre-treated in ZnSO<sub>4</sub> prior to insemination (N=34-150 eggs, 5 trials). B) Incidence of cleavage furrow development from eggs inseminated in 0 or 1 mM ZnSO<sub>4</sub> then transferred, 30 min after sperm addition, to a new solution with 0 or 1 mM ZnSO<sub>4</sub> (N=52 - 256 eggs, 6 trials). C) Inhibition of development from pre-treatment of eggs with 300 μM ZnSO<sub>4</sub> can be reversed with 300 μM ZX1, a cell-impermeant chelator, or 300 μM TPEN, a cell-permeant chelator (N=106 - 200 eggs, 6 trials).

### **3.3.5 Zinc inhibits fertilization, not development or activation**

We have used early embryonic development as an indicator of successful fertilization. Though it is true that an *X. laevis* egg which has not been fertilized will not develop symmetric cleavage furrows, a lack of cleavage furrow development is not necessarily indicative of a lack of fertilization. To determine whether zinc prevents fertilization, rather than blocking activation or developmental processes, I utilized three approaches: electrophysiology, IVF, and chemical activation.

#### **3.3.5.1 Fast block depolarizations are not present in eggs fertilized in extracellular zinc**

To test whether zinc inhibits fertilization, I determined whether eggs inseminated in zinc undergo one of the earliest signs of *X. laevis* fertilization, the fast block to polyspermy. As an external fertilizer, *X. laevis* utilizes an additional polyspermy block immediately after fertilization (Katherine L. Wozniak & Carlson, 2020). During the fast block to polyspermy, sperm can bind, but not enter a depolarized egg (Figure 14 A). The fast block can be observed through whole cell recordings of *X. laevis* eggs during fertilization. I performed whole cell electrophysiology recordings on eggs inseminated in the presence or absence of extracellular zinc to test whether *X. laevis* eggs depolarize after insemination in zinc.

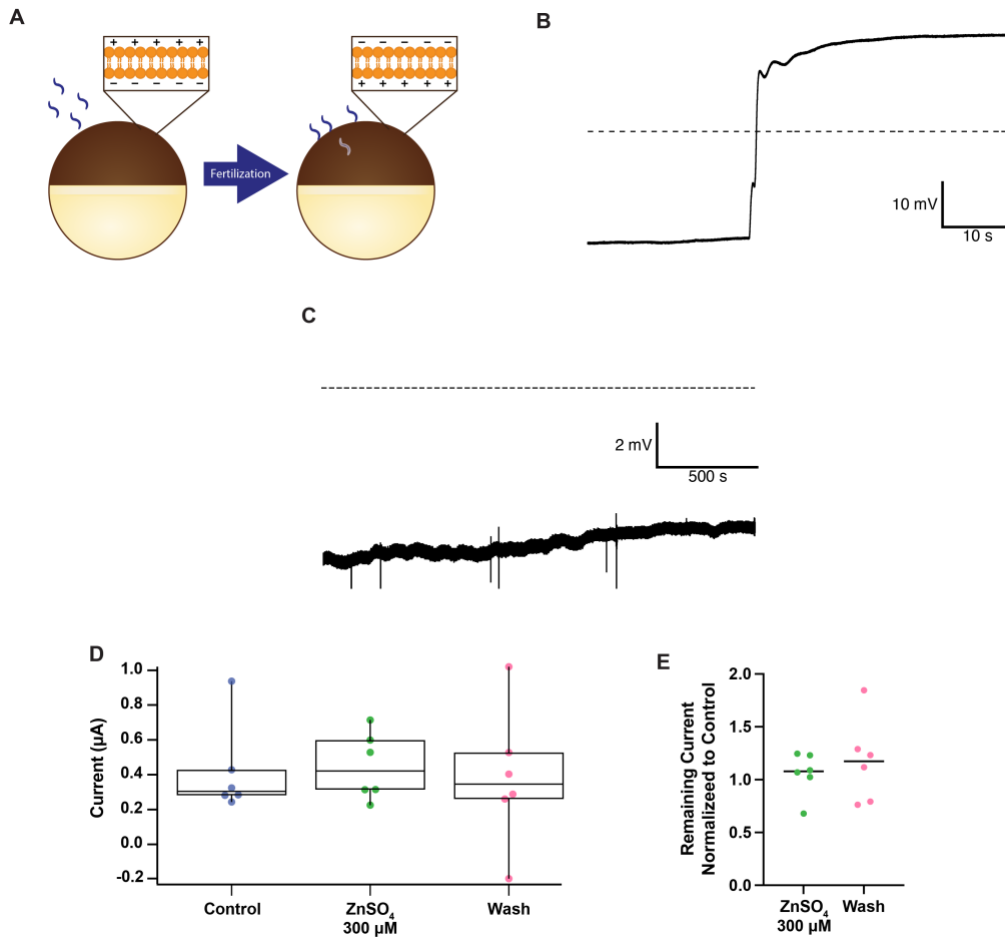


**Figure 14 Eggs inseminated in extracellular zinc do not display fertilization evoked depolarizations**

A) In some external fertilizers such as *X. laevis*, the plasma membrane depolarizes following fertilization. This depolarization allows sperm to bind but not enter the egg. B) A typical membrane depolarization following fertilization recorded via whole cell recording in *X. laevis* (10 trials). C) When a *X. laevis* egg is inseminated in 300  $\mu\text{M}$  extracellular  $\text{ZnSO}_4$ , no rapid membrane depolarization is observed (7 trials). D) Amount of current observed in control or zinc solutions following uncaging of  $\text{IP}_3$  (6 trials). E) Current of subsequent  $\text{IP}_3$  uncaging normalized to control recording (reflecting data in D).

In eggs inseminated in a control solution with no added zinc, I observed a rapid depolarization of the plasma membrane (Figure 14 B), consistent with known fast block depolarizations. In these 10 eggs, average resting potential was  $-9.52 \pm 2.20$  mV, and average fertilization potential was  $21.81 \pm 4.75$  mV. Average time from sperm addition to membrane depolarization was  $6.79 \pm 0.80$  minutes. Average rate of depolarization was  $1.01 \pm 0.45$  mV/ms. In 7 independent trials, I never observed a depolarization of *X. laevis* eggs inseminated in the presence of  $300 \mu\text{M ZnSO}_4$ , even with three subsequent sperm additions over 30-minutes (Figure 14 C). Average resting potential in these trials was  $-2.53 \pm 2.36$ . This lack of membrane depolarization suggests that fertilization is never occurring in the presence of excess extracellular zinc.

One possible explanation for the absence of the fertilization evoked depolarization may be that zinc enters *X. laevis* eggs, and inhibits the calcium activated chloride channel that mediates the depolarization. The  $\text{Ca}^{2+}$  binding site of TMEM16A can bind various transition metals including  $\text{Zn}^{2+}$  (Yuan et al., 2013). Therefore, it is possible that  $\text{Zn}^{2+}$  could bind the  $\text{Ca}^{2+}$  binding site to act as a competitive inhibitor. To test whether extracellular zinc can enter the gamete and inhibit TMEM16A, I performed two electrode voltage clamp experiments on *X. laevis* oocytes loaded with a photo labile  $\text{IP}_3$ . In this technique, the size of currents observed during uncaging is directly related to the number of TMEM16A channels open and can therefore be used to determine whether extracellular  $\text{Zn}^{2+}$  application alters the number of  $\text{IP}_3$  channels activated by uncaging  $\text{IP}_3$ . Water injected oocytes were used as a negative control and never displayed current with UV exposure (N=2). In 6 oocytes clamped at  $-80$  mV, I observed average currents of  $417 \pm 98$  nA in control solution,  $384 \pm 148$  nA in  $300 \mu\text{M ZnSO}_4$ , and  $450 \pm 71.7$  nA control following wash-off. The relative size of TMEM16A currents induced by uncaging of  $\text{IP}_3$  in the presence of  $300 \mu\text{M}$

ZnSO<sub>4</sub> were not outside the range of those uncaged in control solution (Figure 14 D). One-way ANOVA comparing the currents induced in control, 300 μM ZnSO<sub>4</sub>, and wash-off are not significantly different ( $P = 0.9298$ ). Further, comparison of relative current in subsequent uncaging of IP<sub>3</sub> demonstrates the lack of effect by ZnSO<sub>4</sub> in the bath solution (Figure 14 E). Average relative current of oocytes uncaged in the presence of 300 μM ZnSO<sub>4</sub> normalized to previous uncaging in zinc-free solution is  $1.06 \pm 0.08$ . Together, this suggests that zinc did not inhibit TMEM16A channel activity and would not be preventing the appearance of the fertilization evoked depolarization by preventing proper channel activity. Together with the absence of the fast block to polyspermy, an early indicator of fertilization, these data suggest that zinc stops fertilization.

### **3.3.5.2 Delayed chelator-dependent rescue of fertility demonstrates a zinc interruption of fertilization**

To ensure that extracellular zinc blocked fertilization, we examined how rapidly TPEN application recovered cleavage furrow appearance from the zinc-induced block of embryonic development. Eggs were fertilized with or without zinc, then 30 minutes following sperm addition transferred to different solutions with or without TPEN. We predicted that if zinc blocked fertilization, the appearance of cleavage furrows in eggs inseminated in zinc would be shifted by the time of TPEN addition, 30 minutes for these experiments. If zinc blocked another event in early embryonic development, the appearance of cleavage furrows would appear by an intermediate time. We found that under control conditions, approximately half of the eggs developed cleavage furrows 79 minutes after sperm addition ( $\pm 0.3$  min, 5 trials, 26 - 58 eggs Figure 15 A). By contrast, half of the eggs inseminated in zinc, then transferred to TPEN developed cleavage furrows 111 min after sperm addition ( $\pm 0.9$  min), or 81 minutes following transfer to

TPEN (Katherine L. Wozniak et al., 2020). These results reveal that in the presence of zinc, sperm are unable to penetrate the egg. Sperm embedded in the jelly coat and transferred to the TPEN solution fertilize upon zinc chelation. These results indicate that *X. laevis* eggs release zinc upon fertilization to protect the zygote from fertilization by additional sperm.

### **3.3.5.3 Eggs can still be activated chemically in the presence of zinc**

To further explore whether zinc inhibits fertilization, rather than initiation and completion of early embryonic developmental processes, I tested whether eggs could be parthenogenically activated in the presence of zinc using the calcium ionophore ionomycin. I incubated *X. laevis* eggs in solution with or without 300  $\mu\text{M}$   $\text{ZnSO}_4$  for 30 minutes prior to addition of 10  $\mu\text{M}$  ionomycin. Eggs were assessed for cortical contraction and terminal division after 120 minutes. In the presence of zinc, the increased intracellular calcium caused by ionomycin is sufficient to activate eggs ( $100 \pm 0\%$ ) at a rate comparable to that of eggs in a zinc-free solution ( $100 \pm 0\%$ , 4 trials, 92 - 186 eggs; Figure 15 B). Egg activation was assessed by cortical contraction of eggs and development of abortive cleavages. This demonstrates that zinc is not able to disrupt calcium-dependent activation or division in the early embryo.

We also tested whether sperm-dependent activation of eggs occurred in the presence of zinc by transferring fertilized eggs to a zinc-containing solution. Eggs were inseminated in solution with or without 1 mM  $\text{ZnSO}_4$  and incubated for 30 minutes before being transferred to solution with or without 1 mM  $\text{ZnSO}_4$ . Eggs inseminated in zinc-free solution, before being transferred to solution with zinc divided  $89.8 \pm 5.2\%$  of the time, while those never in zinc divided at a similar rate ( $85.5 \pm 8.2\%$ ; Figure 13 B). This also suggests that zinc does not affect sperm-dependent activation.

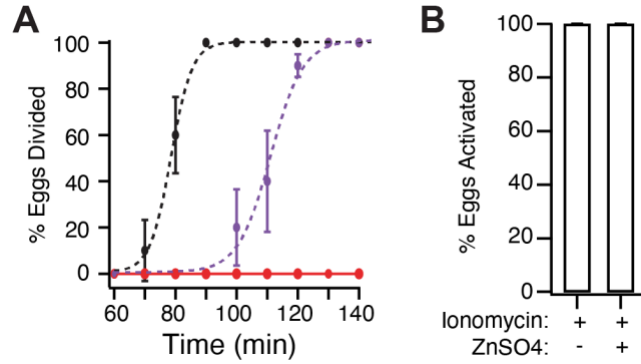


**Figure 15 Extracellular zinc inhibits fertilization, not just development**

A) Proportion of cleavage furrow development from eggs inseminated in and transferred to control conditions (dashed black), inseminated in 300  $\mu\text{M}$   $\text{ZnSO}_4$  and transferred to 600  $\mu\text{M}$  TPEN 30 min following sperm addition (dashed purple), or eggs inseminated in and transferred to 1 mM  $\text{ZnSO}_4$  (solid red;  $N = 26 - 58$  eggs, 7 trials). Plots are fit with sigmoidal functions. B) Eggs pathogenetically activated with calcium ionophore ionomycin undergo activation, marked by cortical contraction and eventual asymmetric terminal cleavage ( $N = 92 - 186$ , 4 trials). Errors are s.e.m.

### **3.3.6 Zinc targets both sperm and egg to stop fertilization**

Fertilization represents the union of two gametes. Therefore, inhibition of fertilization may occur via the disruption of the ability of either gamete to fertilize. To uncover the mechanisms by which zinc disrupts fertilization, we sought to discriminate whether zinc targets eggs or sperm. To do so, we determined whether pretreating each gamete with zinc, then mixing the sperm and eggs together without added zinc, stopped the appearance of cleavage furrows.

#### **3.3.6.1 Zinc inhibition of eggs is concentration dependent**

As previously discussed, eggs pre-treated with 1 mM ZnSO<sub>4</sub> before insemination in zinc-free solution do not develop cleavage furrows (see Section 3.3.4.1; Figure 13 A). By contrast, eggs never exposed to zinc, developed normally. Further, eggs pre-treated in increasing concentrations of zinc demonstrated inhibition of embryonic development in a concentration-dependent manner. Fit of the proportion of developed eggs vs zinc concentration with a sigmoidal function result in an IC<sub>50</sub> of  $73.5 \pm 8.3 \mu\text{M}$  (Figure 16 A, Table 3, 6 trials, 93 – 255 eggs). This concentration is similar to the IC<sub>50</sub> when insemination is performed in zinc (30  $\mu\text{M}$ ; Figure 11 A-B, Table 3). No embryos develop in 300  $\mu\text{M}$  or higher concentrations of ZnSO<sub>4</sub>. This data suggests that the zinc block of fertilization is driven by zinc effects on the egg.

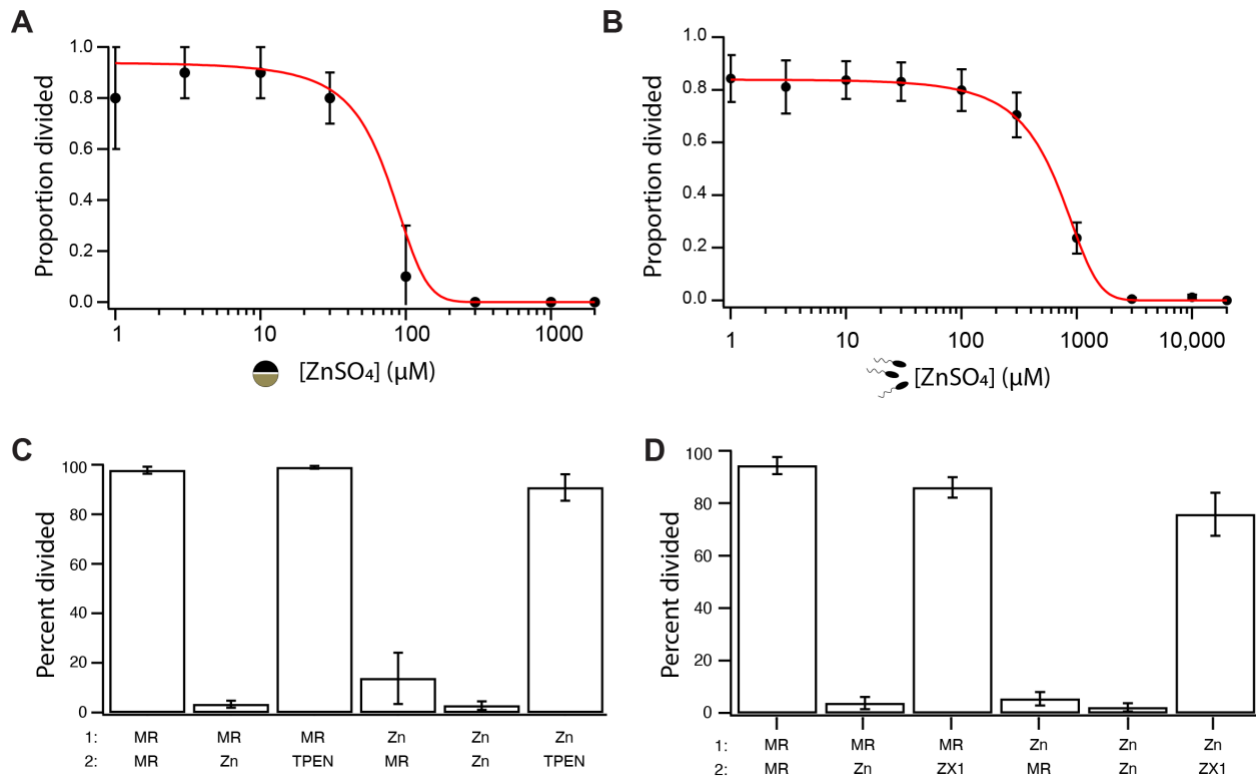


**Figure 16 Zinc inhibits fertilization by interfering with both eggs and sperm.**

A) Eggs pretreated in increasing concentrations of zinc demonstrate a lower proportion of development when used for *in vitro* fertilization (N = 93 - 255 eggs, 6 trials). B) Number of eggs divided decreases with increase in zinc concentration used for sperm pretreatment prior to insemination (N = 121 - 181 eggs, 5 trials). Plots A-B are fit with sigmoidal functions. C-D) Sperm pretreated with 1 mM ZnSO<sub>4</sub> prior to insemination do not lead to developing embryos unless eggs are inseminated in a solution containing 300 μM TPEN (C; N = 156 - 283 eggs, 5 trials) or ZX1 (D; N = 182 - 328 eggs, 4 trials).

### **3.3.6.2 Zinc inhibition of sperm is concentration dependent**

To determine whether zinc targets sperm to disrupt fertilization, we pretreated *X. laevis* sperm by mincing testes in increasing concentrations of zinc approximately 15 min prior to insemination. The embryos were assayed for the development of cleavage furrows 90-120 minutes following sperm addition. Indeed, we observed that fewer eggs developed cleavage furrows when inseminated with sperm pretreated with increasing concentrations of zinc. Fitting incidence of cleavage furrow development against zinc concentration with a sigmoidal function, we determined that the zinc interference of fertilization had a half maximal concentration of  $IC_{50} = 524 \pm 102 \mu\text{M}$  (Figure 16 B, Table 3, 5-21 trials, 152 – 355 eggs). No embryos develop following insemination in sperm minced in 3 mM zinc. Compared to the concentration dependence of fertilizations performed with both gametes in the presence of zinc (Figure 11 A-B), sperm demonstrate a less sensitive concentration response, suggesting that sperm does not drive the zinc block to polyspermy. However, sperm is still responsive to zinc at physiological levels, and therefore should be further explored.

### **3.3.7 Zinc fertilization of *X. laevis* sperm was reversible with zinc chelators**

Having observed that zinc pretreatment was sufficient to stop sperm for fertilizing, we next questioned whether this interaction was reversible using the zinc chelator TPEN. Sperm were pretreated with 1mM  $\text{ZnSO}_4$ , which almost completely stopped fertilization ( $1.40 \pm 0.78\%$  division, 5 trials, 156 – 283 eggs; Figure 16 C). Insemination in 300  $\mu\text{M}$  TPEN did not interfere with fertilization or embryonic development when sperm pretreated in a zinc-free solution were used to inseminate eggs ( $97.4 \pm 0.88\%$  division). When zinc pretreated sperm were used to

inseminate eggs in 300  $\mu$ M TPEN, we observed that TPEN was sufficient to completely reverse the fertility deficit (mean  $90.8 \pm 5.36\%$  division; Figure 16 C). This demonstrates that a non-covalent interaction with sperm components drives the inhibition of fertilization, much like we've seen when eggs alone are treated with zinc and rescued with a chelator (Figure 11 D).

To understand whether intracellular or extracellular zinc in sperm causes a decrease in fertility, we sought to determine whether loss of extracellular zinc rescued the zinc-induced infertility phenotype. The cell impermeant zinc chelator ZX1 was used for this purpose. In 4 independent trials (184 – 334 eggs), sperm pretreated with 1 mM zinc, which is demonstrated to result in a nearly complete loss of fertility ( $3.86 \pm 2.32\%$  division; Figure 16 D) were used to inseminate eggs in solution with or without the cell-impermeant chelator ZX1. When sperm were pretreated in a solution with no added zinc and used to inseminate eggs in 300  $\mu$ M ZX1, no defect of division was observed ( $86.0 \pm 3.9\%$ ). When zinc pretreated sperm were used to inseminate eggs in the presence of 300  $\mu$ M ZX1, we observed a rescue of fertility (mean  $76 \pm 8\%$  of eggs) compared to zinc untreated sperm used to inseminate eggs in control solution ( $94 \pm 3\%$  of eggs; Figure 16 D). This suggests that the chelation of extracellular zinc is sufficient to fully reverse the loss of fertility and suggests that, like in the egg, ZX1 either buffered extracellular zinc important for the block of fertilization or altered the zinc gradient in such a way that intracellular zinc important for the block leaves the cell.

### **3.3.8 Zinc's identity as a divalent transition metal is key for its ability to block fertilization**

The zinc disruption of *X. laevis* fertilization is reversible by chelation (Figure 11 D). This finding thereby suggests zinc acts by binding to a protein or receptor and not by mediating a

chemical reaction (e.g., redox reaction). If extracellular zinc disrupted fertilization through protein coordination, we would expect other transition metals would act similarly. Metal-protein interactions become more potent in a predictable pattern called the Irving-Williams series, which depicts the strength of divalent transition metal-protein complexes:  $\text{Co} < \text{Ni} < \text{Cu} > \text{Zn}$  (R. J. P. Williams, 1987). To uncover how other transition metals in this series altered *X. laevis* fertilization, we inseminated in varying concentrations of extracellular copper, cobalt, or nickel. Development was blocked in a concentration-dependent manner in the presence of all transition metals tested (Figure 17 A-B). Using the half-maximal concentration of each metal that blocks embryonic development, we determined that the potency of the transition metals indeed followed the Irving-Williams series (R. J. P. Williams, 1987): copper acted with the highest affinity and cobalt with the lowest (Figure 17 A-B, Table 3) (Katherine L. Wozniak et al., 2020). This further supports that zinc inhibits fertilization by coordination with extracellular proteins. We propose that release of zinc from the cortical granules upon fertilization modifies the extracellular proteins to block entry by additional sperm.

### **3.3.9 Copper targets both gametes to stop fertilization**

Having demonstrated that zinc's inhibition of fertilization is dependent on its identity as a divalent transition metal, and that zinc can inhibit the fertility of both eggs and sperm, we sought to understand how other divalent transition metals would affect the fertility of individual gametes.

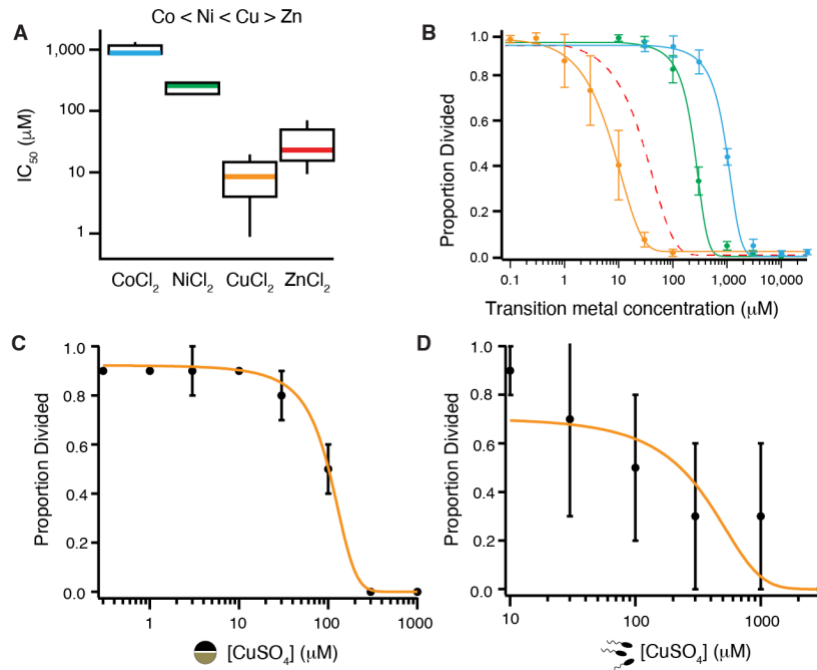


**Figure 17 Divalent transition metals such as copper also effect eggs and sperm**

A) Box plot distributions of the  $IC_{50}$ s of inhibition of appearance of cleavage furrows in *X. laevis* eggs inseminated in cobalt (blue), nickel (green), copper (orange), or zinc (red). B) Proportion of division of *X. laevis* eggs inseminated in varying concentrations of extracellular cobalt (N=148-295 eggs, 5 trials), nickel (N=136-283 eggs, 5 trials), or copper (N=230-321 eggs, 5 trials). C-D) Proportion of eggs that develop cleavage furrows following pretreatment of eggs (C) or sperm (D) in increasing concentrations of copper prior to insemination. Plots are fit with sigmoidal functions.

### **3.3.9.1 Copper block of eggs is concentration dependent**

To characterize the concentration dependence of the copper block on egg fertility, eggs were pretreated in increasing concentrations of extracellular copper. Following 2 washes, pretreated eggs were inseminated in copper-free solution. We observed a decrease in proportion of dividing embryos with increasing concentrations of copper (5 trials, 198 – 336 eggs). Fitting proportion of development against copper concentration with a sigmoidal curve, we calculated an  $IC_{50} = 121.7 \pm 23.2 \mu\text{M}$  (Figure 17 C, Table 3). At 300  $\mu\text{M}$   $\text{CuSO}_4$  and higher concentrations, we don't observe any embryonic development. Like zinc, copper blocks fertilization in pre-treated eggs.

### **3.3.9.2 Copper block of sperm is concentration dependent**

To discriminate whether copper can target sperm to interfere with fertilization, we pretreated sperm with varying concentrations of extracellular copper 15 minutes before addition to eggs and observed the rate of cleavage furrow development. We observe that when sperm were pretreated with higher concentrations of copper, fewer eggs develop. By fitting plots of incidence of cleavage furrow development versus copper concentration with sigmoidal functions, we found a half maximal concentration of  $517.9 \pm 516.3 \mu\text{M}$  (4 trials, 121 – 254 eggs; Figure 17 D, Table 3). This indicates, that like zinc, copper also affects the ability of sperm to fertilize the egg.

## **3.4 Discussion**

Like mammals, fertilization initiates a zinc release from eggs of amphibians and teleost fish (Katherine L. Wozniak et al., 2020). As demonstrated in *X. laevis*, this zinc likely acts to

protect the fertilized egg from polyspermy. Additionally, extracellular zinc inhibits embryonic development in diverse phyla (Figure 18). Although the details on how zinc modifies an egg to prevent sperm entry are yet to be determined, our data suggests that a process that protects fertilized egg from multiple fertilizations is shared between humans and the polyps (*H. symbiologicarpus*) that live on hermit crabs.

Using experiments described here, we were the first to directly test the ability of zinc to prevent fertilization. Though early zygotic developmental milestones are used as a readout for fertilization in most assays, electrophysiological, and developmental data support that no fertilization occurs in the presence of excess extracellular zinc. No fertilization-evoked depolarization, characteristic of the fast block to polyspermy, was observed in *X. laevis* eggs inseminated in extracellular zinc. I also confirmed that TMEM16A, the ion channel that mediates the depolarization, is not inhibited by extracellular zinc which enters the cell. In addition, rescue of the fertility of *X. laevis* eggs inseminated in the presence of zinc was delayed by the time it took to add the zinc chelator TPEN. This suggests that until chelator addition, sperm were unable to enter the egg. Further, extracellular zinc was not able to disrupt activation or division of *X. laevis* eggs either parthenogenetically or following fertilization. These data strongly support that zinc inhibits fertilization altogether.

Though specific mechanisms of zinc inhibition of fertilization are still not clear, data presented gives key insight. We have demonstrated that the zinc interacts with both egg and sperm, with egg driving the inhibition. This reflects the typical view of polyspermy blocks, whereby the egg is largely responsible for keeping sperm out of the egg. Other data from our lab suggests that the extracellular matrix of the egg is modified and maintains a high zinc concentration (Katherine L. Wozniak et al., 2020). This is in some way particular to *X. laevis* and other external fertilizers

with a jelly coat surrounding the egg. However, the jelly coat surrounding the egg is comprised of glycoproteins (Wyrick, Nishihara, & Hedrick, 1974), similar to the composition of the highly conserved vitelline envelope (termed the zona pellucida in mammals) (Bleil & Wassarman, 1980; Wolf et al., 1976; Yurewicz et al., 1975). It was previously found that in mouse eggs, zinc content of the zona pellucida increases by 300% and contributes to hardening of the zona pellucida, which is believed to keep sperm out of the egg (E. L. Que et al., 2017). This further demonstrates the conservation of the slow block to polyspermy, wherein evidence exists for the conservation of the zinc release, the composition of the egg extracellular matrix, the effect of zinc on the hardening of the extracellular matrix, and the importance of the hardening in keeping sperm out of the egg.

Our data also demonstrate that the sperm is affected by zinc. This is a paradigm shifting result suggesting that during the slow block to polyspermy, sperm are not only thwarted by the impenetrable extracellular matrix of the egg, hardened by the released zinc, but also are also themselves made less able to fertilize an unmodified egg. Further exploration of the interaction of extracellular zinc and sperm is covered in Chapter 4.

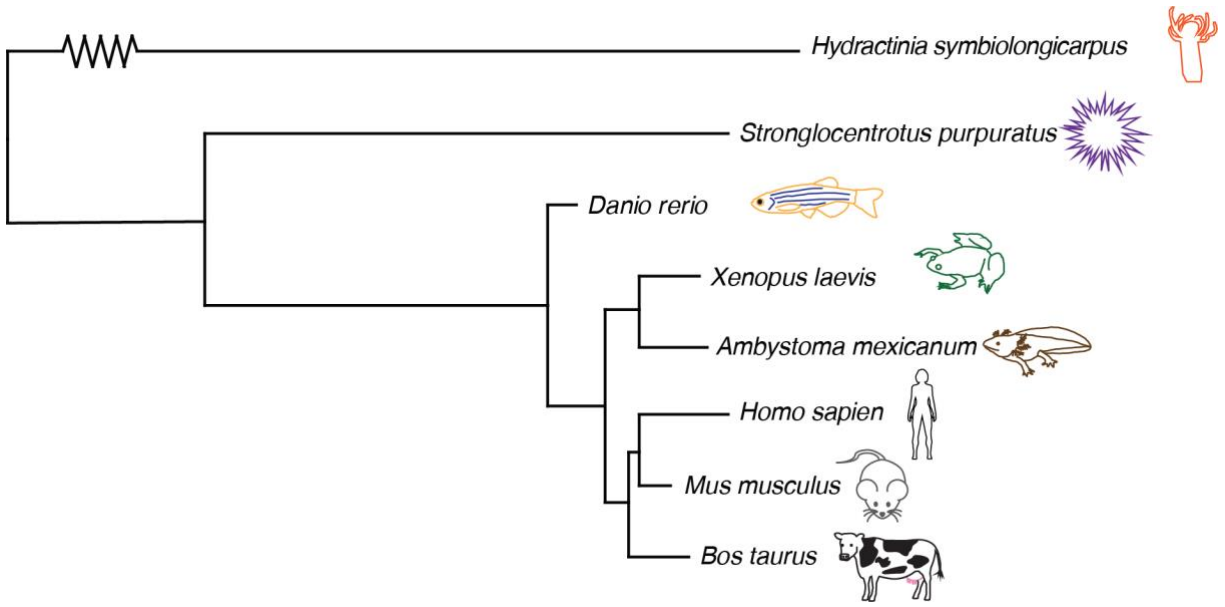


**Figure 18 Zinc protection of eggs is an ancient phenomenon**

Phylogenetic tree of species which demonstrate zinc release at fertilization or egg activation (*D. rerio*, *X. laevis*, *A. mexicanum*, *Homo sapien*, *M. musculus*, *B. taurus*) (Duncan et al., 2016; Kim et al., 2011; Emily L. Que et al., 2018; Katherine L. Wozniak et al., 2020) or zinc protection of eggs from fertilization (*H. symbiolongicarpus*, *S. purpuratus*, *X. laevis*).

## 4.0 Mammalian sperm import extracellular zinc

### 4.1 Introduction

Between mating and fertilization, mammalian sperm encounter high concentrations of zinc at two discrete stages: when mixed with the seminal fluids at mating, and when encountering an already fertilized egg (Figure 19). Seminal fluid has the highest relative zinc content in the body, with measurement of total zinc in human semen ranging from 1-3 mM (Saaranen et al., 1987), compared to serum concentrations of 12-14  $\mu\text{M}$  (Hennigar et al., 2018). Despite this large enrichment of zinc, how this zinc targets sperm and regulates the processes that sperm undergo between mating and fertilization is not yet understood.

Mammalian sperm are distinguished from other animal sperm in that they are unprepared to fertilize at mating, even if placed directly next to an egg (R Yanagimachi, 1988). By mixing with the seminal fluids and spending time in the female reproductive tract, mammalian sperm gain the capacity to fertilize by undergoing processes collectively referred to as “capacitation” (Figure 19, upper track) (R Yanagimachi, 1988). Although sperm encounter high concentrations of zinc between mating and fertilization, capacitation has been studied largely in the absence of zinc. I seek to understand how zinc targets sperm and alters capacitation.

To uncover how zinc regulates mammalian sperm, I am studying mouse and human sperm, as well as porcine and human seminal fluid.

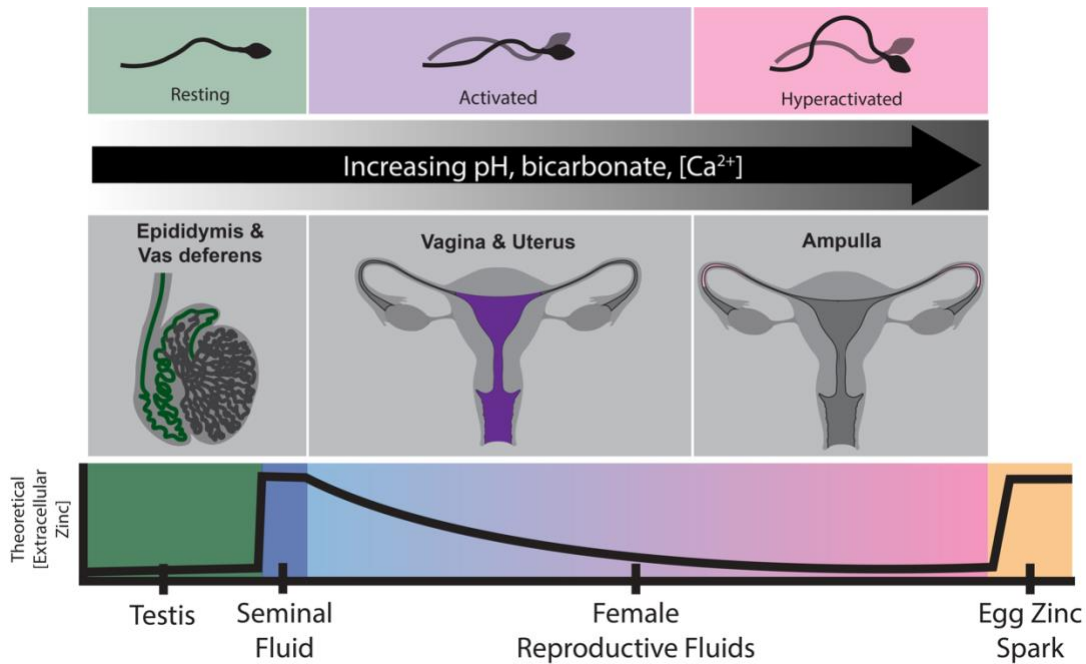


**Figure 19 Mammalian sperm encounter changing conditions throughout fertilization**

Throughout their journey from the male reproductive system, through the female reproductive system towards the egg, sperm encounter changing environments. These cells are mixed into a high zinc environment in the seminal fluid prior to ejaculation into the female reproductive tract. Within the female reproductive tract, zinc levels are unknown. However, it is expected that as sperm move away from the site of deposition, zinc levels will drop, unless the sperm reach a fertilized egg undergoing its zinc spark. It is also known that increasing pH, bicarbonate, and calcium levels induce physiologic changes termed capacitation, which alter sperm behavior, preparing them to fertilize an egg.

## 4.2 Materials and methods

### 4.2.1 Sperm and seminal fluid sources

Mouse (*Mus musculus*) sperm are obtained from the vas deferens and epididymides of retired Swiss Webster breeders. Human semen is donated from patients at the Andrology and Fertility Preservation Laboratory at the UPMC Magee Center for Reproduction and Transplantation. Human samples were surplus from fertility testing which would otherwise be discarded. Porcine semen is obtained commercially (S&S Farms, Ramona, CA).

### 4.2.2 Quantification of labile zinc in seminal fluid

To quantify the labile zinc in human and porcine semen, sperm and other cells were removed by sedimentation and proteins were removed by passage through a 3 kDa centrifugal filter unit. Samples were diluted in a HEPES-buffered saline (HS) solution (135 mM NaCl, 5 mM KCl, 2 mM CaCl<sub>2</sub>, 1 mM MgSO<sub>4</sub>, 20 mM HEPES, 10 mM lactic acid, 5 mM dextrose, 1 mM sodium pyruvate, pH = 7.4) (Anne E. Carlson et al., 2003) with 30 nM of the fluorescent Zn<sup>2+</sup> indicator FluoZin-1. FluoZin-1 fluorescence intensity measurements were recorded using a BioTek Cytation 5 plate reader. Samples were excited with 494 nm light and emission was recorded at 515 nm, with 10-nm slit widths. We corrected for the raw photometric signals by subtracting the background and calculated the labile Zn<sup>2+</sup> by comparing the fluorescent readings against a standard curve fit with a single-site binding model.

### 4.2.3 Quantification of sperm cytoplasmic zinc

Sperm were loaded with cytoplasmic fluorescent  $Zn^{2+}$  indicator FluoZin-3-AM with a final concentration of 5  $\mu M$ . Approximately 0.2% Pluronic (Invitrogen) was used to increase permeability of sperm to FluoZin-3-AM. Sperm were added in HS buffer. For zinc pre-loaded sperm,  $ZnSO_4$  was added for a final concentration of 30  $\mu M$ . Sperm were incubated at room temperature away from light for 30-40 minutes. To wash, sperm suspension was sedimented by centrifugation at 2000 RPM for 5 minutes. This was repeated for 2-3 washes.

FluoZin-3 fluorescence was assayed using BioTek Cytation 5 plate reader, with 492 nm excitation, 514 nm emission light, and 10 nm slit width. Data were corrected for raw photometric signals by subtracting the fluorescence obtained from samples with the  $Zn^{2+}$  chelator TPEN (Arslan et al., 1985) and normalized to the signal of sperm treated with 1 mM of the  $Zn^{2+}$  ionophore pyrithione (Barnett, Kretschmar, & Hartman, 1977) and 1 mM  $Zn^{2+}$ . Normalization allowed us to compare results between independent trials, despite variability between sperm numbers. Technical replicates within each experimental trial, as well as collection of raw FluoZin-3 signal prior to treatment application, allowed us to verify that each sample had roughly the same number of sperm.

## 4.3 Results

### 4.3.1 Quantification of labile zinc in semen

Although the total zinc content of seminal fluids has been reported to be 1-3 mM, most of this zinc is likely bound to various proteins. We therefore sought to quantify the labile zinc present in pig and human seminal fluid. FluoZin-1, rather than FluoZin-3, was chosen for these extracellular measurements as it is suited for measuring labile  $Zn^{2+}$  in solutions with  $\mu M$  concentrations (Gee, Zhou, Qian, & Kennedy, 2002). We found that pig semen contains  $9.6 \mu M$   $Zn^{2+}$  ( $\pm 0.4 \mu M$ ;  $N=8$ ), while human contains  $5.0 \mu M$  ( $\pm 0.7 \mu M$ ;  $N=3$ ). This represents a biologically relevant concentration of labile  $Zn^{2+}$  that we will utilize in our experiments.

### 4.3.2 Mammalian sperm readily take up zinc

To probe whether mammalian sperm can import physiologic concentrations of zinc, I used FluoZin-3 to monitor intracellular zinc before and after zinc application. To do so, I loaded mouse sperm with FluoZin-3. I observed zinc-induced fluorescence immediately after treatment with  $10 \mu M$   $ZnSO_4$  (Figure 20, upper, 4 trials), which approximates the physiological concentration of labile zinc in mammalian seminal fluid (Section 4.3.1). At 60 minutes, sperm treated with  $10 \mu M$   $ZnSO_4$  reached a relative FluoZin-3 fluorescence level of  $0.60 \pm 0.17$  (where relative 0 is fluorescence of sperm treated with 1 mM TPEN, and relative 1 is fluorescence of sperm treated with 1 mM zinc ionophore pyrithione and 1 mM  $ZnSO_4$ ). Treatment with  $30 \mu M$   $ZnSO_4$  resulted in relative fluorescence of  $0.91 \pm 0.11$ , similar to the fluorescence of sperm treated with pyrithione (Figure 20, upper). Human sperm behaved similarly (5 trials). Treatment of FluoZin-3-AM loaded

human sperm demonstrated an increase in fluorescence within minutes of treatment with 10  $\mu\text{M}$   $\text{ZnSO}_4$  and continued to rise over 60 minutes ( $0.41 \pm 0.11$  relative fluorescent units; Figure 20, lower). In sperm from both species, this increase of cytoplasmic zinc continued to increase and stayed stably high for 3 hours in treatment (data not shown). Interestingly, in both mouse and human sperm, addition of the zinc chelator TPEN lowered the FluoZin-3 fluorescence for both mouse and human sperm, with a more dramatic effect observed in human sperm. This demonstrates elevated basal zinc within our sperm samples, with human sperm carrying a larger basal concentration of zinc. This is notable, as our mouse sperm samples are isolated from the epididymis, while human samples are isolated from ejaculate, and have therefore been in contact with zinc-containing seminal fluid.

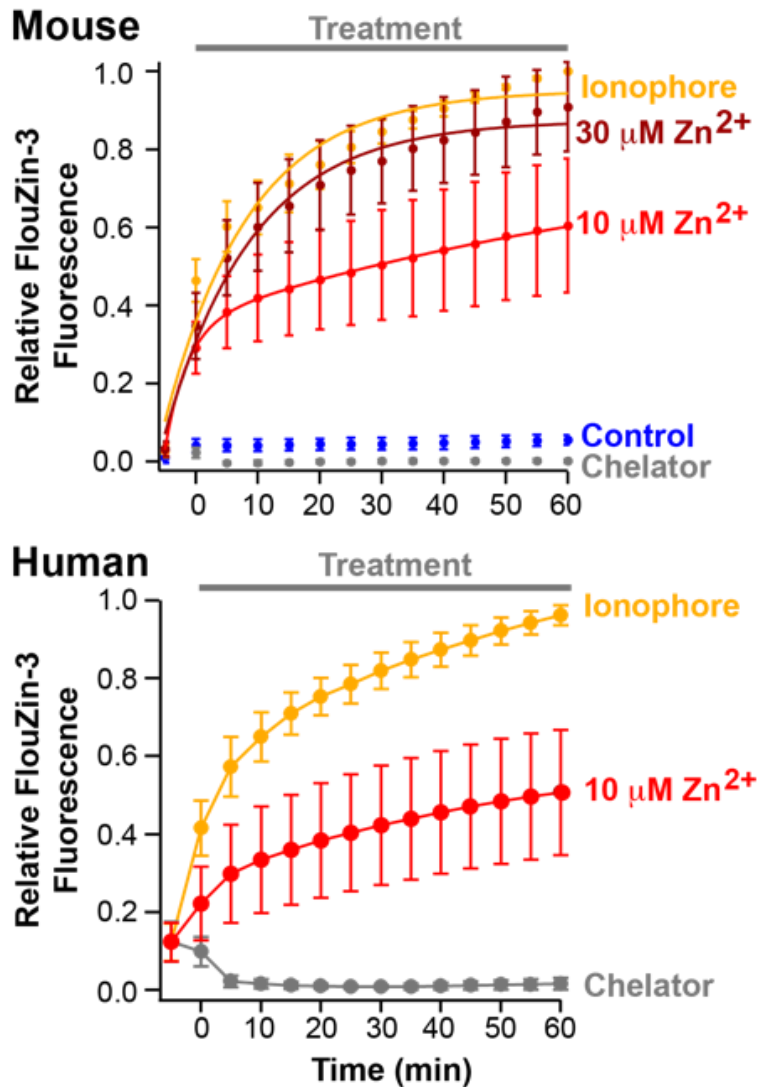


**Figure 20 Mammalian sperm import extracellular zinc**

Measurement of cytoplasmic zinc content of both mouse and human sperm as reported by relative FluoZin-3 fluorescence over time reveals that treatment with 10  $\mu\text{M}$  or 30  $\mu\text{M}$   $\text{Zn}^{2+}$  leads to uptake of zinc into the sperm cytoplasm. Relative 0 level of fluorescence is established by fluorescence of sperm treated with the zinc chelator TPEN, while the relative 1 is established by fluorescence of sperm treated with the zinc ionophore pyrithione and 1mM  $\text{Zn}^{2+}$ .

### 4.3.3 Cytoplasmic zinc decreases in the presence of zinc chelators and capacitating signals

To determine whether sperm maintain elevated cytoplasmic zinc following removal of excess extracellular zinc, I loaded sperm with FluoZin-3 AM and  $30\ \mu\text{M}\ \text{Zn}^{2+}$  for 30 minutes before sedimentation and resuspension in zinc-free control solution (6 independent trials). These sperm retained high cytoplasmic zinc, as indicated by FluoZin-3 fluorescence (average  $0.93 \pm 0.10$  FluoZin-3 fluorescence relative to initial reading). I next explored whether sperm retained elevated cytoplasmic zinc during *in vitro* capacitating incubations. To test this, I loaded sperm with FluoZin-3 AM and  $30\ \mu\text{M}\ \text{Zn}^{2+}$  and then treated these sperm with capacitating incubations, including  $15\ \text{mM}\ \text{HCO}_3^-$  and  $5\ \text{mg/mL}$  bovine serum albumin (BSA) (A. E. Carlson et al., 2005). This resulted in a loss of cytoplasmic zinc (average  $0.19 \pm 0.03$  relative FluoZin-3 fluorescence) similar to sperm treated with  $1\ \text{mM}$  TPEN (average  $0.14 \pm 0.51$  relative FluoZin-3 fluorescence; Figure 21) in both mouse and human sperm. This suggests that capacitation stimulates a reduction of cytoplasmic zinc in mammalian sperm.

Following this result, I sought to determine if either of the active ingredients in *in vitro* capacitating buffer, BSA or  $\text{HCO}_3^-$ , were sufficient to deplete the cytoplasmic zinc. After incubating sperm with FluoZin-3 AM and  $30\ \mu\text{M}$  zinc, I treated with either  $15\ \text{mM}\ \text{HCO}_3^-$  or  $5\ \text{mg/mL}$  BSA. I observed that  $\text{HCO}_3^-$  had no effect on cytoplasmic zinc levels ( $1.0 \pm 0.3$  relative FluoZin-3 fluorescence, 5 trials), compared to sperm treated with control solution ( $1.0 \pm 0.02$  relative FluoZin-3 fluorescence, 4 trials). BSA led to immediate depletion of cytoplasmic zinc ( $0.12 \pm 0.02$  relative FluoZin-3 fluorescence, 5 trials; Figure 22). BSA can chelate zinc, making it difficult to separate direct and indirect effects of the capacitating agent on zinc dynamics.

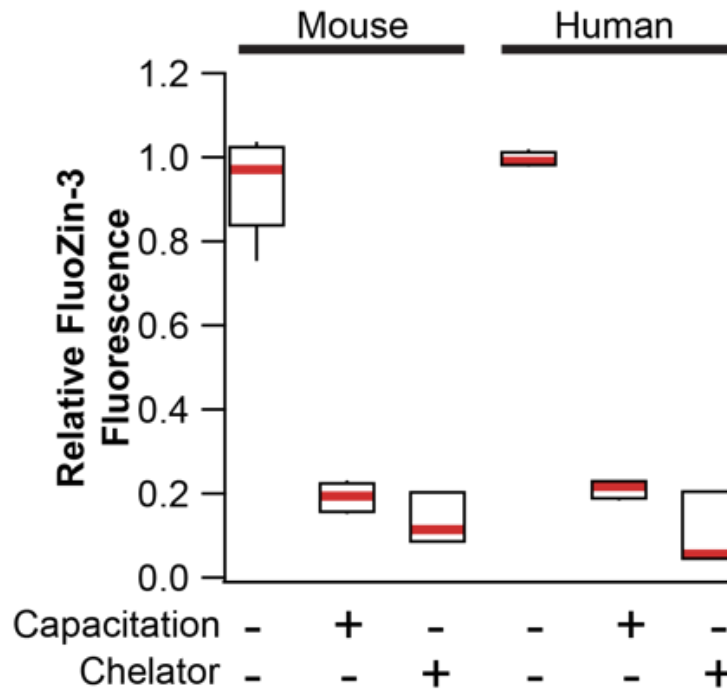


**Figure 21 Chelation and capacitation lead to cytoplasmic zinc loss**

In both mouse and human sperm preloaded with zinc, treatment with either the zinc chelator TPEN or commonly used *in vitro* capacitating conditions (A. E. Carlson et al., 2005) lead to loss of cytoplasmic zinc reported as FluoZin-3 fluorescence relative to levels before treatment.

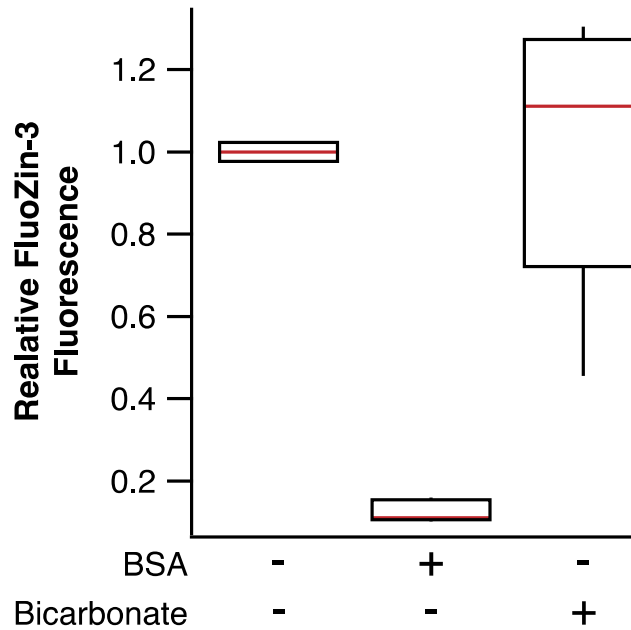


**Figure 22 BSA, but not bicarbonate leads to cytoplasmic zinc depletion**

Individual components of commonly used *in vitro* capacitation conditions, BSA and sodium bicarbonate were tested for their ability to induce loss of cytoplasmic zinc in mouse sperm. Treatment with BSA, not  $\text{HCO}_3^-$ , lead to reduced cytoplasmic zinc, reported as FluoZin-3 fluorescence relative to levels before treatment.

#### **4.3.4 Transcripts for zinc transporters are expressed in the developing sperm**

To identify candidate zinc transporters present in mouse and human sperm, we interrogated RNAseq datasets for mouse and human elongating spermatids (Figure 23) (C. D. Green et al., 2018; Shami et al., 2020). Mature sperm are transcriptionally quiescent, so we predicted that protein present in a mature sperm will be present as RNA transcript in the developing spermatid. From these datasets, we identified all known zinc transporters. RNAseq data suggests the expression of zinc transporters known to localize to the plasma membrane (ZIP1 and ZIP10; Figure 24) (Baltaci & Yuce, 2018; Kambe, Suzuki, & Komori, 2019) in mouse elongating spermatids.

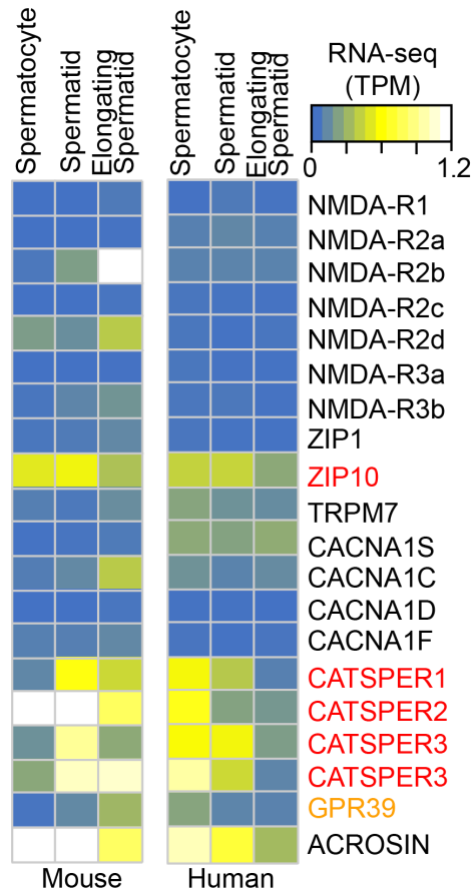


**Figure 23 Transcripts of known or suspected zinc importers in mammalian developing sperm**

Several proteins with known or suspected zinc transporting ability are expressed in the human and mouse developing sperm (C. D. Green et al., 2018; Shami et al., 2020). Candidate proteins to lead to cytoplasmic zinc increase are in red. Acrosin is listed as a known sperm protein.

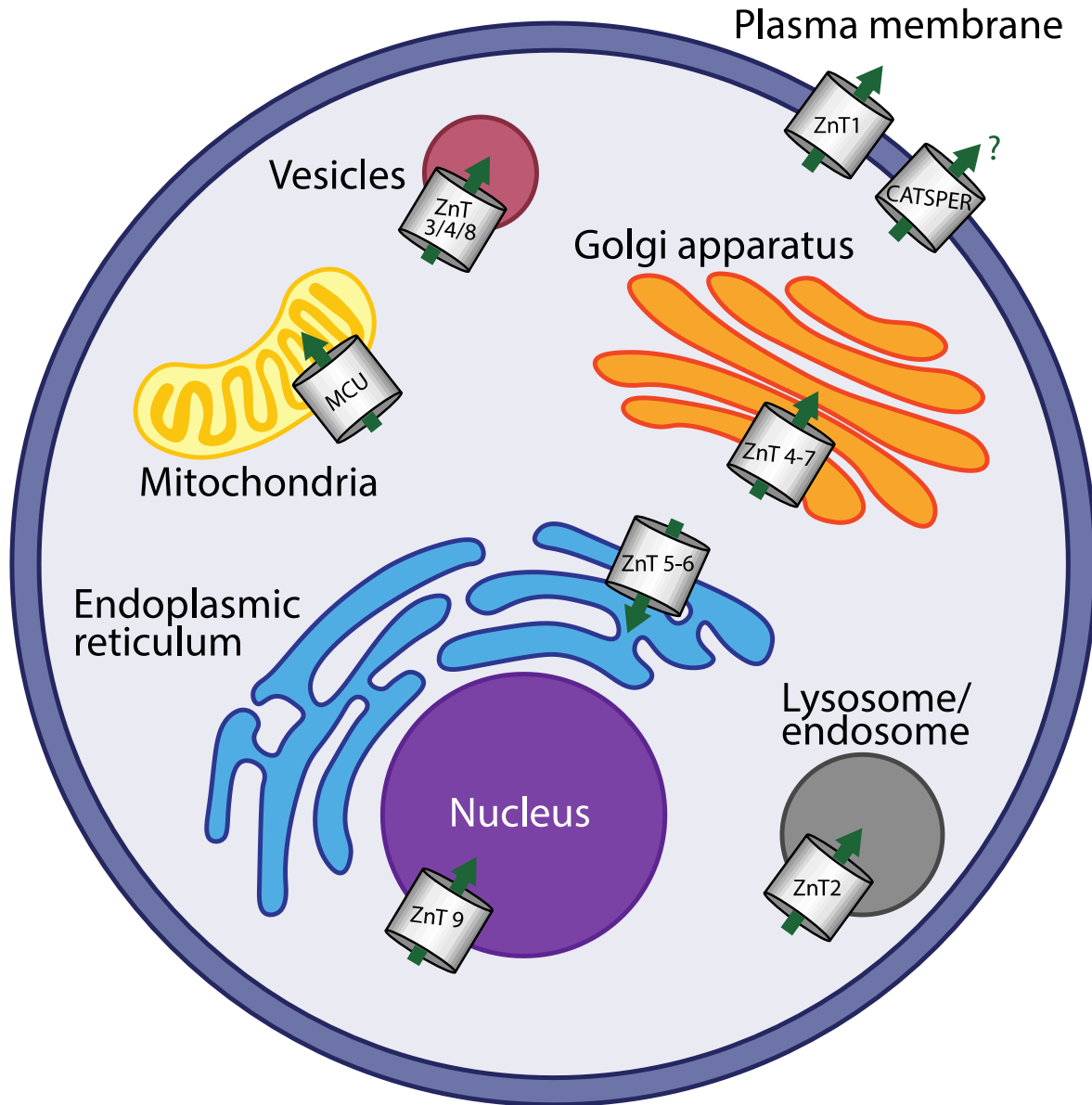


**Figure 24 Known cellular localization of zinc transporters in mammalian sperm**

Several zinc transporters are likely present in mammalian sperm with the ability to shuttle zinc out of the cytoplasm (Baltaci & Yuce, 2018; Kambe et al., 2019) out of the cell, or into subcellular organelles.

#### 4.4 Discussion

I have demonstrated that extracellular zinc enters sperm and is depleted upon treatment with chelators or capacitating incubations. It is not yet clear which transporters or channels move this zinc, or where the zinc goes. It is possible that zinc is transported out of sperm and into the extracellular space during capacitation, or may be shuttled to intracellular organelles.

Continuing work will explore how zinc import affects important sperm functions necessary for fertilization, such as motility, hyperactivation, and the acrosome reaction. Seminal zinc has been explored as a method of predicting male fertility and sperm quality. A large study of fertile and infertile men reported seminal, but not blood zinc levels as significantly lower in their infertile population than in the fertile population, correlating with sperm density, motility, and viability (Chia, Ong, Chua, Ho, & Tay, 2000). It is known that zinc is vital for proper spermatogenesis. However, this supports that zinc is important for maintaining the health of mature sperm.

I believe that it is in reason that capacitating behaviors would be suppressed in increased extracellular zinc, as this mimics the environment where sperm should still be quiescent, before activating within the female reproductive tract (Figure 19). I expect all behaviors important for fertilization to be impeded following increase of cytoplasmic zinc. Zinc inhibition of motility and acrosome reaction have been demonstrated before, though the mechanism was not explored (Riffo et al., 1992). A study using image-based flow cytometry using boar, bull, and human sperm demonstrate that sperm placed in high extracellular zinc (1 mM  $ZnCl_2$ ) tend to retain zinc throughout the entire sperm body (Kerns, Zigo, Drobnis, Sutovsky, & Sutovsky, 2018). However, boar sperm which retained this signature of zinc enrichment through the entire sperm body did not tend to undergo the acrosome reaction, supporting that high cytoplasmic zinc and capacitation are not compatible (Kerns et al., 2018). Further understanding of how sperm import extracellular zinc

will reveal which effects are the result of disruption of intracellular mechanisms. Previous work demonstrated that while the zinc effect on motility was reversible, acrosome reaction was never recovered (Riffo et al., 1992). This suggests independent mechanisms of action. In fact, it was suggested that the inhibition of the acrosome reaction may be through disruption of membrane permeability to potassium (Riffo et al., 1992). Any effect of extracellular zinc on sperm fertility may be leveraged naturally by the zinc spark, and can be leveraged artificially in contraceptives.

Mammalian sperm are exposed to high extracellular zinc at mating, when they are mixed with seminal fluid, which includes the highest concentration of zinc relative to the rest of the body in humans, with free zinc in the  $\mu\text{M}$  range. Therefore, I also examined whether extracellular zinc was capable of entering mammalian sperm. Using both mouse and human sperm, I demonstrated that sperm uptake extracellular zinc into their cytoplasm minutes upon introduction and continue to stably increase for hours. This cytoplasmic zinc was reduced with application of a zinc chelator or by incubation under capacitating conditions. Continuing work will explore how zinc enters and leaves the cytoplasm, and how increased cytoplasmic zinc affects sperm functions such as motility, hyperactivation, and acrosome reaction.

## **5.0 Discussion**

### **5.1 Summary**

This dissertation builds on the foundation of knowledge of *Xenopus laevis* fertilization, expanding our understanding of the molecular mechanisms by which the fast block to polyspermy occurs in the fertilized egg, as well as utilizing this classical developmental model to demonstrate that the extracellular zinc surrounding newly fertilized eggs, modifies eggs and sperm to prevent entry of additional sperm. This dissertation also studied fertilization in diverse species to demonstrate that the zinc protection of eggs from sperm penetration is conserved from Cnidaria to amphibians. Zinc targets both *X. laevis* egg and sperm to stop fertilization. Finally, I also demonstrated that extracellular zinc readily enters mouse and human sperm, where it may regulate sperm physiology.

### **5.2 Future directions**

The impacts of studies on the fast block to polyspermy or the role of zinc in regulating fertilization can have far reaching consequence for the fields of health and conservation, in addition to understanding basic science of fertilization.

## **5.2.1 Further experiments**

### **5.2.1.1 Zinc protection of fertilized eggs**

Our data is the first to directly demonstrate that insemination in extracellular zinc stopped any indication of successful fertilization, such as the development of cleavage furrows. Moving forward, visualization of sperm within the fertilized egg, following *in vitro* fertilization with and without extracellular zinc would be the gold-standard to demonstrate that zinc prohibits sperm entry into the egg. Due to the vast differences in size between the *X. laevis* sperm and the egg, in combination with the strong autofluorescence of the egg cytoplasm, it has been difficult to perform this microscopy. Clearing of the egg cytoplasm following fertilization and fixation, as well as use of flattened, de-jellied eggs should improve visibility and possibility of viewing the sperm.

### **5.2.1.2 Mammalian sperm uptake of extracellular zinc**

I have demonstrated that zinc is enriched in the cytoplasm of both mouse and human sperm when these cells encounter extracellular zinc at levels at or above that measured in the mammalian seminal fluid. Next, we will need to identify the transporters or ion channels that move this zinc and determine whether this zinc ends up in intracellular organelles or remains in the cytoplasm. My data suggests that during capacitation, the zinc imported into the sperm when mixed with the seminal fluid is transported out of sperm and into the extracellular space. In future experiments, inhibition of ZIP1, the zinc transporter predicted to be expressed in the plasma membrane of the sperm cell, could be used to inhibit sperm entry through these transporters. However, ZIP transporters have no pharmacologic inhibitors, so one would need to be developed, or a testis specific KO model created. This will uncover whether ZIP1 mediates zinc entry into mammalian sperm. The cell impermeant zinc chelator ZX1 as well as antibodies against ZIP1 and ZIP10 can

also be used to explore the role of intracellular zinc in fertilization and acrosome reaction. Mouse sperm incubated in ZX1 can be utilized to understand the role of intracellular zinc in hyperactivation. ZX1 will chelate all extracellular zinc, so that any remaining phenotype following zinc treatment can be linked to the action of intracellular zinc. Though there is no antibody shown to work against ZIP1 in *X. laevis*, an antibody against the N-terminal region can be used which is conserved between *M. musculus* and *X. laevis* (Invitrogen PA5-77766). One will need to verify the specificity of these antibodies in both species using Western blots and verify ability to block zinc transport using cells overexpressing ZIP1 or ZIP10.

## **5.2.2 Wider impacts**

### **5.2.2.1 Contraceptives**

About 10% of women worldwide have an unmet need for contraception (United Nations Department of Economic and Social Affairs, 2020). Hormonal birth control has significant side effects that make it a suboptimal choice for many women (Le Guen, Schantz, Régnier-Loilier, & de La Rochebrochard, 2021). Even more significantly, many women have medical conditions that make them unable to tolerate hormonal birth control. Only one long-acting reversible contraceptive is available: the copper IUD. For this reason, development of non-hormonal birth controls is still needed. The copper IUD provides up to 10 years of protection ("ParaGard T 380A (prescribing information),") against pregnancy but has an early removal rate of 25% (Hubacher, Chen, & Park, 2009). This is likely due to the fact that 38% of women report that the copper IUD leads to more painful periods with increased menstrual and intermenstrual pain and bleeding, a side effect unique to this device (Hubacher et al., 2009). Review of studies performed in humans has provided insight into the mechanism of action of copper IUDs, and in turn, their side effects (Ortiz & Croxatto,

2007). This study revealed that the common belief that copper IUDs function by preventing implantation of the embryo via an inflammatory reaction is not supported by the data. Instead, it appears that in almost all cases, fertilization does not occur in the presence of a copper IUD (Ortiz & Croxatto, 2007).

In response to the high rate of pain associated with copper IUDs and the prevalence of early removal, a recent study examined the option of a zinc IUD (Shankie-Williams, Lindsay, Murphy, & Dowland, 2022). In an early study in the rabbit cervix, the zinc IUD underperformed compared to the copper IUD, resulting in a single implantation (Zipper, Medel, & Prager, 1969), resulting in a loss of interest in zinc as a contraceptive option. This imperfect block of fertilization, however, is likely due to the long length of the uterine horn in rabbit, leading to an insufficiently low concentration to prevent fertilization (Shankie-Williams et al., 2022). In fact, the recent study in mouse reported that zinc IUDs are 100% effective, an equal protection from implantation to copper IUDs. The zinc IUD was safe and effective for 16 weeks, and reversible after 12 weeks use with reduced inflammatory damage to the uterine epithelium compared to the copper IUD (Shankie-Williams et al., 2022). This represents a bright future for zinc as a contraceptive.

Due to the high bioavailability of zinc, the body is well prepared to handle excess zinc without causing long-term damage. In both cats (Fagundes et al., 2014) and dogs (Oliveira et al., 2007), zinc gluconate has been tested as an irreversible chemical castration agent. Zinc is also emerging as a useful and safe component for biodegradable bone implants (Yang et al., 2020). In all cases, the noncarcinogenic characteristics and low toxicity of zinc (Bodar et al., 2005) make it a great candidate for long-term medical interventions such as contraceptives.

With continuing examination of the effect of zinc on eggs and sperm, we can uncover other mechanisms to exploit to inhibit fertilization or toxify zygotes and early embryos.

### **5.2.2.2 Environmental concerns due to zinc and copper pollution**

A recent assessment by the European Union has found that zinc and zinc compounds lead to no direct health effects to man (Bodar et al., 2005). However, though zinc toxicity may be low, additive zinc in the environment may lead to issues for non-human species, with freshwater species particularly at risk. US EPA criteria for protection of freshwater aquatic organisms is below 1.84  $\mu\text{M}$  for both short- and long-term protection, while humans can safely consume up to 110-400  $\mu\text{M}$  zinc (EPA, 2009).

As it has been reported, the concentrations of zinc required to suppress fish sperm function exceed those observed in the environment (Hatef, Alavi, Golshan, & Linhart, 2013). Conversely, it was also shown that supplementary dietary zinc improved seminal quality and embryonic survival in rainbow trout (Cite Kazemi) with supplement concentrations up to 1mM (Kocabaş & Kutluyer, 2017). This demonstrates that effects in fish species may be variable by species or delivery type.

Early embryos and larvae have been reported as being particularly sensitive to zinc toxicity. For example, the common active ingredient in commercial antidandruff shampoos is a zinc ionophore, such as zinc pyrithione, a compound with teratogenic effects in zebrafish and Medaka larvae (Goka, 1999). Australian Crimson Spotted Rainbow fish embryos were sensitive to zinc, with deformities occurring in 27% of 3 hour old embryos when treated with 509  $\mu\text{M}$  zinc (N. D. Williams & Holdway, 2000).

The European Union risk assessment modeled crustaceans and algae as the most sensitive of freshwater organisms to zinc toxicity (Bodar et al., 2005). Interestingly, microalgae have been demonstrated to be capable of removing up to 100% of zinc and copper from the freshwater environment (Zhou, Peng, Zhang, & Ying, 2012), demonstrating a possibility for use in metal

bioremediation. However, not all algae demonstrate this tolerance for zinc. A study of algae from Lake Ontario demonstrated that zinc levels of 300 nM were toxic to native species (P. T. S. Wong & Chau, 1990), introducing the possibility of using zinc as an algaecide, which may have limited consequences for other aquatic species. Indeed, environmental zinc levels would need to rise dramatically to endanger freshwater species.

My own data suggests that copper, more so than zinc, may present higher risk in preventing fertilization in externally fertilizing species such as fish, algae, and coral. Agricultural and industrial wastes are common sources of environmental copper (Oliveira-Filho, Lopes, & Paumgarten, 2004). In species of stony coral, *Goniastrea aspera*, fertilization rates dropped in a concentration dependent manner with exposure to extracellular copper (IC<sub>50</sub> ranging 230-630 nM), but not in any concentrations of zinc tested (Reichelt-Brushett & Harrison, 1999). For the soft coral, *Lobophytum compactum*, fertilization rate was found to decrease in response to copper in a dose dependent manner, with an IC<sub>50</sub> of 4 μM, noted to be higher than reported in other marine organisms (Reichelt-Brushett & Michalek-Wagner, 2005). In a tropical freshwater fish species, *Colossoma macropomum*, 12 μM copper was sufficient to decrease sperm motility, and to impair fertilization and rate of embryo hatching (Pinto, Castro, & Val, 2021). In the blue mussel, 1.5 μM copper led to dramatically decreased sperm swimming speed and 0.15 μM led to abnormal development of nearly all embryos (Fitzpatrick, Nadella, Bucking, Balshine, & Wood, 2008).

As we continue to find uses for metals such as zinc and copper in industry, health, agriculture, and animal husbandry, we must continue to understand the specific tolerance of native species. Sensitivity of gametes and embryos can be drastically different between species in the same ecosystem. Copper and zinc have gathered some interest as a potential aquatic herbicides or algaecides (Oliveira-Filho et al., 2004), and as supplements to improve fertility in endangered

species (Kocabaş & Kutluyer, 2017). However, as demonstrated by these reports of contradicting effects, we still need to understand how use will affect the larger ecosystem and other species that share the environment.

## Appendix A Additional Tables

Appendix Table 1 Representative species used for PLC alignment

Class	Infraclass	Order	Species	Common Name
<b>Mammalia</b>		Afrosoricida	<i>Echinops telfairi</i>	Lesser hedgehog tenrec
		Tubulidentata	<i>Orycteropus afer</i> <i>afer</i>	Aardvark
		Hyracoidae	<i>Hyracoidae</i> <i>hyraxes</i>	Hyrax
		Sirenia	<i>Trichechus</i> <i>manatus</i> <i>latirostris</i>	West Indian manatee
		Dermoptera	<i>Galeopterus</i> <i>variegatus</i>	Sunda flying lemur
		Manis pentadactyla	<i>Manis</i> <i>pentadactyla</i>	Chinese pangolin
		Perissodactyla	<i>Equus caballus</i>	Horse
		Artiodactyla	<i>Sus scrofa</i>	Wild boar
		Chiroptera	<i>Rousettus</i> <i>aegyptiacus</i>	Egyptian fruit bat

<b>Aves</b>	Galloanserae	Anseriformes	<i>Branta canadensis</i>	Canada goose
			<i>Anas platyrhynchos</i>	Mallard
			<i>Cygnus atratus</i>	Black swan
		Galliformes	<i>Callipepla squamata</i>	Scaled quail
			<i>Centrocercus minimus</i>	Gunnison grouse
			<i>Numida meleagris</i>	Helmeted guineafowl
	Neoaves	Aegotheliformes	<i>Aegotheles bennettii</i>	Barred owlet-nightjar
		Apodiformes	<i>Chaetura pelagica</i>	Chimney swift
			<i>Calypte anna</i>	Anna's hummingbird
			<i>Hemiprocne comata</i>	Whiskered treeswift
		Balaenicipitiformes	<i>Balaeniceps rex</i>	Shoebill
		Caprimulgiformes	<i>Caprimulgus europaeus</i>	European nightjar
			<i>Nyctibius grandis</i>	Great potoo

			<i>Podargus strigoides</i>	Tawny frogmouth
			<i>Steatornis caripensis</i>	Oilbird
		Charadriiformes	<i>Aptenodytes forsteri</i>	Emperor penguin
			<i>Arenaria interpres</i>	Ruddy turnstone
			<i>Larus smithsonianus</i>	American herring gull
		Ciconiiformes	<i>Egretta garzetta</i>	Little egret
			<i>Ciconia boyciana</i>	Oriental stork
			<i>Nipponia nippon</i>	Crested ibis
		Coliiformes	<i>Colius striatus</i>	Speckled mousebird
			<i>Urocolius indicus</i>	Red-faced mousebird
		Columbiformes	<i>Caloenas nicobarica</i>	Nicobar pigeon
			<i>Columba livia</i>	Rock dove
	Neoaves	Coraciiformes	<i>Chloroceryle aenea</i>	American pygmy kingfisher

			<i>Leptosomus discolor</i>	Cockoo-roller
			<i>Rhinopomastus cyanomelas</i>	Common Scimitarbill
	Neoaves	Cuculiformes	<i>Geococcyx californianus</i>	Greater roadrunner
			<i>Centropus bengalensis</i>	Lesser coucal
			<i>Crotophaga sulcirostris</i>	Groove-billed ani
	Neoaves	Falconiformes	<i>Pandion haliaetus</i>	Osprey
			<i>Cathartes aura</i>	Turkey vulture
			<i>Falco peregrinus</i>	Peregrine falcon
	Neoaves	Galbuliformes	<i>Bucco capensis</i>	Collared puffbird
			<i>Galbula dea</i>	Paradise jacamar
	Neoaves	Gaviiformes	<i>Gavia stellata</i>	Red-throated loon
	Neoaves	Gruiformes	<i>Aramus guarauna</i>	Limpkin
			<i>Psophia crepitans</i>	Grey-winged trumpeter

	Neoaves	Mesitornithiformes	<i>Mesitornis unicolor</i>	Brown mesite
	Neoaves	Musophagiformes	<i>Corythaeola cristata</i>	Great blue turaco
			<i>Corythaixoides concolor</i>	Grey go-away-bird
			<i>Tauraco erythrolophus</i>	Red-crested turaco
	Neoaves	Opisthocomiformes	<i>Opisthocomus hoazin</i>	Hoatzin
	Neoaves	Passeriformes	<i>Callaeas wilsoni</i>	North Island kokako
			<i>Eopsaltria australis</i>	Eastern yellow robin
			<i>Menura novaehollandiae</i>	Superb lyrebird
	Neoaves	Pelecaniformes	<i>Pelecanus crispus</i>	Dalmatian pelican
			<i>Sula dactylatra</i>	Masked booby
			<i>Phalacrocorax brasilianus</i>	Neotropic comorant
	Neoaves	Phoenicopteriformes	<i>Phoenicopterus ruber</i>	American flamingo

	Neoaves	Piciformes	<i>Indicator maculatus</i>	Spotted honeyguide
			<i>Melanerpes aurifrons</i>	Golden-fronted woodpecker
			<i>Pogoniulus pusillus</i>	Red-fronted tinkerbird
	Neoaves	Podicipediformes	<i>Podiceps cristatus</i>	Great crested grebe
	Neoaves	Procellariiformes	<i>Phoebastria albatrus</i>	Short-tailed albatross
			<i>Oceanodroma tethys</i>	Wedge-rumped storm petrel
			<i>Pelecanoides urinatrix</i>	Common diving petrel
	Neoaves	Psittaciformes	<i>Eolophus roseicapilla</i>	Galah
			<i>Lorius garrulus</i>	Chattering lory
			<i>Strigops habroptila</i>	Kakapo
	Neoaves	Sphenisciformes	<i>Aptenodytes forsteri</i>	Emperor penguin
	Neoaves	Strigiformes	<i>Bubo bubo</i>	Eurasian eagle-owl
			<i>Tyto alba</i>	Barn owl

	Neoaves	Trogoniformes	<i>Apaloderma vittatum</i>	Bar-tailed trogon
	Neoaves	Turniciformes	<i>Turnix velox</i>	Little buttonquail
		Struthioniformes	<i>Dromaius novaehollandiae</i>	Emu
<b>Reptilia</b>		Crocodylia	<i>Alligator sinensis</i>	Chinese alligator
		Rhynchocephalia		
		Squamata	<i>Lacerta agilis</i>	Sand lizard
		Testudines	<i>Chelonia mydas</i>	Green sea turtle
<b>Amphibia</b>		Gymnophiona	<i>Geotrypetes seraphini</i>	Gaboon caecilian
		Salientia	<i>Rana temporaria</i>	Common frog
			<i>Bufo bufo</i>	Common toad

## Bibliography

- Aarabi, M., Balakier, H., Bashar, S., Moskovtsev, S. I., Sutovsky, P., Librach, C. L., & Oko, R. (2014). Sperm-derived WW domain-binding protein, PAWP, elicits calcium oscillations and oocyte activation in humans and mice. *FASEB journal : official publication of the Federation of American Societies for Experimental Biology*, 28(10), 4434-4440. doi:10.1096/fj.14-256495 PMID - 24970390
- Aarabi, M., Qin, Z., Xu, W., Mewburn, J., & Oko, R. (2010). Sperm-borne protein, PAWP, initiates zygotic development in *Xenopus laevis* by eliciting intracellular calcium release. *Molecular reproduction and development*, 77(3), 249-256. doi:10.1002/mrd.21140 PMID - 20017143
- Akiyama, T., Ishida, J., Nakagawa, S., Ogawara, H., Watanabe, S., Itoh, N., . . . Fukami, Y. (1987). Genistein, a specific inhibitor of tyrosine-specific protein kinases. *The Journal of biological chemistry*, 262(12), 5592-5595. Retrieved from <https://www.ncbi.nlm.nih.gov/pubmed/3106339>
- Akiyama, T., & Ogawara, H. (1991). Use and specificity of genistein as inhibitor of protein-tyrosine kinases. *Methods in enzymology*, 201, 362-370. Retrieved from <https://www.ncbi.nlm.nih.gov/pubmed/1658553>
- Arslan, P., Virgilio, F. D., Beltrame, M., Tsien, R. Y., & Pozzan, T. (1985). Cytosolic Ca<sup>2+</sup> homeostasis in Ehrlich and Yoshida carcinomas. A new, membrane-permeant chelator of heavy metals reveals that these ascites tumor cell lines have normal cytosolic free Ca<sup>2+</sup>. *Journal of Biological Chemistry*, 260(5), 2719-2727. doi:10.1016/s0021-9258(18)89421-2
- Austin, C. R. (1956). Cortical granules in hamster eggs. *Experimental Cell Research*, 10(2), 533-540.
- Babcock, D. F., Rufo, G. A., Jr., & Lardy, H. A. (1983). Potassium-dependent increases in cytosolic pH stimulate metabolism and motility of mammalian sperm. *Proc Natl Acad Sci U S A*, 80(5), 1327-1331. doi:10.1073/pnas.80.5.1327
- Baltaci, A. K., & Yuce, K. (2018). Zinc transporter proteins. *Neurochemical research*. Retrieved from <https://link.springer.com/article/10.1007/s11064-017-2454-y>
- Barnett, B. L., Kretschmar, H. C., & Hartman, F. A. (1977). Structural characterization of bis(N-oxopyridine-2-thionato)zinc(II). *Inorganic Chemistry*, 16(8), 1834-1838. doi:10.1021/ic50174a002
- Benson, D. A., Cavanaugh, M., Clark, K., Karsch-Mizrachi, I., Lipman, D. J., Ostell, J., & Sayers, E. W. (2017). GenBank. *Nucleic Acids Research*, 45(D1), D37-D42. doi:10.1093/nar/gkw1070
- Bianchi, E., Doe, B., Goulding, D., & Wright, G. J. (2014). Juno is the egg Izumo receptor and is essential for mammalian fertilization. *Nature*, 508(7497), 483-487. doi:10.1038/nature13203
- Bill, C. A., & Vines, C. M. (2020). Phospholipase C. *Adv Exp Med Biol*, 1131, 215-242. doi:10.1007/978-3-030-12457-1\_9

- Bleil, J. D., Beall, C. F., & Wassarman, P. M. (1981). Mammalian sperm-egg interaction: fertilization of mouse eggs triggers modification of the major zona pellucida glycoprotein, ZP2. *Developmental biology*, 86(1), 189-197.
- Bleil, J. D., & Wassarman, P. M. (1980). Structure and function of the zona pellucida: identification and characterization of the proteins of the mouse oocyte's zona pellucida. *Developmental biology*, 76(1), 185-202.
- Bodar, C. W. M., Pronk, M. E. J., & Sijm, D. T. H. M. (2005). The european union risk assessment on zinc and zinc compounds: The process and the facts. *Integrated Environmental Assessment and Management*, 1(4), 301-319. doi:<https://doi.org/10.1002/ieam.5630010401>
- Brawley, S. H. (1991). The fast block against polyspermy in fucoid algae is an electrical block. *Developmental biology*, 144(1), 94-106.
- Burkart, A. D., Xiong, B., Baibakov, B., Jiménez-Movilla, M., & Dean, J. (2012). Ovastacin, a cortical granule protease, cleaves ZP2 in the zona pellucida to prevent polyspermy. *Journal of Cell Biology*, 197(1), 37-44.
- Busa, W. B., Ferguson, J. E., Joseph, S. K., Williamson, J. R., & Nuccitelli, R. (1985). Activation of frog (*Xenopus laevis*) eggs by inositol trisphosphate. I. Characterization of Ca<sup>2+</sup> release from intracellular stores. *Journal of Cell Biology*, 101(2), 677-682. doi:10.1083/jcb.101.2.677
- Busa, W. B., & Nuccitelli, R. (1985). An elevated free cytosolic Ca<sup>2+</sup> wave follows fertilization in eggs of the frog, *Xenopus laevis*. *Journal of Cell Biology*, 100(4), 1325-1329. doi:10.1083/jcb.100.4.1325
- Carlson, A. E., Quill, T. A., Westenbroek, R. E., Schuh, S. M., Hille, H., & Babcock, D. F. (2005). Identical phenotypes of CatSper1 and CatSper2 null sperm. *Journal of Biological Chemistry*, 280. doi:10.1074/jbc.M501430200
- Carlson, A. E., Westenbroek, R. E., Quill, T., Ren, D., Clapham, D. E., Hille, B., . . . Babcock, D. F. (2003). CatSper1 required for evoked Ca<sup>2+</sup> entry and control of flagellar function in sperm. *Proceedings of the National Academy of Sciences of the United States of America*, 100(25), 14864-14868. doi:10.1073/pnas.2536658100 PMID - 14657352
- CDC. (December 31, 2020). ART Success Rates.
- Chamow, S. M., & Hedrick, J. L. (1986). Subunit structure of a cortical granule lectin involved in the block to polyspermy in *Xenopus laevis* eggs. *FEBS letters*, 206(2), 353-357.
- Charbonneau, M., Moreau, M., Picheral, B., Vilain, J. P., & Guerrier, P. (1983). Fertilization of amphibian eggs: a comparison of electrical responses between anurans and urodeles. *Developmental biology*, 98(2), 304-318.
- Chia, S.-E., Ong, C.-N., Chua, L.-H., Ho, L.-M., & Tay, S.-K. (2000). Comparison of Zinc Concentrations in Blood and Seminal Plasma and the Various Sperm Parameters Between Fertile and Infertile Men. *Journal of Andrology*, 21(1), 53-57. doi:<https://doi.org/10.1002/j.1939-4640.2000.tb03275.x>
- Combelles, C. M., & Racowsky, C. (2005). Assessment and optimization of oocyte quality during assisted reproductive technology treatment. *Seminars in reproductive medicine*, 23(3), 277-284. doi:10.1055/s-2005-872456 PMID - 16059834
- Coward, K., Ponting, C. P., Chang, H. Y. Y., Hibbitt, O., Savolainen, P., Jones, K. T., & Parrington, J. (2005). Phospholipase Czeta, the trigger of egg activation in mammals, is present in a non-mammalian species. *Reproduction (Cambridge, England)*, 130(2), 157-163. doi:10.1530/rep.1.00707 PMID - 16049153

- Cross, N. L., & Elinson, R. P. (1980). A fast block to polyspermy in frogs mediated by changes in the membrane potential. *Developmental Biology*, 75(1), 187-198. doi:10.1016/0012-1606(80)90154-2
- Cross, N. L., & Razy-Faulkner, P. (1997). Control of human sperm intracellular pH by cholesterol and its relationship to the response of the acrosome to progesterone. *Biology of reproduction*, 56(5), 1169-1174. doi:10.1095/biolreprod56.5.1169
- Denninger, P., Bleckmann, A., Lausser, A., Vogler, F., Ott, T., Ehrhardt, D. W., . . . Grossmann, G. (2014). Male–female communication triggers calcium signatures during fertilization in Arabidopsis. *Nature Communications*, 5(1), 4645. doi:10.1038/ncomms5645 PMID - 25145880
- Dong, C.-H., Yang, S.-T., Yang, Z.-A., Zhang, L., & Gui, J.-F. (2004). A C-type lectin associated and translocated with cortical granules during oocyte maturation and egg fertilization in fish. *Developmental biology*, 265(2), 341-354.
- Duncan, F. E., Que, E. L., Zhang, N., Feinberg, E. C., O'Halloran, T. V., & Woodruff, T. K. (2016). The zinc spark is an inorganic signature of human egg activation. *Sci Rep*, 6, 24737. doi:10.1038/srep24737
- Elinson, R. P. (1975). Site of sperm entry and a cortical contraction associated with egg activation in the frog *Rana pipiens*. *Developmental biology*. Retrieved from <https://www.sciencedirect.com/science/article/pii/001216067590281X>
- EPA, U. S. (2009). National recommended water quality criteria. *United States Environmental Protection Agency', Office of Water, Office of Science and Technology*.
- Evans, J. P. (2020). Preventing polyspermy in mammalian eggs—Contributions of the membrane block and other mechanisms. *Molecular reproduction and development*, 87(3), 341-349.
- Fagundes, A. K. F., Oliveira, E. C. S., Tenorio, B. M., Melo, C. C. S., Nery, L. T. B., Santos, F. A. B., . . . Silva, V. A. (2014). Injection of a chemical castration agent, zinc gluconate, into the testes of cats results in the impairment of spermatogenesis: A potentially irreversible contraceptive approach for this species? *Theriogenology*, 81(2), 230-236. doi:<https://doi.org/10.1016/j.theriogenology.2013.09.013>
- Feng, Y. L., & Gordon, J. W. (1996). Birth of normal mice after removal of the supernumerary male pronucleus from polyspermic zygotes. *Human reproduction (Oxford, England)*, 11(2), 341-344. doi:10.1093/HUMREP/11.2.341 PMID - 8671222
- Fitzpatrick, J. L., Nadella, S., Bucking, C., Balshine, S., & Wood, C. M. (2008). The relative sensitivity of sperm, eggs and embryos to copper in the blue mussel (*Mytilus trossulus*). *Comparative Biochemistry and Physiology Part C: Toxicology & Pharmacology*, 147(4), 441-449.
- Foltz, K. R., Adams, N. L., & Runft, L. L. (2004). Echinoderm Eggs and Embryos: Procurement and Culture. In *Methods in cell biology* (Vol. 74, pp. 39-74): Academic Press.
- Frank, U., Nicotra, M. L., & Schnitzler, C. E. (2020). The colonial cnidarian *Hydractinia*. *EvoDevo*, 11(1), 7. doi:10.1186/s13227-020-00151-0 PMID - 32226598
- Gagoski, D., Polinkovsky, M. E., Mureev, S., Kunert, A., Johnston, W., Gambin, Y., & Alexandrov, K. (2016). Performance benchmarking of four cell-free protein expression systems. *Biotechnology and Bioengineering*, 113(2), 292-300. doi:10.1002/bit.25814 PMID - 26301602
- Gee, K. R., Zhou, Z.-L., Qian, W.-J., & Kennedy, R. (2002). Detection and Imaging of Zinc Secretion from Pancreatic  $\beta$ -Cells Using a New Fluorescent Zinc Indicator. *Journal of the American Chemical Society*, 124(5), 776-778. doi:10.1021/ja011774y PMID - 11817952

- Glahn, D., Mark, S. D., Behr, R. K., & Nuccitelli, R. (1999). Tyrosine kinase inhibitors block sperm-induced egg activation in *Xenopus laevis*. *Developmental biology*, 205(1), 171-180. doi:10.1006/dbio.1998.9042
- Glahn, D., & Nuccitelli, R. (2003). Voltage-clamp study of the activation currents and fast block to polyspermy in the egg of *Xenopus laevis*. *Development, Growth & Differentiation*, 45(2), 187-197. doi:10.1034/j.1600-0854.2004.00684.x PMID - 12752506
- Goka, K. (1999). Embryotoxicity of Zinc Pyrithione, An Antidandruff Chemical, in Fish. *Environmental Research*, 81(1), 81-83. doi:10.1006/enrs.1998.3944 PMID - 10361029
- Goudeau, H., Depresle, Y., Rosa, A., & Goudeau, M. (1994). Evidence by a voltage clamp study of an electrically mediated block to polyspermy in the egg of the ascidian *Phallusia mammillata*. *Developmental biology*, 166(2), 489-501.
- Green, C. D., Ma, Q., Manske, G. L., Shami, A. N., Zheng, X., Marini, S., . . . Hammoud, S. S. (2018). A Comprehensive Roadmap of Murine Spermatogenesis Defined by Single-Cell RNA-Seq. *Developmental Cell*, 46(5), 651-667.e610. doi:10.1016/j.devcel.2018.07.025 PMID - 30146481
- Green, S. L. (2009). *The laboratory Xenopus sp*: CRC Press.
- Grey, R. D., Bastiani, M. J., Webb, D. J., & Schertel, E. R. (1982). An electrical block is required to prevent polyspermy in eggs fertilized by natural mating of *Xenopus laevis*. *Developmental Biology*, 89(2), 475-484. doi:10.1016/0012-1606(82)90335-9
- Gulyas, B. J. (1980). Cortical granules of mammalian eggs. *International review of cytology*, 63, 357-392.
- Hatef, A., Alavi, S. M. H., Golshan, M., & Linhart, O. (2013). Toxicity of environmental contaminants to fish spermatozoa function in vitro—A review. *Aquatic Toxicology*, 140, 134-144. doi:10.1016/j.aquatox.2013.05.016 PMID - 23792626
- Heasman, J., Holwill, S., & Wylie, C. C. (1991). Fertilization of cultured *Xenopus* oocytes and use in studies of maternally inherited molecules. *Methods in cell biology*, 36, 213-218, 218a, 218b, 219-230. Retrieved from <https://www.sciencedirect.com/science/article/pii/S0091679X08602794>
- Hennigar, S. R., Lieberman, H. R., Fulgoni, V. L., III, & McClung, J. P. (2018). Serum Zinc Concentrations in the US Population Are Related to Sex, Age, and Time of Blood Draw but Not Dietary or Supplemental Zinc. *The Journal of Nutrition*, 148(8), 1341-1351. doi:10.1093/jn/nxy105
- Hill, W. G., Southern, N. M., MacIver, B., Potter, E., Apodaca, G., Smith, C. P., & Zeidel, M. L. (2005). Isolation and characterization of the *Xenopus* oocyte plasma membrane: a new method for studying activity of water and solute transporters. *American Journal of Physiology-Renal Physiology*, 289(1), F217-F224.
- Hinkley Jr, R. E., & Wright, B. D. (1986). Effects of the volatile anesthetic halothane on fertilization and early development in the sea urchin *Lytechinus variegatus*: Evidence that abnormal development is due to polyspermy. *Teratology*, 34(3), 291-301.
- Hiramoto, Y. (1959). Changes in electric properties upon fertilization in the sea urchin egg. *Experimental Cell Research*, 16(2), 421-424. doi:[https://doi.org/10.1016/0014-4827\(59\)90272-1](https://doi.org/10.1016/0014-4827(59)90272-1)
- Ho, H.-C., Granish, K. A., & Suarez, S. S. (2002). Hyperactivated Motility of Bull Sperm Is Triggered at the Axoneme by Ca<sup>2+</sup> and Not cAMP. *Developmental Biology*, 250(1), 208-217. doi:<https://doi.org/10.1006/dbio.2002.0797>

- Hori, R. (1958). On the membrane potential of the unfertilized egg of the medaka, *Oryzias latipes* and changes accompanying activation. *Embryologia*, 4(2), 79-91.
- Hsu, C. Y., Persons, P. E., Spada, A. P., Bednar, R. A., Levitzki, A., & Zilberstein, A. (1991). Kinetic analysis of the inhibition of the epidermal growth factor receptor tyrosine kinase by Lavendustin-A and its analogue. *Journal of Biological Chemistry*, 266(31), 21105-21112. Retrieved from [http://scholar.google.com/scholar?q=Kinetic analysis of the inhibition of the epidermal growth factor receptor tyrosine kinase by Lavendustin-A and its analogue.&btnG=&hl=en&num=20&as\\_sdt=0%2C22](http://scholar.google.com/scholar?q=Kinetic%20analysis%20of%20the%20inhibition%20of%20the%20epidermal%20growth%20factor%20receptor%20tyrosine%20kinase%20by%20Lavendustin-A%20and%20its%20analogue.&btnG=&hl=en&num=20&as_sdt=0%2C22)
- Hu, Q., Duncan, F. E., Nowakowski, A. B., Antipova, O. A., Woodruff, T. K., O'Halloran, T. V., & Wolfner, M. F. (2020). Zinc dynamics during drosophila oocyte maturation and egg activation. *IScience*, 23(7), 101275.
- Hubacher, D., Chen, P.-L., & Park, S. (2009). Side effects from the copper IUD: do they decrease over time? *Contraception*, 79(5), 356-362. doi:10.1016/j.contraception.2008.11.012 PMID - 19341847
- Hummel, W. P., & Kettel, L. M. (1997). Assisted Reproductive Technology: The State of the ART. *Annals of Medicine*, 29(3). doi:10.3109/07853899708999338 PMID - 9240626
- Hwang, S. C., Jhon, D. Y., Bae, Y. S., Kim, J. H., & Rhee, S. G. (1996). Activation of phospholipase C-gamma by the concerted action of tau proteins and arachidonic acid. *The Journal of biological chemistry*, 271(31), 18342-18349. doi:10.1074/jbc.271.31.18342 PMID - 8702475
- Inoda, T., & Morisawa, M. (1987). Effect of osmolality on the initiation of sperm motility in *Xenopus laevis*. *Comparative Biochemistry and Physiology Part A: Physiology*, 88(3), 539-542. doi:10.1016/0300-9629(87)90077-6 PMID - 2892629
- Iwao, Y. (1985). The membrane potential changes of amphibian eggs during species- and cross-fertilization. *Developmental Biology*, 111(1), 26-34. doi:[https://doi.org/10.1016/0012-1606\(85\)90431-2](https://doi.org/10.1016/0012-1606(85)90431-2)
- Jaffe, L. A. (1976). Fast block to polyspermy in sea urchin eggs is electrically mediated. *Nature*, 261(5555), 68-71. doi:10.1038/261068a0
- Jaffe, L. A., & Gould, M. (1985). Polyspermy-Preventing Mechanisms. In C. B. Metz & A. Monroy (Eds.), *Biology of Fertilization* (Vol. 3, pp. 223-250). New York: Academic Press.
- Jaffe, L. F. (1983). Sources of calcium in egg activation: A review and hypothesis. *Developmental Biology*, 99(2), 265-276. doi:10.1016/0012-1606(83)90276-2 PMID - 6352370
- Just, E. E. (1919). The fertilization reaction in *Echinarrachnius parma*: I. Cortical response of the egg to insemination. *The Biological Bulletin*. Retrieved from <https://www.journals.uchicago.edu/doi/pdfplus/10.2307/1536454>
- Kadamur, G., & Ross, E. M. (2013). Mammalian phospholipase C. *Annu Rev Physiol*, 75(1), 127-154.
- Kambe, T., Suzuki, E., & Komori, T. (2019). Zinc Transporter Proteins: A Review and New View from Biochemistry. In T. Fukada & T. Kambe (Eds.), *Zinc Signaling* (Second Ed ed., pp. 23-56). Singapore: Springer Nature Singapore Pte Ltd.
- Karadge, U. B., Gosto, M., & Nicotra, M. L. (2015). Allorecognition Proteins in an Invertebrate Exhibit Homophilic Interactions. *Current Biology*, 25(21), 2845-2850. doi:10.1016/j.cub.2015.09.030
- Kay, V. J., & Robertson, L. (1998). Hyperactivated motility of human spermatozoa: a review of physiological function and application in assisted reproduction. *Human Reproduction Update*, 4(6), 776-786. doi:10.1093/humupd/4.6.776

- Kazemi, E., Sourinejad, I., Ghaedi, A., Johari, S. A., & Ghasemi, Z. (2020). Effect of different dietary zinc sources (mineral, nanoparticulate, and organic) on quantitative and qualitative semen attributes of rainbow trout (*Oncorhynchus mykiss*). *Aquaculture*, *515*, 734529. doi:10.1016/j.aquaculture.2019.734529
- Kerns, K., Zigo, M., Drobnis, E. Z., Sutovsky, M., & Sutovsky, P. (2018). Zinc ion flux during mammalian sperm capacitation. *Nature Communications*, *9*(1), 2061. doi:10.1038/s41467-018-04523-y PMID - 29802294
- Kim, A. M., Bernhardt, M. L., Kong, B. Y., Ahn, R. W., Vogt, S., Woodruff, T. K., & O'Halloran, T. V. (2011). Zinc Sparks Are Triggered by Fertilization and Facilitate Cell Cycle Resumption in Mammalian Eggs. *ACS Chem Biol*, *6*(7), 716-723. doi:10.1021/cb200084y
- Kline, D. (1988). Calcium-dependent events at fertilization of the frog egg: Injection of a calcium buffer blocks ion channel opening, exocytosis, and formation of pronuclei. *Developmental Biology*, *126*(2), 346-361. doi:10.1016/0012-1606(88)90145-5
- Kline, D., Jaffe, L. A., & Tucker, R. P. (1985). Fertilization potential and polyspermy prevention in the egg of the nemertean, *Cerebratulus lacteus*. *Journal of Experimental Zoology*, *236*(1), 45-52. doi:<https://doi.org/10.1002/jez.1402360107>
- Kocabaş, M., & Kutluyer, F. (2017). In Vitro Effect of Zinc: Evaluation of the Sperm Quality of Endangered Trout *Salmo Coruhensis* and Rainbow Trout *Oncorhynchus Mykiss* and Fertilizing Capacity. *International Journal of Aquaculture and Fishery Sciences*, 046-050. doi:10.17352/2455-8400.000028
- Kong, B. Y., Duncan, F. E., Que, E. L., Xu, Y., Vogt, S., O'Halloran, T. V., & Woodruff, T. K. (2015). The inorganic anatomy of the mammalian preimplantation embryo and the requirement of zinc during the first mitotic divisions. *Developmental Dynamics*, *244*(8), 935-947. doi:10.1002/dvdy.24285
- Kotdawala, A. P., & Kumar, S. (2012). Addition of zinc to human ejaculate prior to cryopreservation prevents freeze-thaw-induced DNA damage and preserves sperm function.
- Le Guen, M., Schantz, C., Régnier-Loilier, A., & de La Rochebrochard, E. (2021). Reasons for rejecting hormonal contraception in Western countries: A systematic review. *Social Science & Medicine*, *284*, 114247. doi:<https://doi.org/10.1016/j.socscimed.2021.114247>
- Lee-Liu, D., Méndez-Olivos, E. E., Muñoz, R., & Larraín, J. (2017). The African clawed frog *Xenopus laevis*: A model organism to study regeneration of the central nervous system. *Neuroscience Letters*, *652*, 82-93. doi:<https://doi.org/10.1016/j.neulet.2016.09.054>
- Lindemann, C. B., & Goltz, J. S. (1988). Calcium regulation of flagellar curvature and swimming pattern in triton X-100--extracted rat sperm. *Cell Motil Cytoskeleton*, *10*(3), 420-431. doi:10.1002/cm.970100309
- Lishko, P. V., Kirichok, Y., Ren, D., Navarro, B., Chung, J.-J., & Clapham, D. E. (2012). The control of male fertility by spermatozoan ion channels. *Annual review of physiology*, *74*, 453.
- Lishko, P. V., Kirichok, Y., Ren, D., Navarro, B., Chung, J. J., & Clapham, D. E. (2012). The control of male fertility by spermatozoan ion channels. *Annu Rev Physiol*, *74*, 453-475. doi:10.1146/annurev-physiol-020911-153258
- Maeno, T., Morita, H., & Kuwabara, M. (1956). Potential measurements on the eggs of Japanese killi-fish, *Oryzias latipes*. *Mem. Fac. Sci. Kyushu Univ., Ser. B*, *2*, 87-94.
- McClay, D. R. (2011). Evolutionary crossroads in developmental biology: sea urchins. *Development*, *138*(13), 2639-2648. doi:10.1242/dev.048967

- McPherson, S. M., McPherson, P. S., Mathews, L., Campbell, K. P., & Longo, F. J. (1992). Cortical localization of a calcium release channel in sea urchin eggs. *Journal of Cell Biology*, 116(5), 1111-1121. doi:10.1083/jcb.116.5.1111
- Mendoza, A. D., Sue, A., Antipova, O., Vogt, S., Woodruff, T. K., Wignall, S. M., & O'Halloran, T. V. (2022). Dynamic zinc fluxes regulate meiotic progression in *Caenorhabditis elegans*†. *Biology of reproduction*, 107(2), 406-418. doi:10.1093/biolre/ioac064
- Metz, C. (2012). *Biology Of Fertilization V3: The Fertilization Response Of the Egg* (Vol. 3): Elsevier.
- Milostić-Srb, A., Včev, A., Tandara, M., Marić, S., Kuić-Vadlja, V., Srb, N., & Holik, D. (2020). IMPORTANCE OF ZINC CONCENTRATION IN SEMINAL FLUID OF MEN DIAGNOSED WITH INFERTILITY. *Acta Clinica Croatica*, 59(1), 154-160. doi:10.20471/acc.2020.59.01.19 PMID - 32724287
- Miyazaki, S.-i., & Hirai, S. (1979). Fast polyspermy block and activation potential: Correlated changes during oocyte maturation of a starfish. *Developmental biology*, 70(2), 327-340.
- Mizushima, S., & Sasanami, T. (2017). Fertilization 2: Polyspermic Fertilization. In T. Sasanami (Ed.), *Avian Reproduction. Advances in Experimental Medicine and Biology* (Vol. 1001): Springer, Singapore.
- Mizushima, S., Takagi, S., Ono, T., Atsumi, Y., Tsukada, A., Saito, N., & Shimada, K. (2007). Possible role of calcium on oocyte development after intracytoplasmic sperm injection in quail (*Coturnix japonica*). *Journal of Experimental Zoology Part A: Ecological Genetics and Physiology*, 307A(11), 647-653. doi:10.1002/jez.a.418 PMID - 17899613
- Nishibe, S., Wahl, M. I., Hernandez-Sotomayor, S. M., Tonks, N. K., Rhee, S. G., & Carpenter, G. (1990). Increase of the Catalytic Activity of Phospholipase C- $\gamma$ 1 by Tyrosine Phosphorylation. *Science*, 250(4985), 1253-1256. doi:10.1126/science.1700866
- Nomikos, M., Elgmati, K., Theodoridou, M., Georgilis, A., Gonzalez-Garcia, J. R., Nounesis, G., . . . Lai, F. A. (2011). Novel regulation of PLC $\zeta$  activity via its XY-linker. *Biochemical Journal*, 438(Pt 3), 427-432. doi:10.1042/bj20110953 PMID - 21767260
- Nomikos, M., Kashir, J., & Lai, F. A. (2017). The role and mechanism of action of sperm PLC-zeta in mammalian fertilisation. *Biochemical Journal*, 474(21), 3659-3673. doi:10.1042/BCJ20160521
- Nomikos, M., Swann, K., & Lai, F. A. (2012). Starting a new life: Sperm PLC-zeta mobilizes the Ca<sup>2+</sup> signal that induces egg activation and embryo development. *BioEssays*, 34(2), 126-134. doi:<https://doi.org/10.1002/bies.201100127>
- Nomizu, T., Falchuk, K. H., & Vallee, B. L. (1993). Zinc, iron, and copper contents of *Xenopus laevis* oocytes and embryos. *Molecular Reproduction and Development*, 36(4), 419-423. doi:10.1002/mrd.1080360403
- Oliveira, E. C. S., Moura, M. R., Silva, V. A., Peixoto, C. A., Saraiva, K. L. A., de Sá, M. J. C., . . . de Pinho Marques, A. (2007). Intratesticular injection of a zinc-based solution as a contraceptive for dogs. *Theriogenology*, 68(2), 137-145. doi:<https://doi.org/10.1016/j.theriogenology.2007.03.026>
- Oliveira-Filho, E. C. d., Lopes, R. M., & Paumgarten, F. J. R. (2004). Comparative study on the susceptibility of freshwater species to copper-based pesticides. *Chemosphere*, 56(4), 369-374. doi:10.1016/j.chemosphere.2004.04.026 PMID - 15183999
- Onoda, T., Iinuma, H., Sasaki, Y., Hamada, M., Isshiki, K., Naganawa, H., . . . Umezawa, K. (1989). Isolation of a novel tyrosine kinase inhibitor, lavendustin A, from *Streptomyces*

- griseolavendus. *Journal of natural products*, 52(6), 1252-1257. Retrieved from <https://www.ncbi.nlm.nih.gov/pubmed/2614420>
- Ortiz, M. E., & Croxatto, H. B. (2007). Copper-T intrauterine device and levonorgestrel intrauterine system: biological bases of their mechanism of action. *Contraception*, 75(6), S16-S30. doi:10.1016/j.contraception.2007.01.020 PMID - 17531610
- Pan, E., Zhang, X.-a., Huang, Z., Krezel, A., Zhao, M., Tinberg, Christine E., . . . McNamara, James O. (2011). Vesicular Zinc Promotes Presynaptic and Inhibits Postsynaptic Long-Term Potentiation of Mossy Fiber-CA3 Synapse. *Neuron*, 71(6), 1116-1126. doi:10.1016/j.neuron.2011.07.019
- ParaGard T 380A (prescribing information). (2014). Retrieved from <http://www.paragard.com/pdf/PARAGARD-PI.pdf>
- Peterfi, T., & Rothschild, V. (1935). Bio-electric transients during fertilisation. *Nature*, 135(3421), 874-875.
- Pinto, G. L., Castro, J. d. S., & Val, A. L. (2021). Copper and cadmium impair sperm performance, fertilization and hatching of oocytes from Amazonian fish *Colossoma macropomum*. *Chemosphere*, 266, 128957. doi:10.1016/j.chemosphere.2020.128957 PMID - 33218723
- Qi, H., Moran, M. M., Navarro, B., Chong, J. A., Krapivinsky, G., Krapivinsky, L., . . . Clapham, D. E. (2007). All four CatSper ion channel proteins are required for male fertility and sperm cell hyperactivated motility. *Proc Natl Acad Sci U S A*, 104(4), 1219-1223. doi:10.1073/pnas.0610286104
- Que, E. L., Duncan, F. E., Bayer, A. R., Philips, S. J., & Roth, E. W. (2017). Zinc sparks induce physiochemical changes in the egg zona pellucida that prevent polyspermy. *Integrative Biology*, 9(2), 91-180. doi:10.1039/C6IB00212A
- Que, E. L., Duncan, F. E., Lee, H. C., Hornick, J. E., Vogt, S., Fissore, R., . . . Woodruff, T. K. (2018). Bovine eggs release zinc in response to parthenogenetic and sperm-induced egg activation. *Theriogenology*, Available Online.
- Reichelt-Brushett, A. J., & Harrison, P. L. (1999). The Effect of Copper, Zinc and Cadmium on Fertilization Success of Gametes from Scleractinian Reef Corals. *Marine Pollution Bulletin*, 38(3), 182-187. doi:10.1016/s0025-326x(98)00183-0
- Reichelt-Brushett, A. J., & Michalek-Wagner, K. (2005). Effects of copper on the fertilization success of the soft coral *Lobophytum compactum*. *Aquatic Toxicology*, 74(3), 280-284. doi:10.1016/j.aquatox.2005.05.011 PMID - 15998546
- Reinhart, D., Ridgway, J., & Chandler, D. E. (1998). *Xenopus laevis* fertilisation: analysis of sperm motility in egg jelly using video light microscopy. *Zygote*, 6(2), 173-182. doi:10.1017/S0967199498000100
- Riffo, M., Leiva, S., & Astudillo, J. (1992). Effect of zinc on human sperm motility and the acrosome reaction. *International Journal of Andrology*(15), 229-237. doi:10.1111/j.1365-2605.1992.tb01343.x
- Runft, L. L., Jaffe, L. A., & Mehlmann, L. M. (2002). Egg activation at fertilization: where it all begins. *Developmental Biology*, 245(2), 237-254. doi:10.1006/dbio.2002.0600
- Runft, L. L., Watras, J., & Jaffe, L. A. (1999). Calcium release at fertilization of *Xenopus* eggs requires type I IP(3) receptors, but not SH2 domain-mediated activation of PLCgamma or G(q)-mediated activation of PLCbeta. *Developmental biology*, 214(2), 399-411. doi:10.1006/dbio.1999.9415
- Ryu, S. H., Cho, K. S., Lee, K. Y., Suh, P. G., & Rhee, S. G. (1987). Purification and characterization of two immunologically distinct phosphoinositide-specific

- phospholipases C from bovine brain. *Journal of Biological Chemistry*, 262(26), 12511-12518. doi:10.1016/s0021-9258(18)45235-0
- Saaranen, M., Suistomaa, U., Kantola, M., Saarikoski, S., & Vanha-Perttula, T. (1987). Lead, magnesium, selenium and zinc in human seminal fluid: comparison with semen parameters and fertility. *Human Reproduction*, 2(6), 475-479.
- Sanders, S. M., Ma, Z., Hughes, J. M., Riscoe, B. M., Gibson, G. A., Watson, A. M., . . . Baxevanis, A. D. (2018). CRISPR/Cas9-mediated gene knockin in the hydroid *Hydractinia symbiolongicarpus*. *BMC genomics*, 19(1), 1-17.
- Santella, L., Vasilev, F., & Chun, J. T. (2012). Fertilization in echinoderms. *Biochemical and Biophysical Research Communications*, 425(3), 588-594. doi:<https://doi.org/10.1016/j.bbrc.2012.07.159>
- Santi, C. M., Orta, G., Salkoff, L., Visconti, P. E., Darszon, A., & Treviño, C. L. (2013). K<sup>+</sup> and Cl<sup>-</sup> channels and transporters in sperm function. *Curr Top Dev Biol*, 102, 385-421. doi:10.1016/b978-0-12-416024-8.00014-3
- Sato, K., Iwasaki, T., Tamaki, I., Aoto, M., Tokmakov, A. A., & Fukami, Y. (1998). Involvement of protein-tyrosine phosphorylation and dephosphorylation in sperm-induced *Xenopus* egg activation. *FEBS letters*, 424(1-2), 113-118. doi:10.1016/S0014-5793(98)00123-9
- Sato, K., Tokmakov, A. A., Iwasaki, T., & Fukami, Y. (2000). Tyrosine kinase-dependent activation of phospholipase C $\gamma$  is required for calcium transient in *Xenopus* egg fertilization. *Developmental biology*, 224(2), 453-469. doi:10.1006/dbio.2000.9782 PMID - 10926780
- Scheer, B. T., Monroy, A., Santangelo, M., & Riccobono, G. (1954). Action potentials in sea urchin eggs at fertilization. *Experimental Cell Research*, 7(1), 284-287.
- Schneider, C. A., Rasband, W. S., & Eliceiri, K. W. (2012). NIH Image to ImageJ: 25 years of image analysis. *Nat Methods*, 9(7), 671-675. doi:10.1038/nmeth.2089
- Schroeder, B. C., Cheng, T., Jan, Y. N., & Jan, L. Y. (2008). Expression Cloning of TMEM16A as a Calcium-Activated Chloride Channel Subunit. *Cell*, 134(6), 1019-1029. doi:10.1016/j.cell.2008.09.003
- Session, A. M., Uno, Y., Kwon, T., Chapman, J. A., Toyoda, A., Takahashi, S., . . . Rokhsar, D. S. (2016). Genome evolution in the allotetraploid frog *Xenopus laevis*. *Nature*, 538(7625), 336-343. doi:10.1038/nature19840
- Shami, A. N., Zheng, X., Munyoki, S. K., Ma, Q., Manske, G. L., Green, C. D., . . . Hammoud, S. S. (2020). Single-Cell RNA Sequencing of Human, Macaque, and Mouse Testes Uncovers Conserved and Divergent Features of Mammalian Spermatogenesis. *Developmental Cell*, 54(4), 529-547.e512. doi:10.1016/j.devcel.2020.05.010 PMID - 32504559
- Shankie-Williams, K. N., Lindsay, L. A., Murphy, C. R., & Dowland, S. N. (2022). Zinc as a non-hormonal contraceptive: an alternative to the copper intrauterine device (IUD). *Reproduction*, 164(4), 135-142. doi:10.1530/rep-22-0155 PMID - 35929835
- Shen, S. S., & Buck, W. R. (1993). Sources of calcium in sea urchin eggs during the fertilization response. *Developmental biology*, 157(1), 157-169.
- Snow, P., Yim, D. L., Leibow, J. D., Saini, S., & Nuccitelli, R. (1996). Fertilization stimulates an increase in inositol trisphosphate and inositol lipid levels in *Xenopus* eggs. *Developmental Biology*, 180(1), 108-118. doi:10.1006/dbio.1996.0288
- Sørensen, M. B., Bergdahl, I. A., Hjøllund, N. H. I., Bonde, J. P. E., Stoltenberg, M., & Ernst, E. (1999). Zinc, magnesium and calcium in human seminal fluid: relations to other semen

- parameters and fertility. *MHR: Basic science of reproductive medicine*, 5(4), 331-337. doi:10.1093/molehr/5.4.331 PMID - 10321804
- Stanković, H., & Mikac-Dević, D. (1976). Zinc and copper in human semen. *Clinica Chimica Acta*, 70(1), 123-126. doi:10.1016/0009-8981(76)90013-9 PMID - 947613
- Stauss, C. R., Votta, T. J., & Suarez, S. S. (1995). Sperm motility hyperactivation facilitates penetration of the hamster zona pellucida. *Biology of reproduction*, 53(6), 1280-1285. doi:10.1095/biolreprod53.6.1280
- Stein, P., Savy, V., Williams, A. M., & Williams, C. J. (2020). Modulators of calcium signalling at fertilization. *Open Biology*, 10(7), 200118. doi:10.1098/rsob.200118 PMID - 32673518
- Suarez, S. S. (2008). Control of hyperactivation in sperm. *Human Reproduction Update*, 14(6), 647-657. doi:10.1093/humupd/dmn029 PMID - 18653675
- Suarez, S. S., Vincenti, L., & Ceglia, M. W. (1987). Hyperactivated motility induced in mouse sperm by calcium ionophore A23187 is reversible. *J Exp Zool*, 244(2), 331-336. doi:10.1002/jez.1402440218
- Suzuki, H., Ju, J.-C., & Yang, X. (2000). Surface Ultrastructural Alterations of Bovine Oocytes after Parthenogenetic Activation. *Cloning*, 2(2), 69-78. doi:10.1089/152045500436096 PMID - 16218861
- Swann, K. (2020). The soluble sperm factor that activates the egg: PLCzeta and beyond. *Reproduction*, 160(1), V9-V11. doi:10.1530/rep-20-0079 PMID - 32485666
- Swann, K., & Lai, F. A. (2016). The sperm phospholipase C-zeta and Ca<sup>2+</sup> signalling at fertilization in mammals. *Biochem Soc Trans*, 44(1), 267-272. doi:10.1042/bst20150221
- Swanson, W. J., & Vacquier, V. D. (2002). The rapid evolution of reproductive proteins. *Nat Rev Genet*, 3(2), 137-144. doi:10.1038/nrg733
- Tembo, M., Lara-Santos, C., Rosenbaum, J. C., & Carlson, A. E. (2022). PIP2 and Ca<sup>2+</sup> regulation of TMEM16A currents in excised inside-out patches. *bioRxiv*, 2022.2008.2030.505925. doi:10.1101/2022.08.30.505925
- Tholl, N., Naqvi, S., McLaughlin, E., Boyles, S., Bieber, A. L., & Chandler, D. E. (2011). Swimming of *Xenopus laevis* sperm exhibits multiple gears and its duration is extended by egg jelly constituents. *Biol Bull*, 220(3), 174-185. doi:10.1086/BBLv220n3p174
- Tian, J., Gong, H., & Lennarz, W. J. (1999). *Xenopus laevis* sperm receptor gp69/64 glycoprotein is a homolog of the mammalian sperm receptor ZP2. *Proceedings of the National Academy of Sciences*, 96(3), 829-834.
- Tokuhiro, K., & Dean, J. (2018). Glycan-Independent Gamete Recognition Triggers Egg Zinc Sparks and ZP2 Cleavage to Prevent Polyspermy. *Developmental Cell*, 46, 627-640. Retrieved from <https://www.sciencedirect.com/science/article/pii/S1534580718306051>
- Tyler, A., Monroy, A., Kao, C. Y., & Grundfest, H. (1956). MEMBRANE POTENTIAL AND RESISTANCE OF THE STARFISH EGG BEFORE AND AFTER FERTILIZATION. *The Biological Bulletin*, 111(1), 153-177. doi:10.2307/1539191
- Ueda, Y., Yoshizaki, N., & Iwao, Y. (2002). Acrosome Reaction in Sperm of the Frog, *Xenopus laevis*: Its Detection and Induction by Oviductal Pars Recta Secretion. *Developmental Biology*, 243(1), 55-64. doi:10.1006/dbio.2001.0541 PMID - 11846477
- United Nations Department of Economic and Social Affairs, P. D. (2020). *World Family Planning 2020 Highlights: Accelerating action to ensure universal access to family planning*
- Visconti, P. E., Galantino-Homer, H., Moore, G. D., Bailey, J. L., Ning, X., Fornes, M., & Kopf, G. S. (1998). The molecular basis of sperm capacitation. *Journal of Andrology*, 19(2), 242-248. doi:10.1002/j.1939-4640.1998.tb01994.x PMID - 9570749

- Wahl, M. I., Jones, G. A., Nishibe, S., Rhee, S. G., & Carpenter, G. (1992). Growth factor stimulation of phospholipase C-gamma 1 activity. Comparative properties of control and activated enzymes. *Journal of Biological Chemistry*, 267(15), 10447-10456. doi:10.1016/s0021-9258(19)50039-4
- Wallace, R. A., Jared, D. W., Dumont, J. N., & Sega, M. W. (1973). Protein incorporation by isolated amphibian oocytes III. Optimum incubation conditions. *Journal of Experimental Zoology*, 184(3), 321-333. doi:<https://doi.org/10.1002/jez.1401840305>
- Webb, D. J., & Nuccitelli, R. (1985). Fertilization potential and electrical properties of the *Xenopus laevis* egg. *Developmental Biology*, 107(2), 395-406. doi:10.1016/0012-1606(85)90321-5
- Whitaker, M. J., & Steinhardt, R. A. (1983). Evidence in support of the hypothesis of an electrically mediated fast block to polyspermy in sea urchin eggs. *Developmental biology*, 95(1), 244-248.
- Williams, N. D., & Holdway, D. A. (2000). The effects of pulse-exposed cadmium and zinc on embryo hatchability, larval development, and survival of Australian crimson spotted rainbow fish (*Melanotaenia fluviatilis*). *Environmental Toxicology*, 15(3), 165-173. doi:10.1002/1522-7278(2000)15:3<165::aid-tox3>3.0.co;2-q
- Williams, R. J. P. (1987). The biochemistry of zinc. *Polyhedron*, 6(1). Retrieved from [www.sciencedirect.com](http://www.sciencedirect.com)
- Wilson, E. B. (1925). *The cell in development and heredity*: Macmillan.
- Wolf, D. P., Nishihara, T., West, D. M., Wyrick, R. E., & Hedrick, J. L. (1976). Isolation, physicochemical properties, and the macromolecular composition of the vitelline and fertilization envelopes from *Xenopus laevis* eggs. *Biochemistry*, 15(17), 3671-3678.
- Wong, J. L., & Wessel, G. M. (2006). Defending the zygote: search for the ancestral animal block to polyspermy. *Curr Top Dev Biol*, 72, 1-151. doi:10.1016/s0070-2153(05)72001-9
- Wong, P. T. S., & Chau, Y. K. (1990). Zinc toxicity to freshwater algae. *Toxicity Assessment*, 5(2), 167-177. doi:<https://doi.org/10.1002/tox.2540050205>
- Wozniak, K. L., Bainbridge, R. E., Summerville, D. W., Tembo, M., Phelps, W. A., Sauer, M. L., . . . Carlson, A. E. (2020). Zinc protection of fertilized eggs is an ancient feature of sexual reproduction in animals. *PLOS Biology*, 18(7), e3000811. doi:10.1371/journal.pbio.3000811 PMID - 32735558
- Wozniak, K. L., & Carlson, A. E. (2020). Ion channels and signaling pathways used in the fast polyspermy block. *Molecular Reproduction and Development*, 87(3), 350-357. doi:10.1002/mrd.23168 PMID - 31087507
- Wozniak, K. L., Mayfield, B. L., Duray, A. M., Tembo, M., Beleny, D. O., Napolitano, M. A., . . . Carlson, A. E. (2017). Extracellular Ca<sup>2+</sup> Is Required for Fertilization in the African Clawed Frog, *Xenopus laevis*. *PLoS One*, 12(1), e0170405. doi:10.1371/journal.pone.0170405
- Wozniak, K. L., Phelps, W. A., Tembo, M., Lee, M. T., & Carlson, A. E. (2018). The TMEM16A channel mediates the fast polyspermy block in *Xenopus laevis*. *J Gen Physiol*, 150, 1249-1259. doi:10.1085/jgp.201812071
- Wozniak, K. L., Phelps, W. A., Tembo, M., Lee, M. T., & Carlson, A. E. (2018). The TMEM16A channel mediates the fast polyspermy block in *Xenopus laevis*. *J Gen Physiol*. doi:10.1085/jgp.201812071

- Wozniak, K. L., Tembo, M., Phelps, W. A., Lee, M. T., & Carlson, A. E. (2018). PLC and IP3-evoked Ca<sup>2+</sup> release initiate the fast block to polyspermy in *Xenopus laevis* eggs. *J Gen Physiol*, *150*, 1239-1248. doi:10.1085/jgp.201812069
- Wozniak, K. L., Tembo, M., Phelps, W. A., Lee, M. T., & Carlson, A. E. (2018). PLC and IP3-evoked Ca(2+) release initiate the fast block to polyspermy in *Xenopus laevis* eggs. *J Gen Physiol*. doi:10.1085/jgp.201812069
- Wühr, M., Freeman, R. M., Presler, M., Horb, M. E., Peshkin, L., Gygi, S., & Kirschner, M. W. (2014). Deep proteomics of the *Xenopus laevis* egg using an mRNA-derived reference database. *Current biology : CB*, *24*(13), 1467-1475. doi:10.1016/j.cub.2014.05.044
- Wyrick, R. E., Nishihara, T., & Hedrick, J. L. (1974). Agglutination of Jelly Coat and Cortical Granule Components and the Block to Polyspermy in the Amphibian *Xenopus laevis*. *Proceedings of the National Academy of Sciences*, *71*(5), 2067-2071. doi:10.1073/pnas.71.5.2067 PMID - 4525317
- Yanagimachi, R. (1970). THE MOVEMENT OF GOLDEN HAMSTER SPERMATOZOA BEFORE AND AFTER CAPACITATION. *Reproduction*, *23*(1), 193-196. doi:10.1530/jrf.0.0230193 PMID - 5472441
- Yanagimachi, R. (1988). Mammalian Fertilization. In E. Knobil & J. D. Neill (Eds.), *The Physiology of Reproduction* (Vol. 1, pp. 135-185). New York: Raven Press.
- Yang, H., Jia, B., Zhang, Z., Qu, X., Li, G., Lin, W., . . . Zheng, Y. (2020). Alloying design of biodegradable zinc as promising bone implants for load-bearing applications. *Nature Communications*, *11*(1), 401. doi:10.1038/s41467-019-14153-7
- Yuan, H., Gao, C., Chen, Y., Jia, M., Geng, J., Zhang, H., . . . An, H. (2013). Divalent Cations Modulate TMEM16A Calcium-Activated Chloride Channels by a Common Mechanism. *The Journal of Membrane Biology*, *246*(12), 893-902. doi:10.1007/s00232-013-9589-9
- Yurewicz, E. C., Oliphant, G., & Hedrick, J. L. (1975). Macromolecular composition of *Xenopus laevis* egg jelly coat. *Biochemistry*, *14*(14), 3101-3107.
- Zeng, Y., Oberdorf, J. A., & Florman, H. M. (1996). pH regulation in mouse sperm: identification of Na(+)-, Cl(-)-, and HCO<sub>3</sub>(-)-dependent and arylaminobenzoate-dependent regulatory mechanisms and characterization of their roles in sperm capacitation. *Developmental Biology*, *173*(2), 510-520. doi:10.1006/dbio.1996.0044
- Zhou, G.-J., Peng, F.-Q., Zhang, L.-J., & Ying, G.-G. (2012). Biosorption of zinc and copper from aqueous solutions by two freshwater green microalgae *Chlorella pyrenoidosa* and *Scenedesmus obliquus*. *Environmental Science and Pollution Research*, *19*(7), 2918-2929. doi:10.1007/s11356-012-0800-9 PMID - 22327643
- Zinc Fact Sheet for Health Professionals. (2022, 08/28/2022). Retrieved from <https://ods.od.nih.gov/factsheets/zinc-HealthProfessional/>
- Zipper, J., Medel, M., & Prager, R. (1969). Suppression of fertility by intrauterine copper and zinc in rabbits. A new approach to intrauterine contraception. *American journal of obstetrics and gynecology*, *105*(4), 529-534.